AFRL-VS-HA-TR-98-0001

EXPANDED CAPABILITIES FOR THE IONOSPHERIC FORECAST MODEL

R. W. Schunk
J. J. Sojka
J. V. Eccles

Space Environment Corporation
399 North Main, Suite 325
Logan, UT 84321

20 December 1997

Final Report
12 May 1994 to 30 September 1997

Approved for public release; distribution unlimited

19980413 036

[DTIC QUALITY INSPECTED 8]

"This technical report has been reviewed and is approved for publication."

JOHN RETTERER
Contract Manager

ROBERT MORRIS
Branch Chief

DAVID HARDY
Division Director

This report has been reviewed by the ESC Public Affairs Office (PA) and is releasable to the National Technical Information Service (NTIS).

Qualified requestors may obtain additional copies from the Defense Technical Information Center (DTIC). All others should apply to the National Technical Information Service (NTIS).

If your address has changed, if you wish to be removed from the mailing list, of if the addressee is no longer employed by your organization, please notify AFRL/VSOS-IM, 29 Randolph Road, Hanscom AFB, MA 01731-3010. This will assist us in maintaining a current mailing list.

Do not return copies of this report unless contractual obligations or notices on a specific document require that it be returned.

4. TITLE AND SUBTITLE Expanded Capabilities for the Ionospheric Forecast Model	5. FUNDING NUMBERS PE 63707F PR 4026 TA GL WU MB
6. AUTHOR(S) R.W. Schunk, J.J. Sojka, and J.V. Eccles	Contract F19628-94-C-0046

7. PERFORMING ORGANIZATION NAME(S) AND ADDRESS(ES) Space Environment Corporation 399 North Main, Suite 325 Logan, Utah 84321	8. PERFORMING ORGANIZATION REPORT NUMBER

9. SPONSORING/MONITORING AGENCY NAME(S) AND ADDRESS(ES) Air Force Research Laboratory 29 Randolph Road Hanscom AFB, MA 01731-3010 Contract Manager: John Retterer/VSB	10. SPONSORING/MONITORING AGENCY REPORT NUMBER AFRL-VS-HA-TR-98-0001

11. SUPPLEMENTARY NOTES

12a. DISTRIBUTION/AVAILABILITY STATEMENT Approved for public release; distribution unlimited	12b. DISTRIBUTION CODE

13. ABSTRACT (Maximum 200 words)

The Ionospheric Forecast Model (IFM) is a computationally efficient, user-friendly, model of the global ionosphere that was developed for operational use at the Space Forecast Center. The model provides 12-hour forecasts for the global distributions of the molecular (NO^+, $O2^+$, $N2^+$) and O^+ densities, and the electron and ion temperatures, at E and F region altitudes (90-1000 km). The model also contains a simple algorithm for predicting H^+ densities in the F region. The IFM is self-contained and is run by specifying a few simple parameters and geophysical indices. With support from this contract, the capabilities of the IFM were expanded in order to improve the reliability of its predictions. This involved the extension of the model to 1600 km, and the development of a K_p forecast algorithm, which was needed in order to obtain forecasts for the time-dependent convection and precipitation patterns. An extensive validation of the IFM was also conducted, including both climatology and storm simulations. In addition, the IFM was modified so that it could be coupled to the Thermospheric Forecast Model (TFM). As part of this effort, we developed the necessary coupling algorithms. Finally, we initiated the construction of a global dynamo model.

14. SUBJECT TERMS Ionospheric Model; Forecast; Ion and Electron Densities and Temperatures; Peak Densities and Heights			15. NUMBER OF PAGES 148
			16. PRICE CODE

17. SECURITY CLASSIFICATION OF REPORT Unclassified	18. SECURITY CLASSIFICATION OF THIS PAGE Unclassified	19. SECURITY CLASSIFICATION OF ABSTRACT Unclassified	20. LIMITATION OF ABSTRACT SAR

Table of Contents

EXECUTIVE SUMMARY

The Ionospheric Forecast Model (IFM) is a computationally efficient, user-friendly, model of the global ionosphere that was developed for operational use at the Space Forecast Center. The model provides 12-hour forecasts for the global distributions of the molecular (NO^+, $O2^+$, $N2^+$) and O^+ densities, and the electron and ion temperatures, at E and F region altitudes (90-1000 km). The model also contains a simple algorithm for predicting H^+ densities in the F region. The inputs needed by the IFM are the global distributions of the neutral gas parameters (densities, temperatures, and winds), the electric field (magnetospheric and dynamo), the auroral electron precipitation, and the topside electron heat flux. In the original version of the IFM, specific empirical models or simplified expressions for all of these global inputs were adopted, and they were included as an integral part of the IFM. This original version of the IFM is therefore self-contained and is run by specifying a few simple parameters and geophysical indices. With support from this contract, the capabilities of the IFM were expanded in order to improve the reliability of its predictions. This involved the extension of the model to 1600 km, and the development of a K_p forecast algorithm, which was needed in order to obtain forecasts for the time-dependent convection and precipitation patterns. An extensive validation of the IFM was also conducted, including both climatology and storm simulations. In addition, the IFM was modified so that it could be coupled to the Thermospheric Forecast Model (TFM), which is under development at Phillips Laboratory. As part of this effort, we developed the necessary coupling algorithms. Finally, we initiated the construction of a global dynamo model, so that in the future the dynamo electric fields can be incorporated in the IFM in a self-consistent manner.

1. INTRODUCTION

With previous support from Phillips Laboratory, we developed a computationally efficient, user-friendly, Ionospheric Forecast Model (IFM) for the Space Forecast Center. The model calculates the 3-dimensional, time-dependent evolution of the global ionosphere at altitudes between 90 and 1000 km. The IFM provides predictions for the density distributions of four major ions (NO^+, O_2^+, N_2^+, O^+) at E-region altitudes, two major (NO^+, O^+) and two minor (N_2^+, O_2^+) ions at F-region altitudes, and the ion and electron temperatures at both E and F region altitudes. The IFM also contains a simple prescription for calculating H^+ densities in the F-region. The spatial resolution of the model in the vertical direction is 4 km in the E-region and 20 km in the F-region, which is more than adequate to resolve all of the ionization peaks. The IFM takes account of all of the important chemical and physical processes, including field-aligned diffusion, cross-field electrodynamic drifts, thermospheric winds, protonospheric exchange fluxes, energy-dependent chemical reactions, neutral composition changes, several ion production sources (auroral electron precipitation, solar UV and EUV radiation, resonantly scattered solar radiation, starlight), electron thermal conduction, and a host of local heating and cooling processes. The IFM also takes account of the offset between the geomagnetic and geographic poles.

The inputs needed by the IFM are included as an integral part of the model. The main global inputs are the neutral atmospheric densities, temperatures and winds, the magnetospheric and dynamo electric fields, and the auroral electron precipitation pattern. In the original version of the model (IFM-1), specific empirical models were adopted for all of the required 'global' inputs. However, the IFM was constructed in a modular form so that when improved inputs become available, they can be 'plugged in' with no impact on the rest of the model.

The IFM-1 is driven by a few simple parameters and geophysical indices. Depending on the specification, the IFM outputs a variety of parameters, including global snapshots of N_mF2, h_mF2, N_mE, and h_mE, density and temperature contours at a fixed altitude, density and temperature profiles versus altitude at specified locations, and the total electron content (TEC).

With support from this Air Force contract, we expanded the capabilities of the Ionospheric Forecast Model in order to provide more reliable forecasts. The work involved the following five primary tasks: (1) Support for the delivery and technical transition of IFM-1; (2) Support for the development of the Coupled Ionosphere-Thermosphere Forecast Model (CITFM), which involved the construction of coupling algorithms; (3) Development of improved plasma convection and particle precipitation patterns, which are important inputs for the IFM in the high-latitude domain; (4) Development of improved models for the equatorial electric fields, which are the main drivers of the low-latitude ionosphere; and (5) Validation of the IFM in all latitudinal domains and for a range of geophysical conditions. In the subsections that follow, more details are given of the work completed in these five primary areas.

1

2. IFM DELIVERY AND TRANSITION SUPPORT

2.1 IFM Delivery Schedule

Three versions of the IFM have been delivered to both the Air Force and Hughes STX, which is the company responsible for implementing the IFM on the computers at the Space Forecast Center. The delivery schedule was as follows:

(a) IFM-1 delivered September 1994.
(b) IFM-2 delivered September 1995.
(c) IFM-2 with user interface delivered January 1996.
(d) IFM-2 for VMS operating system delivered June 1996.
(e) IFM-3 (test version) for a top altitude of 1600 km delivered April 1997.
(f) IFM-3 (final version) delivered September 1997.

The IFM-1 model was delivered at the scheduled delivery date of September 1994. However, the Air Force was not ready to transition the model until September 1995. In the mean time, we continued the validation of the IFM and when the Air Force was ready to transition the IFM in September 1995, we sent them the most recent version (IFM-2). After delivery, the Space Forecast Center (SFC) requested that we provide a user interface to the IFM that was similar to the PRISM interface. The IFM-2 version with the user interface was delivered January 1996. The IFM's delivered up to that time were for a UNIX operating system and the SFC subsequently requested a version of IFM-2 that could be run on a VMS operating system, which was delivered June 1996. Later, the SFC requested a version of the IFM that had a top altitude of 1600 km, instead of 1000 km. A 'beta' version of this extended model (IFM-3), was delivered to Hughes STX in April 1997 and the 'final' version was delivered to the Air Force in September 1997. Also, in order to protect the IFM from improper usage, protection software was developed to prevent an erroneous model initialization.

2.2 Hughes STX Transition Support

Since September 1995, when the transition of the IFM began, we have worked with Hughes STX in order to provide a smooth transition of the model. Only a few issues have arisen during this time, most of which had to do with the operating systems on the SFC and Hughes STX computers. Working together with Hughes STX, these issues were quickly resolved. The only problem detected with the IFM was a minor software problem with an ancillary subroutine we separately supplied at the request of the SFC. This subroutine calculates N_mF2, h_mF2, N_mE, h_mE, and TEC after the IFM has been run and a global data base of electron densities has been created. After detection by Hughes STX, the minor software problem was trivial to correct. Further details concerning our interactions with Hughes STX are given in previous reports presented at the Model Review Meetings.

3. CITFM DEVELOPMENT SUPPORT

The neutral densities, temperatures, and winds are important input parameters for the Ionospheric Forecast Model. Currently, these parameters are obtained from the MSIS atmospheric model and the Hedin wind model (Hedin et al, 1988; Hedin, 1987). These empirical models should be more than adequate during sustained levels of geomagnetic activity. However, during changing magnetic activity, a coupled ionosphere-thermosphere model could yield more reliable forecasts because the time delays and feedback mechanisms that are inherent in the system are properly described. Because of this fact, Phillips Laboratory initiated the development of a Thermospheric Forecast Model (TFM), which is based on the physical model of the coupled ionosphere-thermosphere system developed by Fuller-Rowell and Rees (1980). Like the IFM, the Thermospheric Forecast Model is user-friendly and computationally efficient.

The Ionospheric Forecast Model provides global distributions of the ion and electron densities and temperatures over the altitude range from 90 to 1600 km at specified times. Likewise, the Thermospheric Forecast Model provides global distributions of the neutral densities, temperatures, and winds at altitudes from 90 to 500 km at specified times. During the tenure of this contract, we worked with PL scientists in an effort to identify issues that needed to be addressed so that the models could be coupled in an optimum way. One of the issues addressed relates to the spatial coordinates inherent in the two models. The IFM is based on an Euler-Lagrange hybrid scheme. The equations are solved along a magnetic field line using a fixed spatial grid, and the flux tubes of plasma are followed as they drift across $\underline{B}$ in response to dynamo and magnetospheric electric fields. The TFM, on the other hand, has fixed latitude and longitude grids, and the vertical spatial grid is tied to pressure levels, not altitude. Another issue addressed concerned the time at which the two models need to communicate with each other in relation to the CPU time required to get to the 'communication' time. In particular, the IFM is more CPU intensive than the TFM and algorithms had to be developed that force the TFM to wait for the IFM to 'catch up'. Finally, both codes had to be modified so that they would accept the same plasma convection and particle precipitation drivers.

With regard to the philosophy underlying the coupling of the IFM and TFM, it was decided that in order to keep a modular form the best approach was for the two models to communicate through an external, Global Spatial Grid. This approach had the added advantage in that the global inputs needed by both the IFM and TFM (low and high latitude electric fields, magnetic field, particle precipitation) could also be specified on the global grid. To establish such a setup, it was first necessary to remove the empirical models for convection, precipitation, neutral densities, winds, and the geomagnetic field from the IFM. It was then necessary to create modules so the IFM could access the Global Grid for all of these inputs. This required the development of algorithms that would automatically interpolate values on the Global Grid to the IFM internal grids. The IFM outputs are also supplied to the Global Grid.

A schematic of the IFM-TFM coupling configuration is shown in Figure 1. The IFM and TFM operate as separate codes on the computer, with wait commands to allow synchronized time stepping and information exchange. The data exchange occurs every x minutes (15 minutes typically) via the Global Grid. At the time of an exchange, the IFM acquires new global distributions for the electric field, magnetic field, and auroral oval from empirical models as well as the neutral densities, temperatures, and winds from the TFM. At this time, the IFM also supplies the ion densities and temperatures to the Global Grid for

3

use by the TFM. The two numerical models then run independently until the next time for a data exchange. As noted above, an advantage of this coupling configuration is its modular form. Different atmospheric models can be easily inserted in place of the TFM with no impact on the rest of the system, as can different models for convection, precipitation, and the geomagnetic field.
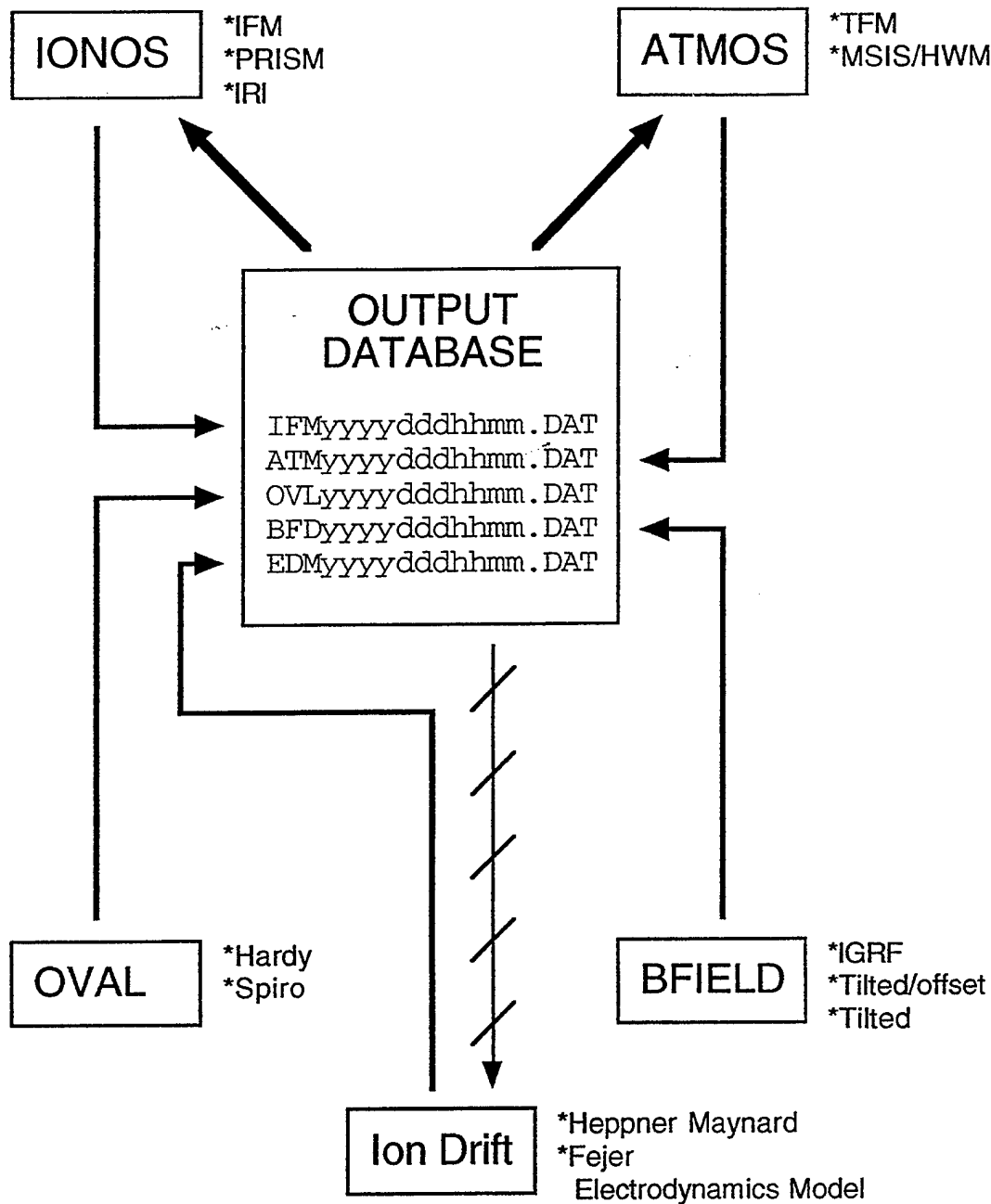
```
  IONOS        *IFM              ATMOS        *TFM
               *PRISM                         *MSIS/HWM
               *IRI


                     OUTPUT
                     DATABASE

                  IFMyyyydddhhmm.DAT
                  ATMyyyydddhhmm.DAT
                  OVLyyyydddhhmm.DAT
                  BFDyyyydddhhmm.DAT
                  EDMyyyydddhhmm.DAT


  OVAL         *Hardy            BFIELD       *IGRF
               *Spiro                         *Tilted/offset
                                              *Tilted


              Ion Drift    *Heppner Maynard
                           *Fejer
                           Electrodynamics Model
```

Figure 1. The IFM-TFM Coupling Configuration.

4

4. IMPROVED CONVECTION AND PRECIPITATION INPUTS

At high latitudes, the main inputs to the IFM are the plasma convection and particle precipitation patterns. The electric fields act to transport plasma over large distances and are a significant heat source for the ions owing to the consequent ion-neutral frictional interactions. The elevated ion temperatures then affect the chemical reaction rates, topside plasma scale heights, and the electron-ion energy transfer rate. Auroral electron precipitation, on the other hand, is an important heat source for the thermal electrons, and it is an important source of plasma via impact ionization. In the first two versions of the IFM that have been delivered to the Air Force (IFM-1,2), specific empirical models were adopted for the plasma convection (Heppner and Maynard, 1987) and electron precipitation (Hardy et al, 1985) patterns. However, during the tenure of this contract, work was done in an effort to improve the way these important inputs are used.

4.1 Kp Forecast Algorithm

In the IFM-1 and IFM-2, the plasma convection and particle precipitation patterns vary with time according to the way the magnetic indice K_p varies with time. Therefore, when the IFM is used in a forecast mode, it is necessary to forecast the K_p variation in order to forecast the time-dependent convection and precipitation patterns. Of course, the obvious way to forecast K_p is to use persistence, but that is not adequate if the current K_p value is either high or low.

During the contract period, we developed a forecast algorithm that is far superior to persistence. Given the current K_p value, this algorithm provides a 12-hour forecast of what K_p should be. The algorithm was developed using 40 years of K_p data (from 1950 to 1990). The algorithm development was based on the *most likely* K_p trend given the current K_p value. The algorithm provides K_p forecasts for different solar cycle ranges, as determined by the F10.7 index. Figures 2 and 3 show K_p forecasts for solar cycle ranges of 60<F10.7<100 and 200<F10.7<300, respectively. In each figure, the current K_p value is given at 0 hours, and integer values from 1 to 6 have been selected. The values to the right of 0 hours show what the future K_p is *most likely* to be (according to 40 years of data). For example, consider the F10.7 range from 60-100. If the current K_p=6, then in 15 hours the most likely K_p value will be 4.

The RMS error of the K_p forecast algorithm is significantly better than that for persistence forecasts. Therefore, this K_p forecast algorithm was included in the IFM-3 version delivered to the Air Force in April 1997.
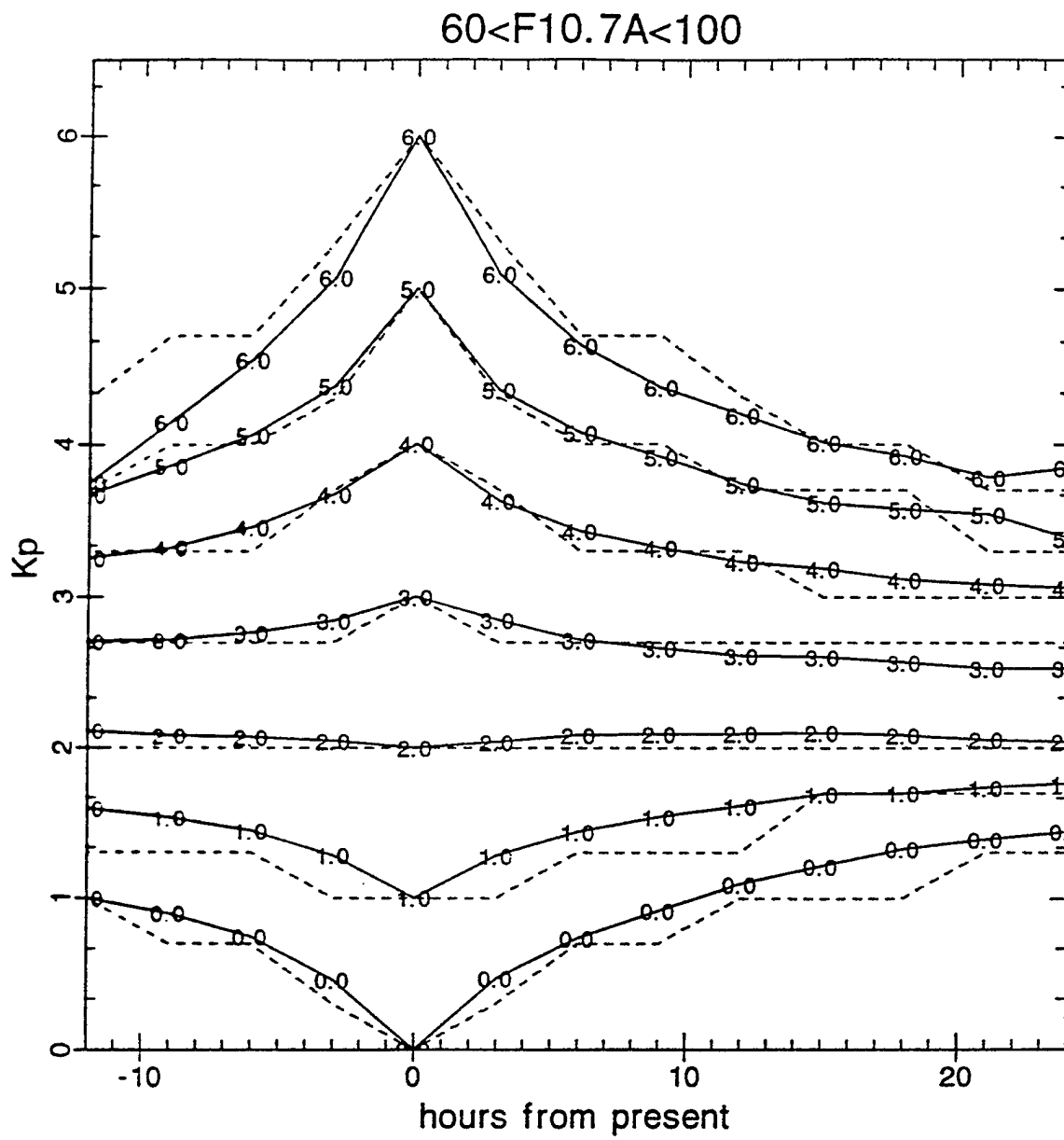
5

60<F10.7A<100

Figure 2.   K$_p$ forecasts for the solar cycle range 60<F10.7<100.
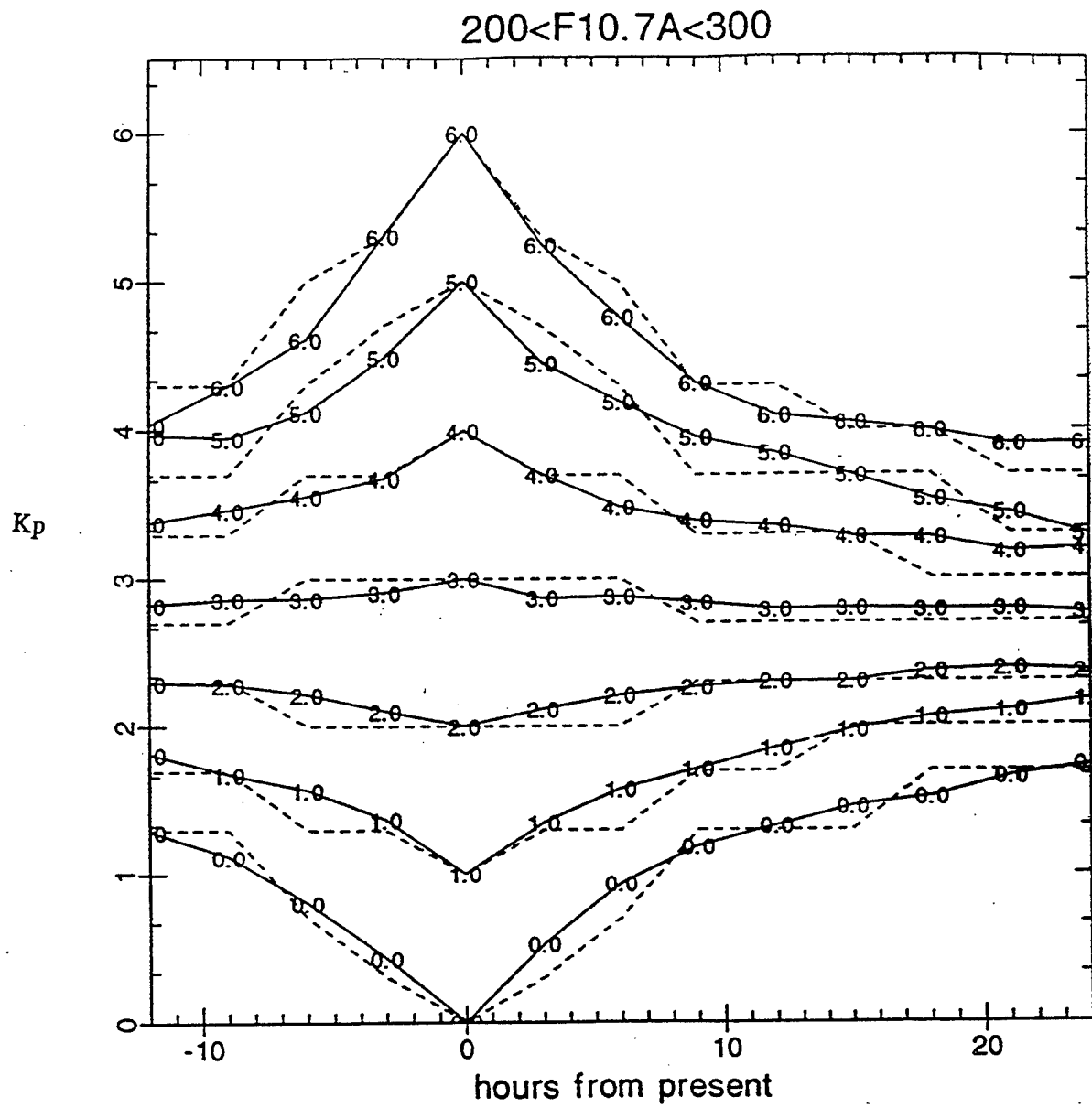
6

200<F10.7A<300

Figure 3. K_p forecasts for the solar cycle range 200<F10.7<300.

7

4.2 DMSP-J4 Data Assimilation

In the future, the ultimate way to use the IFM is to adjust the *empirical* convection and precipitation patterns in response to real-time satellite measurements. The DMSP satellites provide in situ measurements of both plasma drifts and electron precipitation along the satellite orbits at an altitude of 800 km. For example, the J4 particle data provide information on the spatial extent of the auroral oval as well as on the energy flux and characteristic energy of the precipitating electrons. When these data are available, they can be used to adjust the empirical model of the auroral oval developed by Hardy et al (1985), which should yield more reliable ionospheric predictions, especially during geomagnetic storms.

Figure 4 shows contours of the precipitating electron energy flux obtained from the empirical model developed by Hardy et al (1985) for three levels of K_p (0,3, and 5). It is apparent that as K_p increases, the auroral oval expands and the precipitation becomes more intense, as expected. When the magnetic activity level is steady, the Hardy model is very reliable. However, during geomagnetic storms, the empirical model can differ significantly from the actual precipitation. This is shown in Figure 5, where the DMSP-J4 particle measurements are compared with the predictions of the Hardy model during a 15-hour storm period. The solid lines show the precipitating electron energy flux measured by the F-11 satellite as it crossed the northern polar region. The dashed lines show the corresponding predictions obtained from the Hardy model. During this 15-hour period, the K_p index varied from 2.7 at 22:28 UT, to 5.0, and then to 1.7 at 12:03 UT. At times the Hardy model provides a reliable representation of the electron energy flux, but at other times it is off by a significant amount. Clearly, if the Hardy empirical model could be adjusted with the aid of real-time particle measurements, the resulting auroral oval would be more reliable.

With funding from this contract, we developed a data assimilation algorithm that ingests J4 particle data into the Hardy empirical model. The algorithm can handle up to 4 DMSP satellites simultaneously. When data from 4 satellites are available, more than 40% of the auroral oval can be modified with our data assimilation algorithm. The algorithm can also take account of discrete auroral arcs. Figures 6-8 show three examples of how the algorithm adjusts the Hardy empirical model in response to real-time J4 particle measurements. In each figure, the top dial shows the modified auroral oval and the bottom dial shows the auroral oval obtained from the Hardy model. Figure 6 shows a case where the modifications are small. For the case shown in Figure 7, multiple arcs were seen by 3 of the 4 DMSP satellites, and our data ingestion algorithm successfully modified the Hardy empirical model to account for these arcs. Finally, Figure 8 shows a case where our data ingest algorithm was able to capture the cusp precipitation, which resulted in a significant modification of the Hardy empirical model on the dayside.
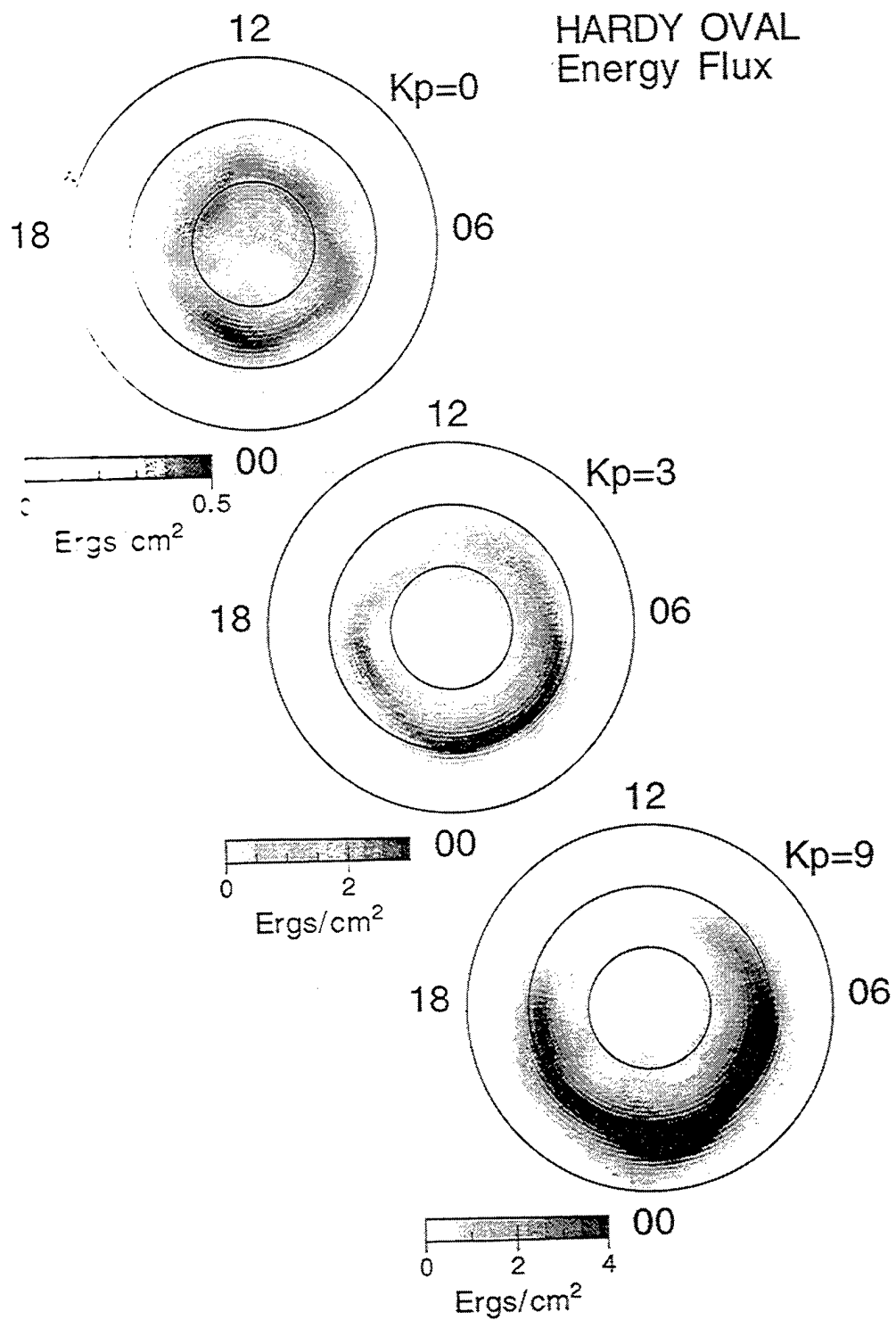
Figure 4. Contours of the auroral electron energy flux obtained from the Hardy empirical model for three values of K_p.

9

Precipitation Model versus J4 Data
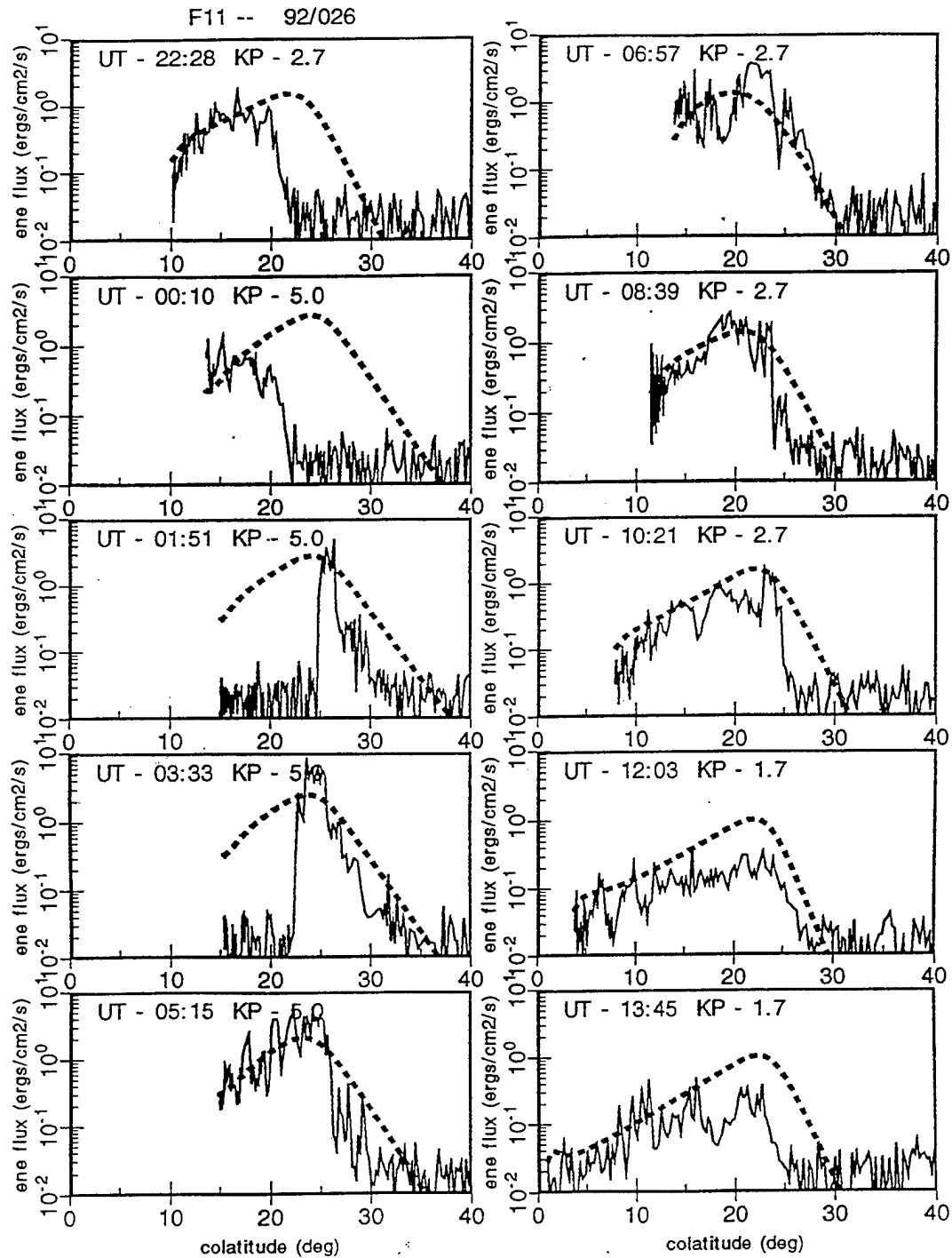
Storm Example

Figure 5. Comparisons of the auroral electron energy flux obtained from the Hardy empirical model (dashed curves) with the energy flux measured by the DMSP F-11 satellite (solid curves).
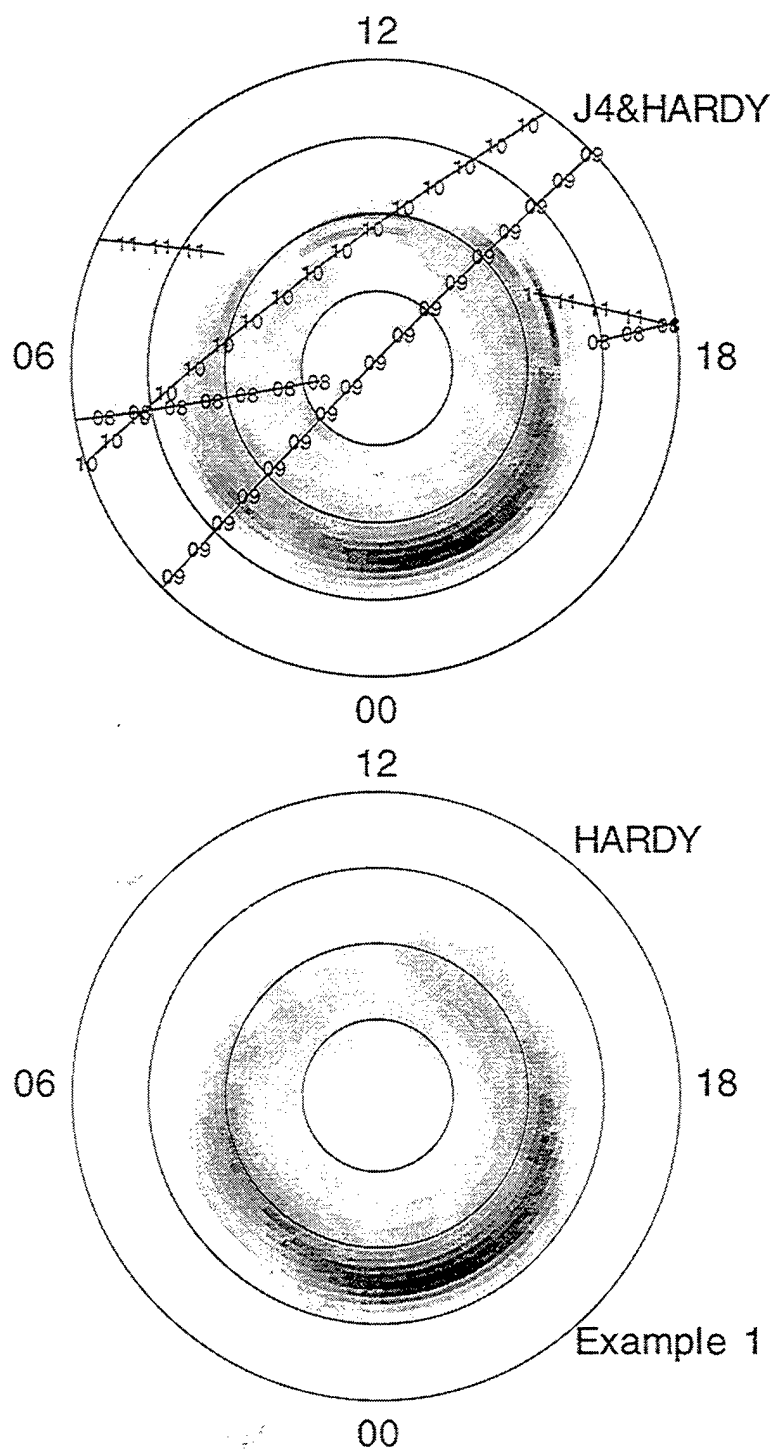
10

YEAR=1992 DAY=27 UT=09:00 KP=2.7

12

J4&HARDY

06

18

00

12

HARDY

06

18

Example 1

00

Figure 6. Comparison of modified and unmodified auroral ovals for a case when the modifications are small.

11

YEAR=1992   DAY=27   UT=17:00   KP=2.3
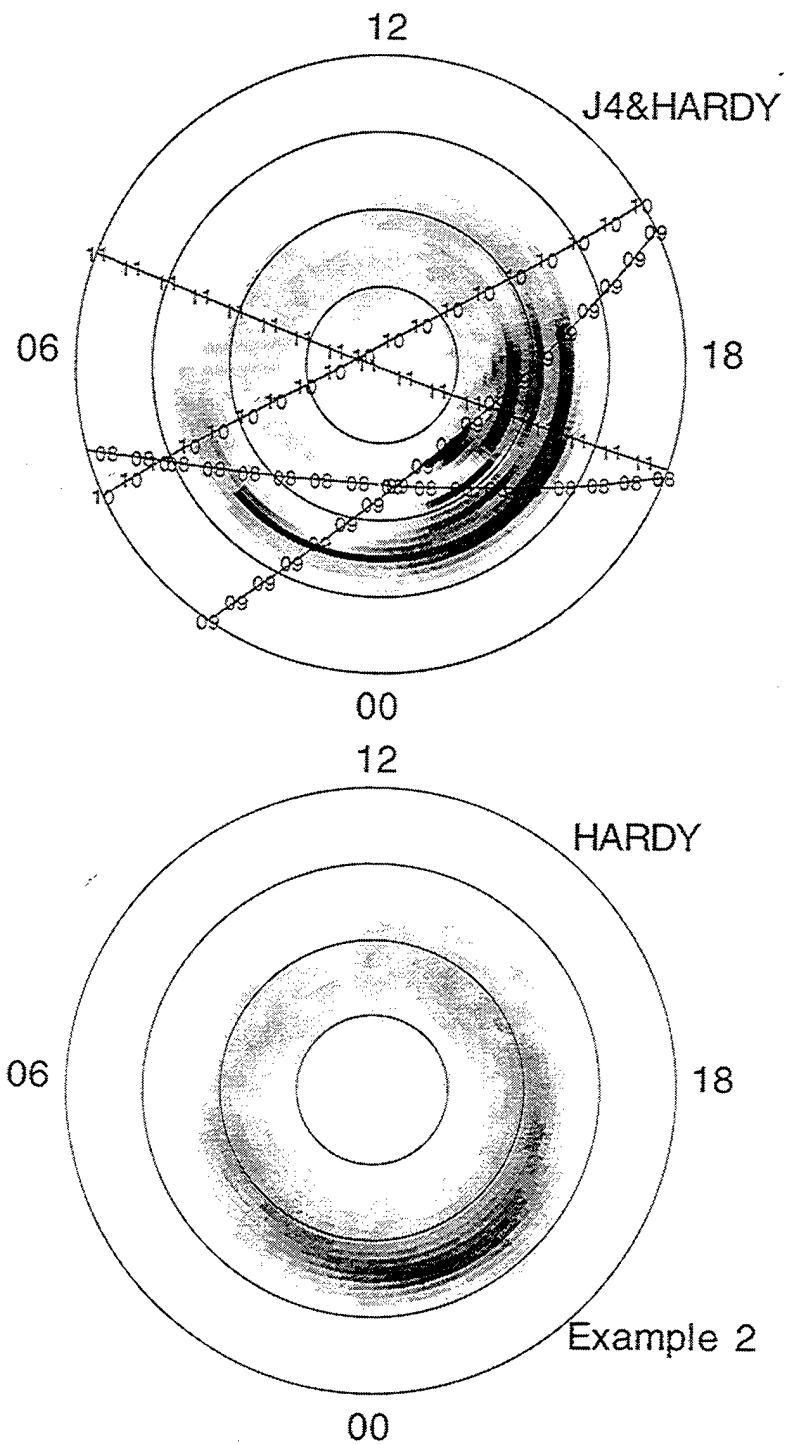
Figure 7.   Comparison of modified and unmodified auroral ovals for a case when multiple
arcs were seen by three DMSP satellites.

YEAR=1992　DAY=25　UT=10:00　KP=1.0
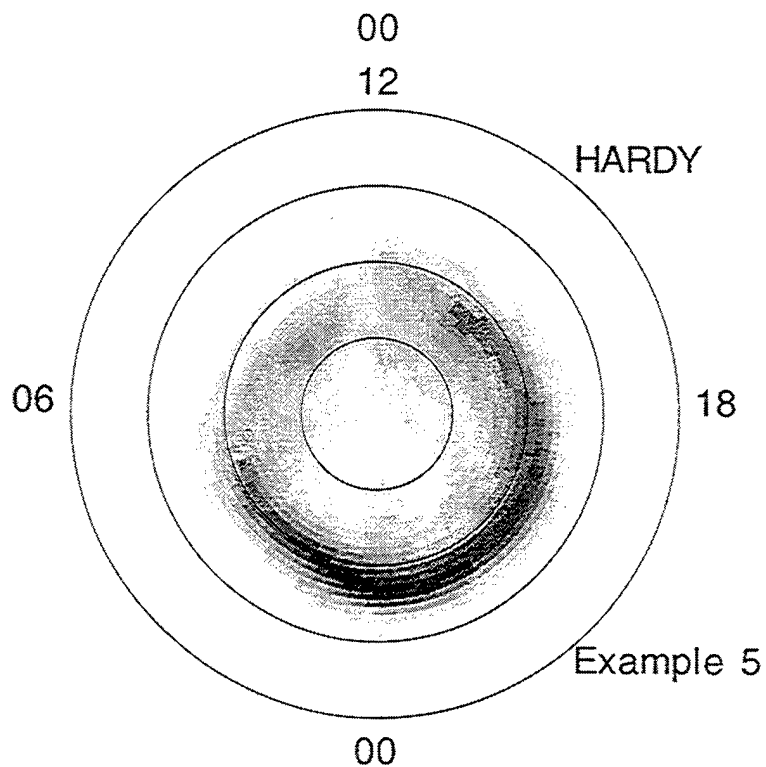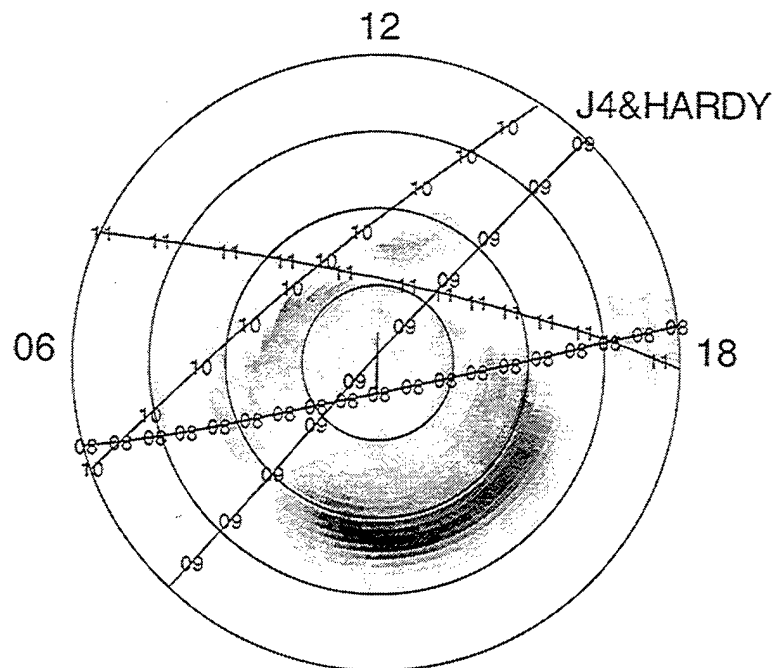
Figure 8.　Comparison of modified and unmodified auroral ovals for a case when the DMSP satellites captured the precipitation in the cusp.

13

5. EQUATORIAL ELECTRODYNAMICS

The most important input parameter for the IFM at low latitudes is the distribution of the dynamo electric fields. These electric fields are generated when the thermospheric wind transports ions across magnetic field lines. The electric fields are generated at E- and F1-region altitudes and then mapped along the geomagnetic field to higher altitudes due to the high conductivity of the ionosphere. The electric field generally induces an upward plasma drift during the day and a downward drift at night. At dusk, however, just before the reversal from upward to downward plasma drifts, there is a prereversal enhancement in the upward drift (at about 1800 LT). This upward drift lifts the F-layer to altitudes as high as 500 km, which acts to produce a sharp density gradient below the ionization peak. These conditions can lead to the Rayleigh-Taylor instability and then spread-F. When spread-F occurs, the resulting scintillations can have a significant effect on military systems and operations. Therefore, for reliable IFM predictions, it is important to have the best possible model for the low-latitude dynamo electric fields.

5.1 Fejer Empirical Model

When the IFM was first developed, there were very few empirical models of equatorial electric fields. The most extensive study published up to that time was the one conducted by Richmond et al (1980). These scientists used a harmonic expansion, including UT terms, to model incoherent scatter radar measurements of plasma drifts obtained in two distinct longitude regions. Their empirical model was built with data acquired over a wide range of seasonal conditions, but the data were restricted to low geomagnetic activity and solar maximum. The electric potentials obtained with their model varied markedly with UT and season, but the magnitudes of the derived equatorial electric fields were lower than those found in other studies. Nevertheless, this model was the only published equatorial electric field model that was suitable as an input to the IFM and it was incorporated into the first version of the IFM.

Subsequent to the incorporation of the Richmond et al (1980) equatorial electric field model into the IFM, Fejer et al (1995) developed a more comprehensive model. The Fejer empirical model of vertical drifts (east-west electric fields) was constructed from a large data base of Atmospheric Explorer-E satellite data and Jicamarca incoherent scatter radar measurements. The empirical model takes account of diural, seasonal, and solar cycle variations. It also covers four longitude sectors, including the Atlantic (320°), American (260°), Pacific (180°), and Indian (80°) sectors. Typical results obtained from this equatorial electric field model are shown in Figure 9, where vertical drifts are plotted versus local time in the four longitude sectors and for three seasons. Clearly seen in most of the plots is the prereversal enhancement in the upward drift at about 1800 LT.

As part of the work support with this contract, we replaced the Richmond et al (1980) empirical model that was in the IFM with the more comprehensive Fejer et al (1995) empirical model. After this change, the model was thoroughly tested to ensure that it was robust.

AE-E 1978-79   Kp ≤ 3

MAR-APR SEP-OCT   MAY-AUG   NOV-FEB

VERTICAL DRIFT (m/s)

$\bar{\phi}=80°E$

$\bar{\phi}=180°E$

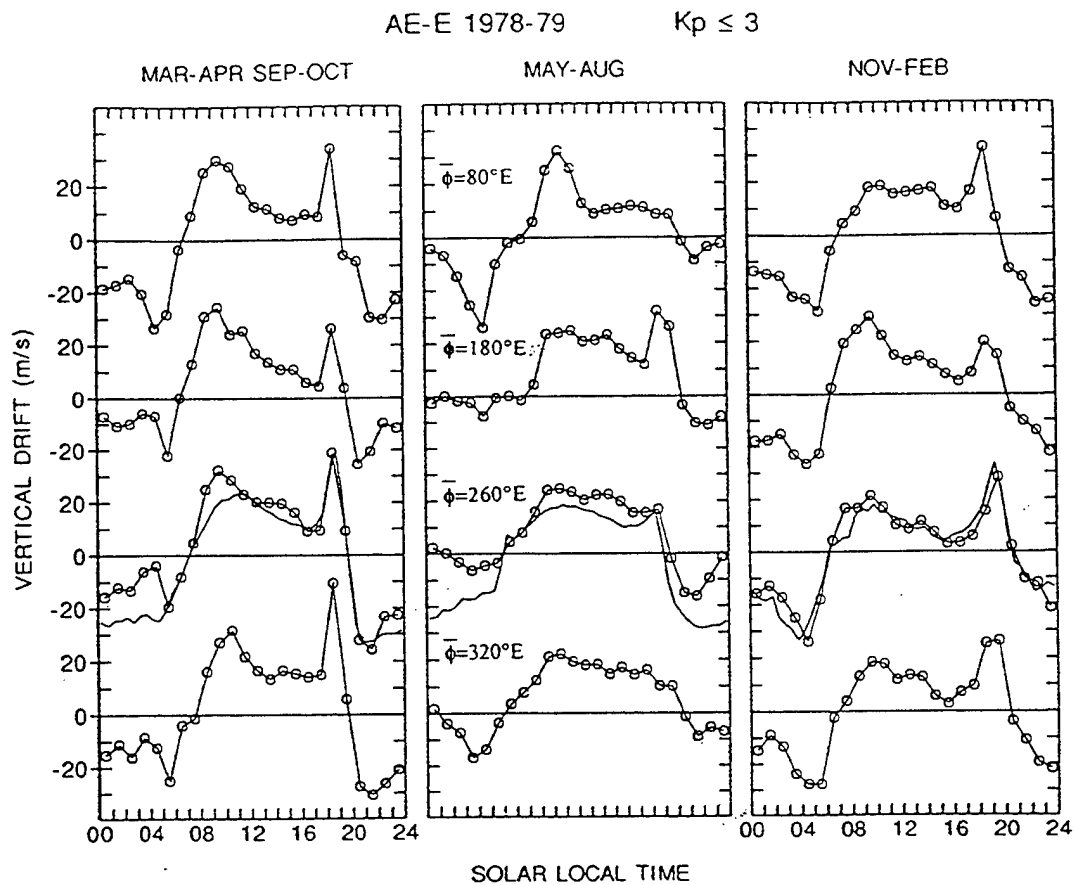$\bar{\phi}=260°E$

$\bar{\phi}=320°E$

SOLAR LOCAL TIME

Figure 9. Empirical model of vertical plasma drifts in four longitude sectors and for three seasons. The results are for low magnetic activity and moderate to high solar activity. Also shown are the seasonal Jicamarca drift patterns for similar solar flux and geomagnetic conditions. From Fejer et al (1995).

15

5.2 Global Dynamo Model

As noted above, dynamo electric fields are the primary source of vertical plasma drifts in the low latitude ionosphere, and they contribute to the plasma motions at middle and high latitudes. Since these electric fields are an important input to both the IFM and the CITFM, more reliable forecasts would be obtained if these dynamo electric fields were self-consistently calculated. Consequently, as part of this contract work, Phillips Laboratory directed us to initiate the development of a global, dynamo electric field model. The model is supposed to be a robust, user-friendly version of the research code originally developed by David Crain as part of his Ph.D. dissertation. To turn this research code into an operational model requires the following tasks:

(a) Verify and review the theoretical formulation.
(b) Improve the numerical algorithm for the potential solver.
(c) Assimilate ionospheric inputs.
(d) Test the dynamo model with different wind models.
(e) Couple the dynamo model to ionospheric and simple wind models to test the overall coupling scheme.
(f) Run the dynamo model for a wide range of geophysical conditions.
(g) Validate the results with geophysical data.

We have already made substantial progress on the dynamo model. In particular, the theoretical formulation has already been reviewed and no additional terms were needed. The numerical scheme for the potential solver has been stabilized and testing has been initiated to see how robust it is. However, in the future, it would be useful to consider other numerical schemes so as to obtain the most computationally efficient algorithm. The dynamo model has a modular configuration so that any element of the model can be changed without impacting the rest of the model. The main elements of the dynamo model are:

1. Conductivity module
2. Wind module
3. Geomagnetic field module
4. Field-line integration model
5. Potential Solver
6. Electric field and vertical and zonal drift calculator

These modules can be different models or they can be inputs supplied by measurements. For example, the conductivity module calculates ionospheric conductivities using plasma densities supplied by the IRI, PRISM, or the IFM. Likewise, the magnetic field can be a centered dipole, an offset-tilted dipole, or the IGRF.

The global dynamo model outputs the potential distribution on a 5° latitude by 5° longitude spatial grid at 20-minute time intervals. From this output, the zonal and meridional components of both the dynamo electric field and the plasma drift are calculated.

16

Under this contract, the modular structure of the dynamo model has been completed and, as noted above, the numerical scheme has been stabilized. However, thorough testing is needed of both of these model features for a range of geophysical conditions and for different inputs to the modules. Specifically, the dynamo model should be tested for all combinations of the following:

- Solar Maximum, Medium, Minimum
- Summer, Winter, Equinox
- IFM and PIM Plasma Densities
- Analytical, MSIS, CTIP, and DE-2 Winds
- Centered Dipole, Offset-Tilted Dipole, and IGRF Magnetic Field

This amount to 216 runs of the global dynamo model, and a successful completion of these runs will verify that the numerical scheme is indeed stable and that the model is robust. It would also be useful to acquire a large data base of equatorial plasma drifts that can be used to validate the model results.

During the tenure of this contract, we have already conducted 24 of the 216 simulations and we have already collected some equatorial data. Figures 10-12, show sample results from the global dynamo model. Figure 10 shows a snapshot of the global potential distribution, while Figures 11 and 12 show vertical and zonal plasma drifts calculated by the dynamo model as well as drifts measured at Jicamarca. The results are for moderate solar activity, equinox, an offset tilted dipole $\underline{B}$ field, MSIS atmospheric densities, winds supplied by Fuller-Rowell's CTIP model, and PIM ionospheric conductivities.

PIM and CTIP (TFM) Wind 12 UT Equinox
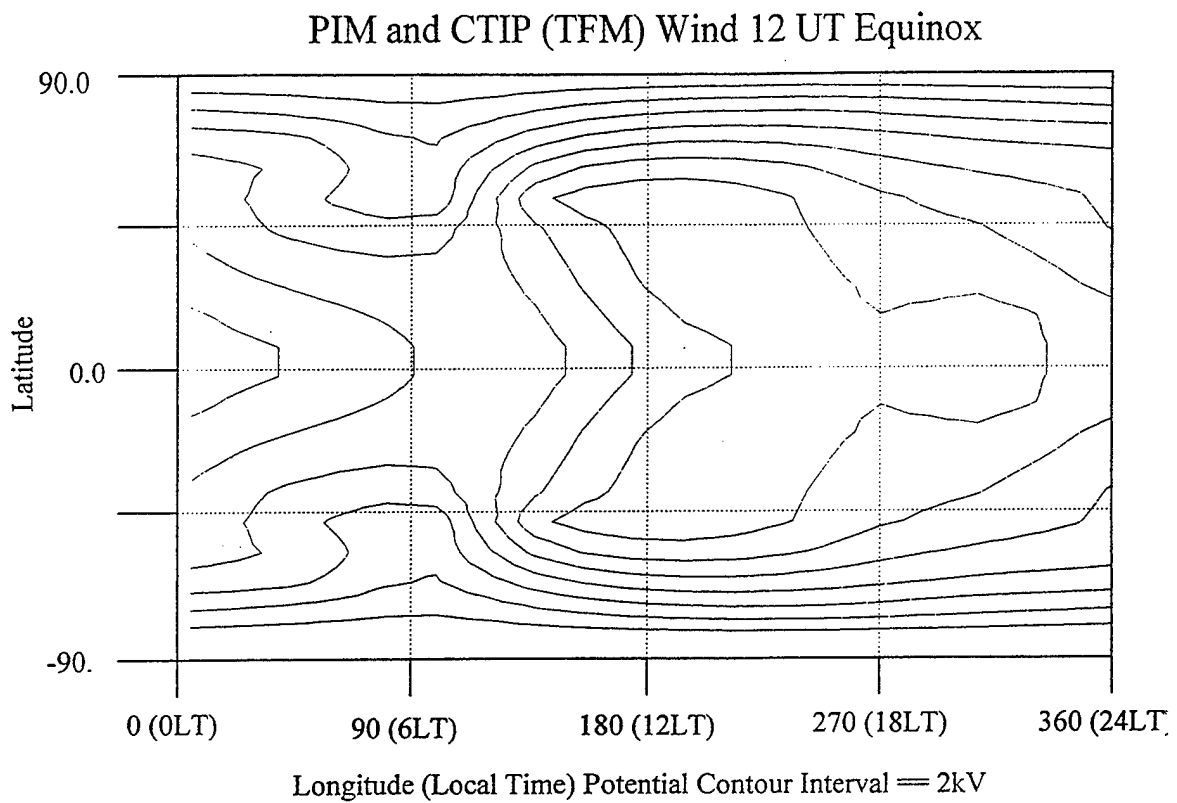
Figure 10. Snapshot of the global distribution of the electric potential induced by thermospheric winds.

PIM/CTIP 1and 12 UT Vertical Drifts
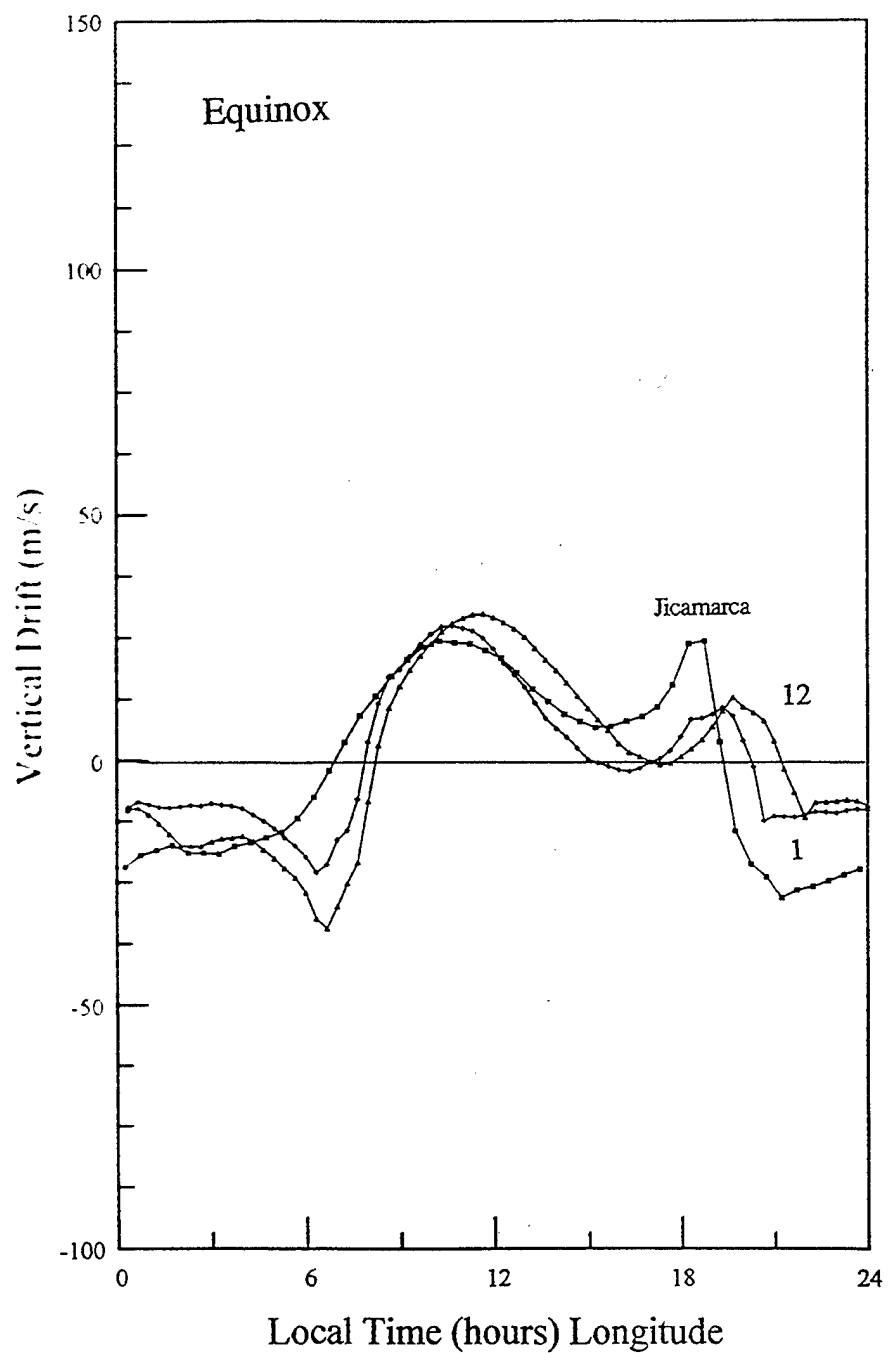
Figure 11. Local time variation of the vertical plasma drifts at 1 and 12 UT calculated by the dynamo model at the Jicamarca location. Also shown are the corresponding radar measurements.

19

PIM/CTIP Zonal Drifts (1 and 12 UT)
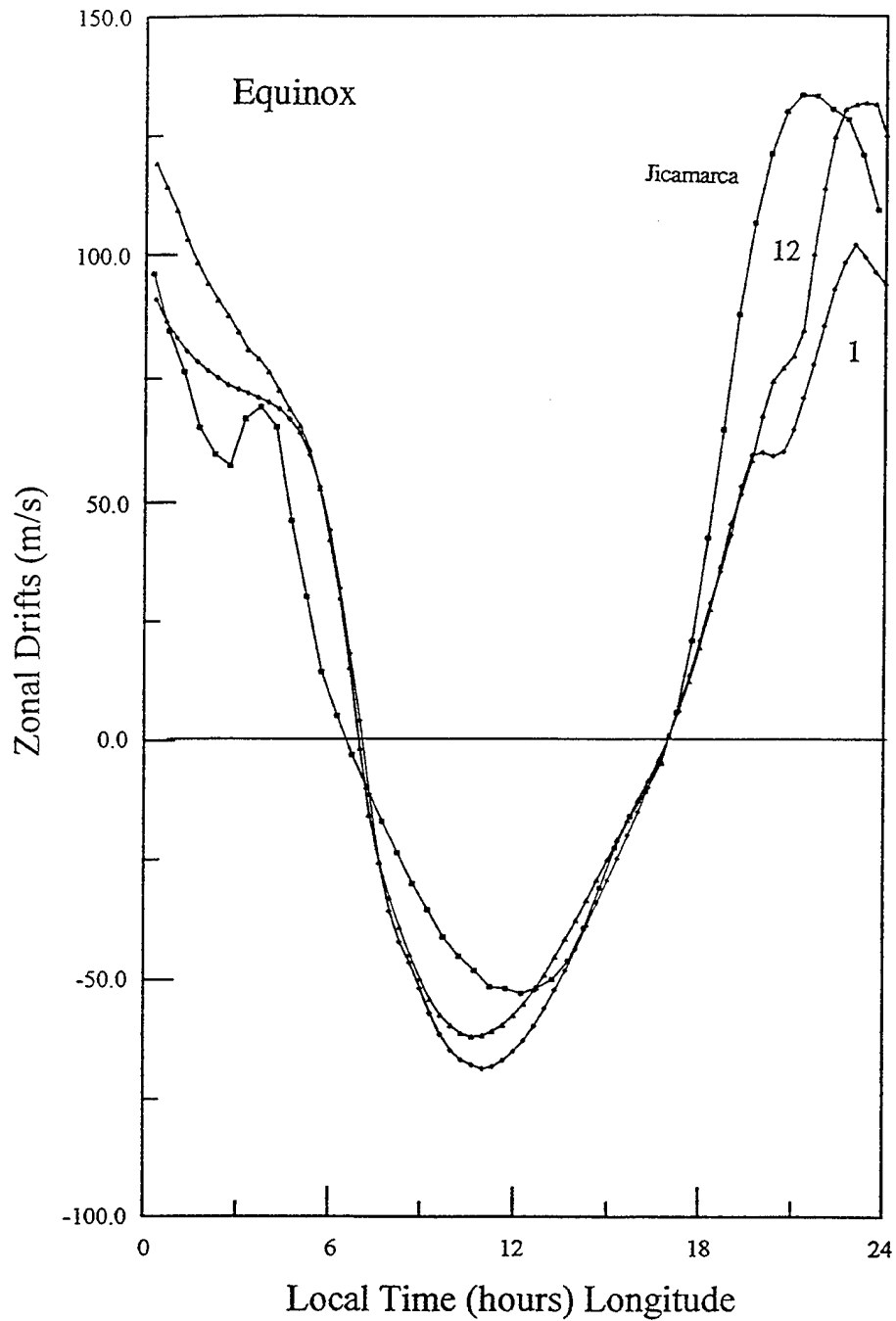
Figure 12. Local time variation of the zonal plasma drifts at 1 and 12 UT calculated by the dynamo model at the Jicamarca location. Also shown are the corresponding radar measurements.

20

6. IFM VALIDATION

During the 3-year contract period, the IFM has been extensively validated using a wide range of data types and for a range of geophysical conditions. A thorough validation of the IFM requires a fairly large data base of measurements, including measurements to define the initial ionosphere, measurements to define the time evolution of geomagnetic activity, and adequate ionospheric observations during the forecast period against which the forecast can be compared. Also, because of the extreme variability of the ionosphere, the validation needs to be conducted for different geomagnetic activity levels, universal times, seasons, and solar flux levels.

To date, the IFM validation has covered the following:

- Ionospheric Domains

    - Low Latitudes
    - Mid-Latitudes
    - High Latitudes ⟶ Northern Hemisphere
    - High Latitudes ⟶ Southern Hemisphere

- Ionospheric Altitudes

    - E-Region
    - F-Region
    - Topside Ionosphere

- Magnetic Activity Conditions

    - Quiet Geomagnetic Activity
    - Moderately Disturbed
    - Major Storm

- Seasonal Conditions

    - Summer
    - Winter
    - Equinox

- Solar Cycle Levels

    - Solar Minimum
    - Solar Maximum

The data in the validation program included the following:

- PRIMO Measurements

    - Solar Minimum - Summer
    - Solar Minimum - Winter
    - Solar Maximum - Summer
    - Solar Maximum - Winter

- DMSP Satellites F8, F9, F10, and F11

    - Simultaneous Measurements
    - January 21-29, 1992   (9 Days)
    - February 11-21, 1992   (11 Days)

- Ionospheric Sounders

    - NGDC SELDADS Data ⟶ 29 Stations
    - NOAA Worldwide Data Base for years 1957-1975 and 1976-1992

- Australian Measurements

    - Four DMSP Satellites
    - Four Ionosondes

- Space Shuttle TSS-1R Flight

    - Ne Along Orbit

- MSX Satellite

    - H^+ and O^+ Along Orbit

6.1 Summary of PRIMO Validation

The PRIMO measurements were relevant to the mid-latitude ionosphere and they were primarily obtained from ionosondes and incoherent scatter radars. At the time the IFM was compared to the PRIMO data base, the thermospheric wind that was contained in the IFM was based on just a simple analytical wind model. From this validation effort we found the following:

1. Solar Minimum - Summer

Both N_mF_2 and h_mF_2 were in good agreement with the measurements during both the day and at night.

2. Solar Minimum - Winter

22

N_mF_2 throughout the daytime and in the early evening was in good agreement with the measurements, but the pre-dawn secondary maximum in N_mF_2 that was observed was not adequately reproduced. Also, the calculated h_mF_2 was a little too high (20 km) compared to the measurements.

3. Solar Maximum - Summer

The daytime N_mF_2 and h_mF_2 that were calculated by the IFM were too high and that led to erroneous nighttime values. As a result of this model-data comparison, it was concluded that the simple analytical wind used in the IFM was not adequate and that the HWM wind (Hedin et al, 1988) would yield more reliable ionosphere predictions.

4. Solar Maximum - Winter

Both the daytime and nighttime N_mF_2 and h_mF_2 values calculated by the IFM were too high. Again, the conclusion was that the problem could be solved by replacing the simple analytical wind with the HWM model.

As a result of the above model-data comparisons, the simple analytical wind in the IFM was replaced with the HWM model and the above model-data discrepancies were resolved.

6.2 Summary of DMSP Validation

The DMSP spacecraft (F8, F9, F10, and F11) were in 800 km orbits, and they provided in situ measurements of electron density along the satellite tracks. In general, the electron density variations along the satellite orbits that were calculated by the IFM were in good agreement with the measured features. In particular, the calculated and observed boundaries of high-latitude features were in good agreement. The IFM was even able to properly model the increase in density observed during a weak geomagnetic storm (1200 UT on 26 January 1992). However, with regard to magnitudes, the DMSP densities were, on average, higher than the modeled densities by 10 to 25%. In addition, the modeled electron density troughs were deeper than observed at certain universal times.

6.3 Summary of SELDADS Validation

The SELDADS measurements correspond to an extensive data base of low-altitude electron density profiles obtained from ionosondes. Upon comparing the IFM E-region densities with the SELDADS data, deficiencies in the calculated electron densities were noticed. These deficiencies were corrected by updating some of the absorption and ionization cross sections, updating the EUV-to-F10.7 dependencies for improved ionization rates due to the solar flux, and adding a solar zenith angle dependence to the nocturnal production rates that are associated with resonantly scattered solar radiation.

With regard to the comparison of the calculated F-region densities with the SELDADS measurements, there was generally good agreement. However, the ionosonde measurements displayed a distinct night-to-night variability in the electron density that was

not reproduced by the IFM. At times, the measurements indicated that the electron density could even increase for a time period during the night. The inability of the IFM to model these features was deduced to be related to the adopted thermospheric wind model (Hedin et al, 1988), which is an empirical model. Hence, it is not expected to correctly describe the night-to-night wind variability.

6.4 Summary of Ionosonde - DMSP Validation

For the period 1-31 January 1991, we were able to acquire an extensive dataset of simultaneous ionosonde and DMSP satellite measurements for the Australian sector. The ionosonde data were acquired at Vanimo, Darwin, Townsville, and Norfolk Island. This dataset allowed us to compare the electron densities calculated by the IFM and the measurements simultaneously at E-region, F-region, and topside altitudes for this period.

At E-region altitudes, ionosonde observations were available only during daylight hours, when f_oE was greater than a megahertz. The daytime variation of the E-layer was essentially the same at all four stations. In this southern (summer) hemisphere, the solar flux was the main factor controlling the variation of the electron density, and winds, electric fields, and interlhemispheric transport had a small effect on the densities. Throughout the entire month, there was excellent agreement between the calculated and measured E-region electron densities, with density differences of less than 10%.

In the F-region, the low magnetic activity, combined with the summer conditions, resulted in a diural variation of N_mF2 that was repeated day-after-day throughout the month at all four stations. The standard deviation of the observed N_mF2 over the 31-day period was 19.5% for Vanimo, 25% for Darwin, 19.4% for Townsville, and 18.5% for Norfolk Island. In general, the calculated and observed N_mF2 agreed to within these standard deviations, with two exceptions. First, at the two lowest latitude stations, Vanimo (located under the anomaly) and Darwin (located under the anomaly shoulder), the IFM densities were too low from prenoon to about 1400 LT. This difference in calculated and measured densities was attributed to the fact that the Fejer empirical model of equatorial electric fields cannot properly account for the day-to-day variation of these dynamo fields, which is not unexpected. Another model-data discrepancy occurred at the most paleward station (Norfolk Island). A comparison of the IFM densities with the Norfolk Island data indicated that the model densities decay too rapidly, and to values that are too low, in the post-midnight to pre-dawn time period. This discrepancy was attributed to either the inadequacy of the Hedin wind model or the lack of a protonospheric exchange flux at 1600 km in the IFM. Further work is needed to correct this deficiency in the IFM.

At the time the Australian ionosonde data were taken, four DMSP satellites (F8, F9, F10, and F11) also measured in situ electron densities at 800 km. However, the satellite data were available for only one day (22 January 1992). The DMSP measurements were extracted when the satellites passed near the Australian stations (they were within $+/- 15^o$ longitude of the stations). The agreement between the modeled and measured electron densities was generally very good. Only near the 2100 LT sector was the agreement between modeled and measured densities not adequate. In this time sector, the calculated electron densities were significantly larger than those measured. The main cause of this discrepancy could not be clearly identified.

24

More details concerning the IFM validation program that was conducted during the 3-year contract period are given in the Appendix.

References

Fejer, B.G., E.R. de Paula, R.A. Heelis, and W.B. Hanson, Global equatorial ionospheric vertical plasma drifts measured by the AE-E satellite, *J. Geophys. Res.*, 100, 5769-5776, 1995.

Fuller-Rowell, T.J., and D. Rees, A three-dimensional, time dependent, global model of the thermosphere, *J. Atmos. Sci.*, 37, 2545-2567, 1980.

Hardy, D.A., M.S. Gussenhoven, and E. Holeman, A statistical model of auroral electron precipitation, *J. Geophys. Res.*, 90, 4229-4238, 1985.

Hedin, A.E., MSIS-86 Thermospheric Model, *J. Geophys. Res.*, 92, 4649-4662, 1987.

Hedin, A.E., N.W. Spencer, and T.L. Killeen, Empirical global model of upper thermosphere winds based on Atmosphere and Dynamics Explorer satellite data, *J. Geophys. Res.*, 93, 9959-9978, 1988.

Heppner, J.P., and N.C. Maynard, Empirical high-latitude electric field models, *J. Geophys. Res.*, 92, 4467-4489, 1987.

Richmond, A.D., et al, An empirical model of quiet-day ionospheric electric fields at middle and low latitudes, *J. Geophys. Res.*, 85, 4658-4664, 1980.

APPENDIX

Validation Presented At

October 24, 1994
Models Review Meeting
Colorado Springs, Colorado

IFM1 VALIDATION

- STREAMLINED VERSUS FULL MODEL

- PHYSICS & CHEMISTRY

- PRIMO COMPARISONS

SUMMARY OF PRIMO VALIDATION

- ### Solar Minimum - Summer

  Both NmF2 and hmF2 are in very good agreement with observations. Indeed, agreement appears to be better than the TDIM results.

- ### Solar Minimum - Winter

  NmF2 through daytime and early evening is good but the predawn secondary maximum is not well reproduced. HmF2 may be a little high (≈ 20 km). Comparable to TDIM results.

- ### Solar Maximum - Summer

  Daytime NmF2 and hmF2 are too high. Default wind has no downward drift on dayside. Such a wind would lower and reduce NmF2. With a lower sunset NmF2 an automatically improved nighttime NmF2 would be achieved. Need to implement MSIS-Wind model which has a daytime wind.

- ### Solar Maximum - Winter

  Both daytime and nightime NmF2 and hmF2 are too large. Nighttime wind is too strong. Replacing wind with MSIS-WIND would reduce nightime wind and introduce a daytime wind that would lower layer and decrease daytime NmF2.

Phase 3 IFM VALIDATION OVERVIEW

- Forecast starts from a full specification of the ionosphere, obtained from PRISM, or from an IFM COLD START.

- Forecast needs the time evolution of:
    - geomagnetic activity (Kp)
    - auroral precipitation
    - magnetospheric electric field

- Forecast provides a full specification of the ionosphere.

- Validation data base requires :

    a)   ionosphere defined at start time,

    b)   time evolution of geomagnetic activity and associated magnetospheric inputs,

    c)   and adequate ionospheric observations during forecast period against which to compare.

- Validation needs to be done for various conditions:
    - seasonal
    - solar cycle
    - Universal Time
    - geomagnetic activity levels

INITIAL CONDITION

either   use PRISM output at start time, which requires:

DISS   ionospheric electron density profiles

DMSP (IES)   topside plasma parameters

DMSP (J/4)   auroral precipitation and boundaries

$Kp/F_{10.7}$ geomagnetic activity and solar conditions

Note: this can be augmented with other ionospheric sounder data (ionosondes, Incoherent Scatter Radars (ISR), etc)

or   use IFM in Cold Start mode, which would require as little as

$Kp/F_{10.7}$ geomagnetic activity and solar conditions over the prior 6 hours.

Note: However, to improve the start time conditions the following information would be of value:

DISS
DMSP (IES and J/4)
other ionospheric sounders
IMF if available

FORECAST CONDITIONS

Level 0 Zeroth order run scenario

Kp forecast based upon persistence/forecast

Data required: none

Level 1 Knowledge of the Kp evolution

by using data from a historic data period.

Data required: Kp(t), $0 \leq t \leq$ end forecast

Level 2 Knowledge of the evolution of Kp as well as
magnetospheric inputs

Data required: Kp (t), $0 \leq t \leq$ end forecast
DMSP (IES)   electric field
DMSP (J/4)   aurora

VALIDATION DATA BASE

- Should include winter-equinox-summer.
  Should include storm and quiet geomagnetic conditions.
  Solar cycle is difficult, but many instruments were running
  during the last solar maximum.

- Need: a) DISS and other ionospheric soundings.
           b) DMSP and other magnetospheric inputs.

- From December 1991 through April 2, 1992 there were 4
  DMSP satellites; F8, F9, F10, and F11.
  (Then there were 3 through August 2, 94; F8, F10, F11).

- Quiet periods

December 5-9, 1991	4 days
January 21-26, 1992	6 days
February 11-16, 1992	6 days
April 9-14, 1992	6 days

- Disturbed periods

February 17-21, 1992	5 days(major storm)
January 27-29, 1992	3 days(moderately disturbed)
April, 15-16, 1992	2 days(isolated disturbance)

- Prioritization of combined periods

1. January 21-29, 1992	9 days
2. February 11-21, 1992	11 days
3. April 9-16, 1992	8 days
4. December 5-9, 1992	4 days

- These are subsets of the 5 month long data base requested
  in IFM quarterly presentation on 2 February, 1994.

Validation Presented At

May 3, 1995
Models Review Meeting
Colorado Springs, Colorado

VALIDATION DATA BASE

- Should include winter-equinox-summer.
  Should include storm and quiet geomagnetic conditions.
  Solar cycle is difficult, but many instruments were running
  during the last solar maximum.

- Need: a) DISS and other ionospheric soundings.
           b) DMSP and other magnetospheric inputs.

- From December 1991 through April 2, 1992 there were 4
  DMSP satellites; F8, F9, F10, and F11.
  (Then there were 3 through August 2, 94; F8, F10, F11).

- Quiet periods
December 5-9, 1991	4 days
January 21-26, 1992	6 days
February 11-16, 1992	6 days
April 9-14, 1992	6 days

- Disturbed periods
February 17-21, 1992	5 days(major storm)
January 27-29, 1992	3 days(moderately disturbed)
April, 15-16, 1992	2 days(isolated disturbance)

- Prioritization of combined periods

1. January 21-29, 1992	9 days
2. February 11-21, 1992	11 days
3. April 9-16, 1992	8 days
4. December 5-9, 1992	4 days

- These are subsets of the 5 month long data base requested
in IFM quarterly presentation on 2 February, 1994.

VALIDATION PERIOD 1

- January 21-29, 1992 (9 days)

- Winter in the Northern Hemisphere

- Quiet 6 days followed by 3 slighty disturbed days

- Data Sets Obtained

<u>DMSP SSIES</u> from Phillips Laboratory, Hanscom AFB supplied by Peter Sultan. Data from satellites F8, F9, F10, and F11 were available on each day during the study period. A total of 36 files (one per day and satellite) for the scintillation meter and another 36 for the drift meter were obtained. This corresponds to about 540 MBytes of data.

<u>Ionospheric Sounders</u> from NGDC supplied by Ray Conkright. The entire SELDADS data base for the Month of January 1992 was supplied. This does include certain DISS sounders that were operational. A total of 43 stations, but only 29 have useable data.
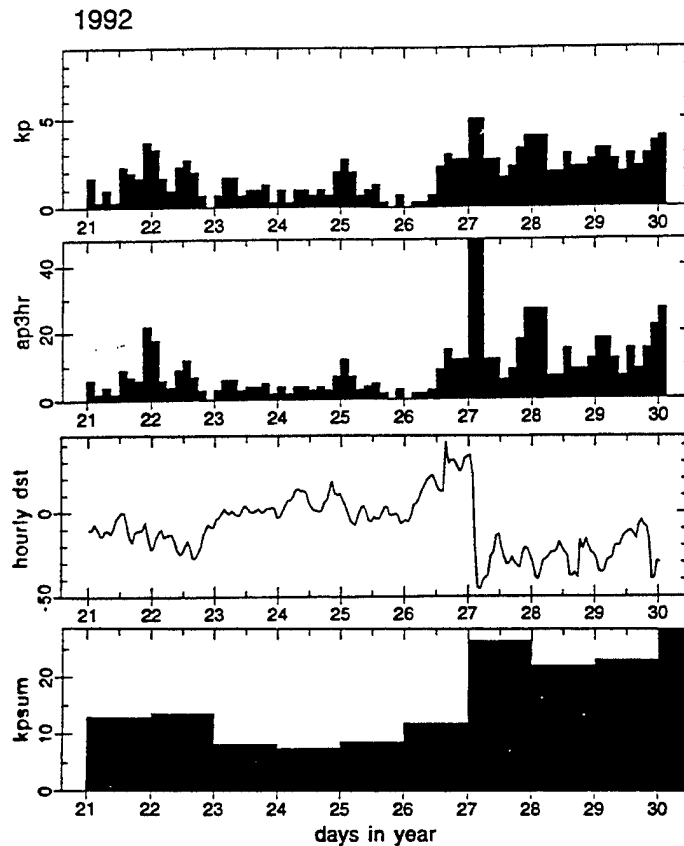
1992

- Kp averages about 1 for the first 6 days.

- ap averages about 5 for the first 6 days.

- Kp and ap increase rapidly at about 0000 UT on the 27 January 1992.

- Dst drops by 80γ at this time.

- The last 3 days are moderably disturbed.

- Kp averages about 3 for the last 3 days.

1992
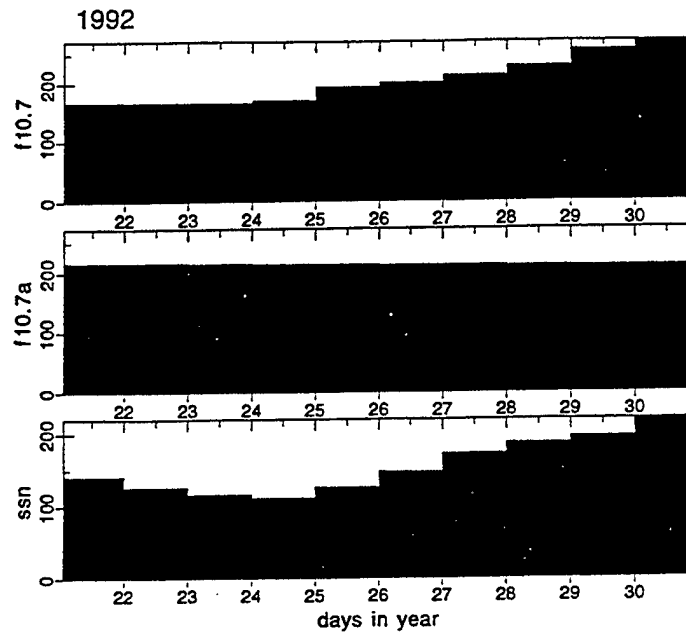
- F10.7 steadily increases from 160 units to over 250 units on the ninth day.

- This corresponds to going from a solar medium level to a high solar maximum level in 9 days.

- The sunspot number almost doubles in this time period.

- Is this a problem? Empirical models tend to be based on "monthly" medians and averages.

DMSP SSIES   Validation Period 1 Data Base

- Four DMSP satellites were in orbit F8, F9, F10, and F11 and both the scintillation and drift meter data was obtained.

- At this time only the electron density deduced from the SSIES scintillation meter has been compared with the model.

- DMSP electron density data is available every second along the satellite track. This corresponds to a distance ~ 7.5 km.

- In a nearly polar orbit this distance corresponds to latitude. The typical IFM latitudinal bin width ranges from 2° to 5°. Which at an altitude of 840 km corresponds to distances for 250 to 630 km respectively.

- There are between 33 and 84 DMSP electron density measurements per IFM bin for a perfectly meridional satellite orbit. The actual number ranges from a few to over 100.

- Hence the DMSP electron density data is averaged to produce mean observed electron densities, one per IFM bin crossed by the satellite.

- Magnetic local time and polar cap distribution of orbit trajectories for one day is shown in the following 2 pages.
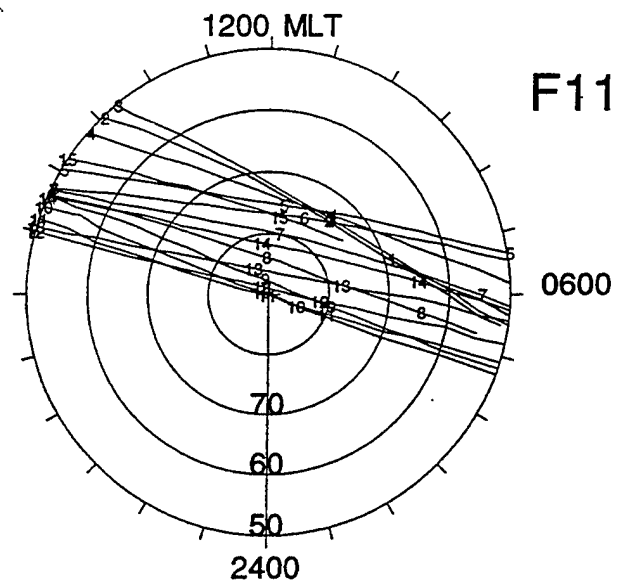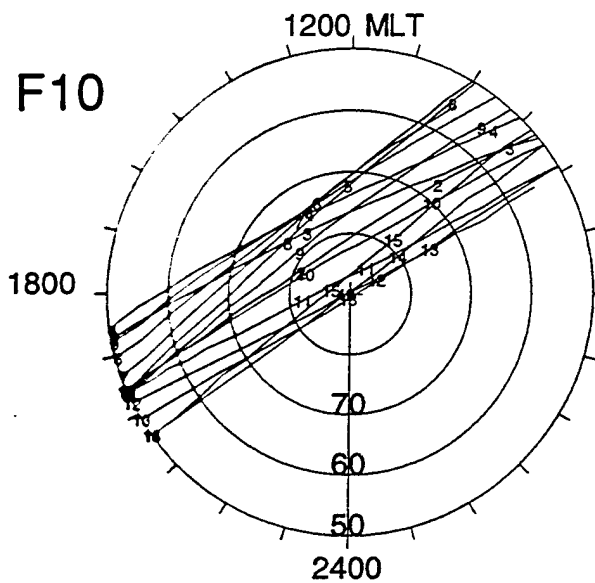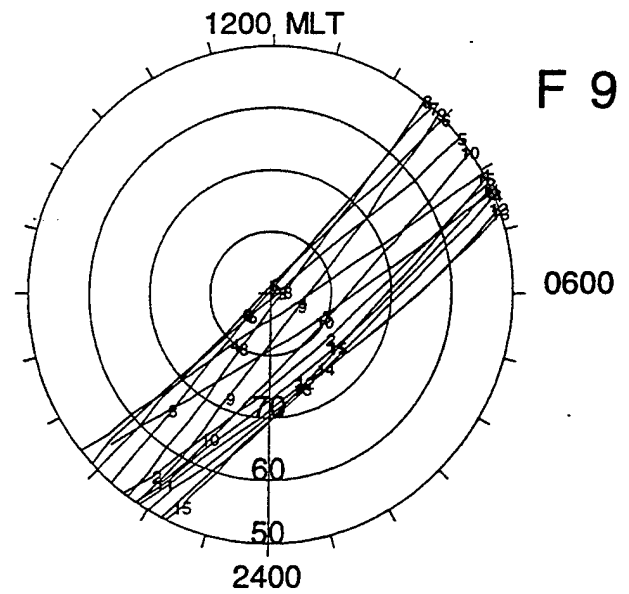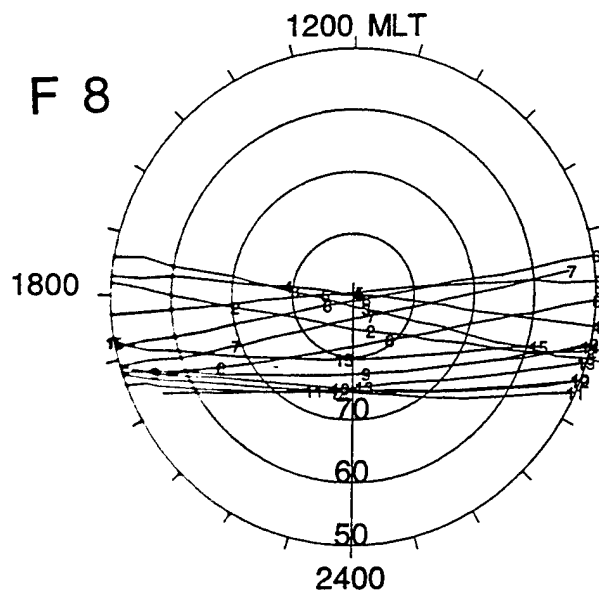
- DMSP northern hemisphere orbits (labeled sequentially 1 through 15) for 24 hours during validation period 1.

42

- DMSP southern hemisphere orbits (labeled sequentially 1 through 15) for 24 hours during validation period 1.

selected orbit: 4
year:1992 month: 1 day:22

ORBIT # 5 PHASE ANGLE

45
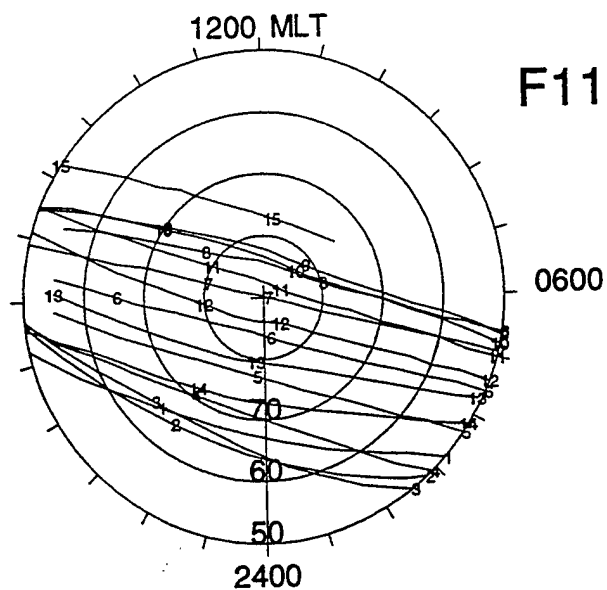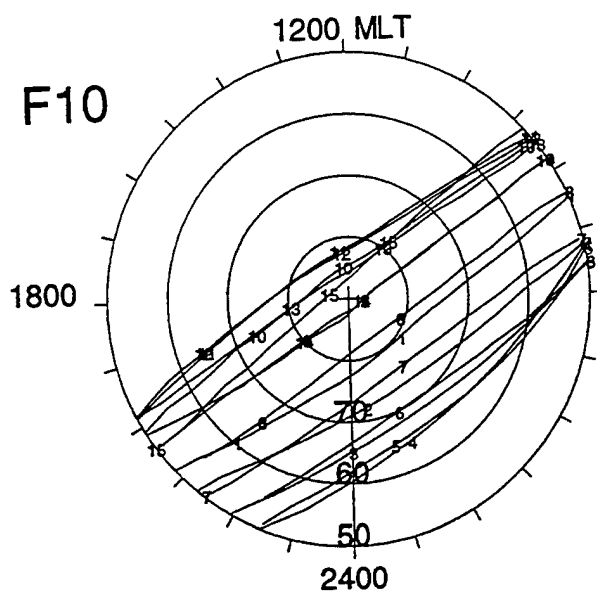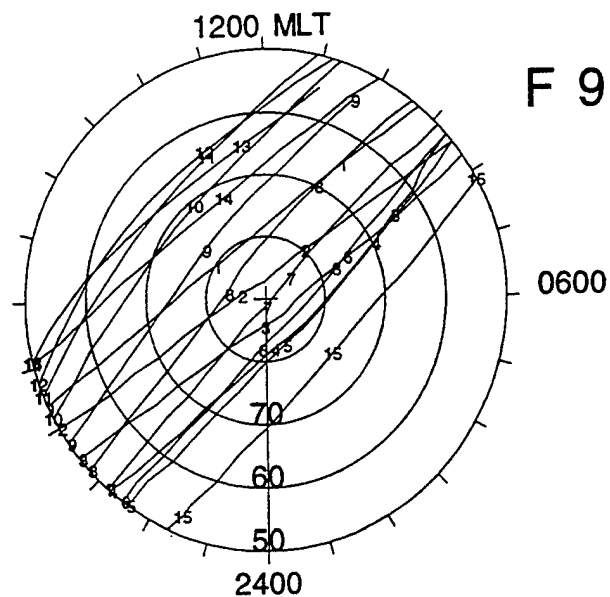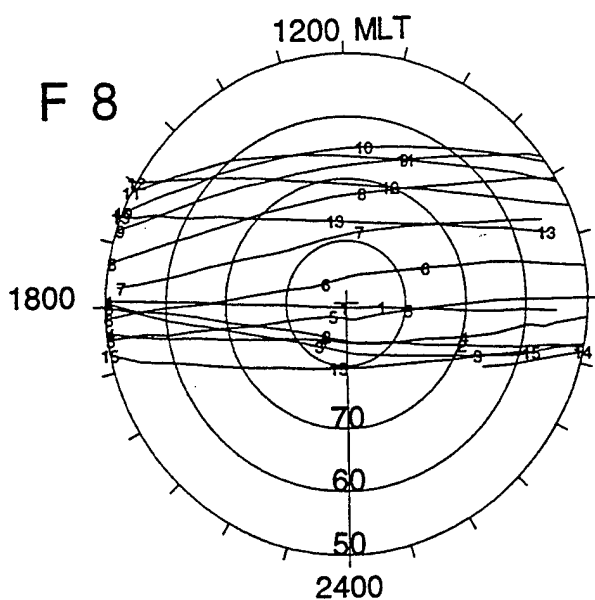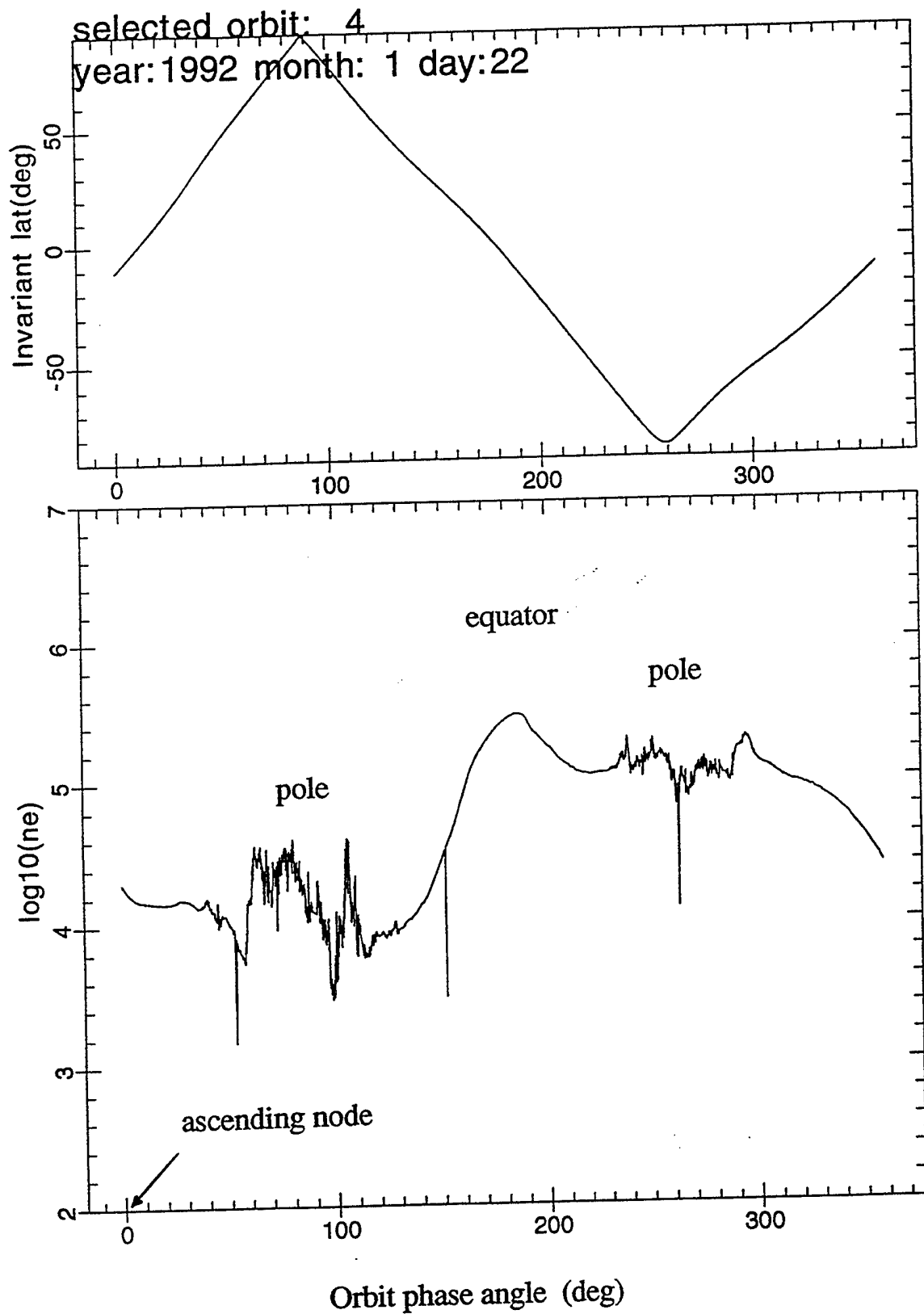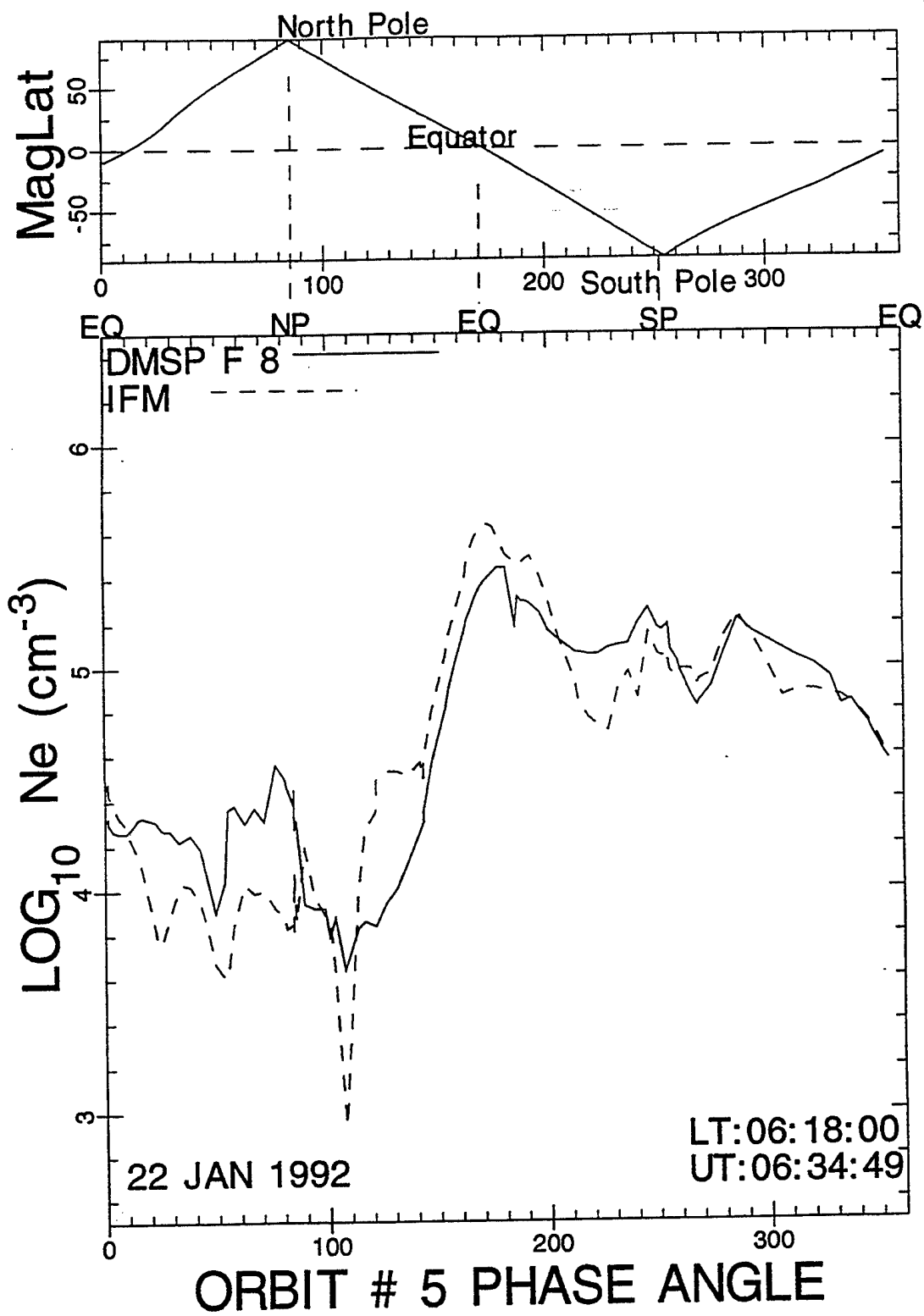
- The electron density at 840 km varies by 2 orders of magnitude over an orbit.

- Highest densities for F8 are at the post 1800 MLT equator.

- Lowest densities are in the winter polar region.

- IFM density structure correlate well with that observed.

- Over the 2 orders of magnitude range the absolute densities track those observed very well. There are some systematic differences.

- The following comparison figures will be used to illucidate some of these effects.

- Empirical precipitation fluxes along the F8 orbit (prior figure) are given below to aid in making auroral region comparisons. Note this auroral variation is different for each pass and each DMSP satellite.

Hardy et al [1987] oval

simulated aurora along DMSP F8 orbit #5

phase angle (0 to 360 deg)

North Pole

MagLat

Equator

South Pole

EQ   NP   EQ   SP   EQ

DMSP F 9 ———

IFM − − −

LOG$_{10}$ Ne (cm^{-3})

LT:09:18:00
UT:11:18:19

22 JAN 1992

ORBIT # 8 PHASE ANGLE

North Pole

MagLat

Equator

North Pole

EQ   NP   EQ   SP   EQ

DMSP F11 ———
IFM — — —

LOG_{10} Ne (cm^{-3})

LT:16:22:00
UT:01:14:22

22 JAN 1992

ORBIT # 2 PHASE ANGLE
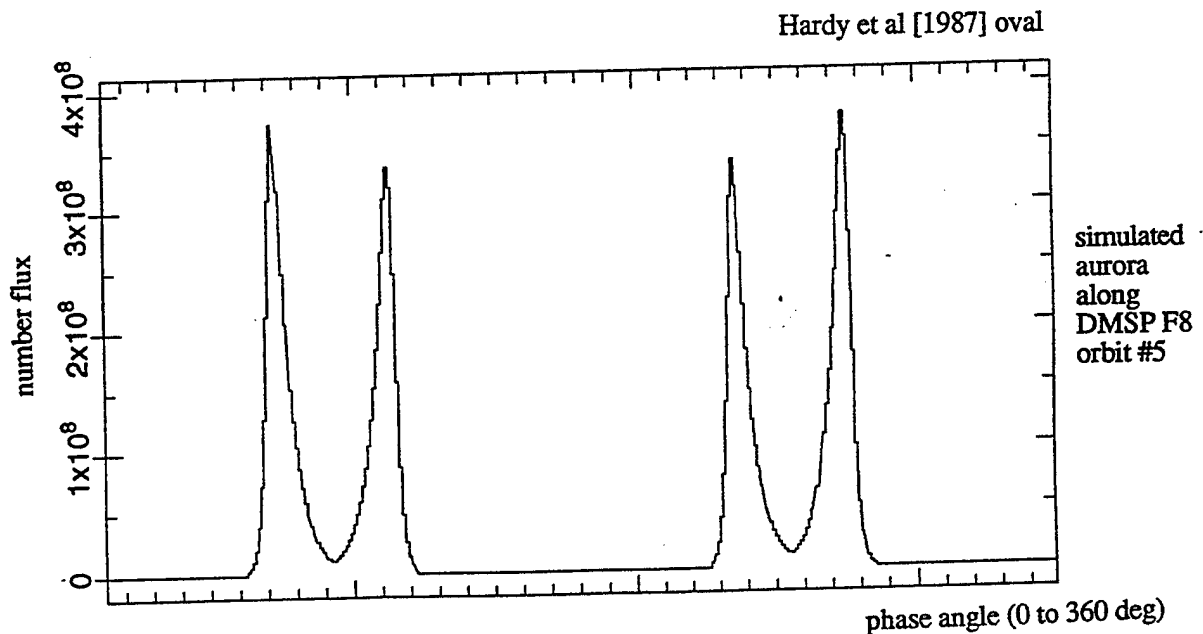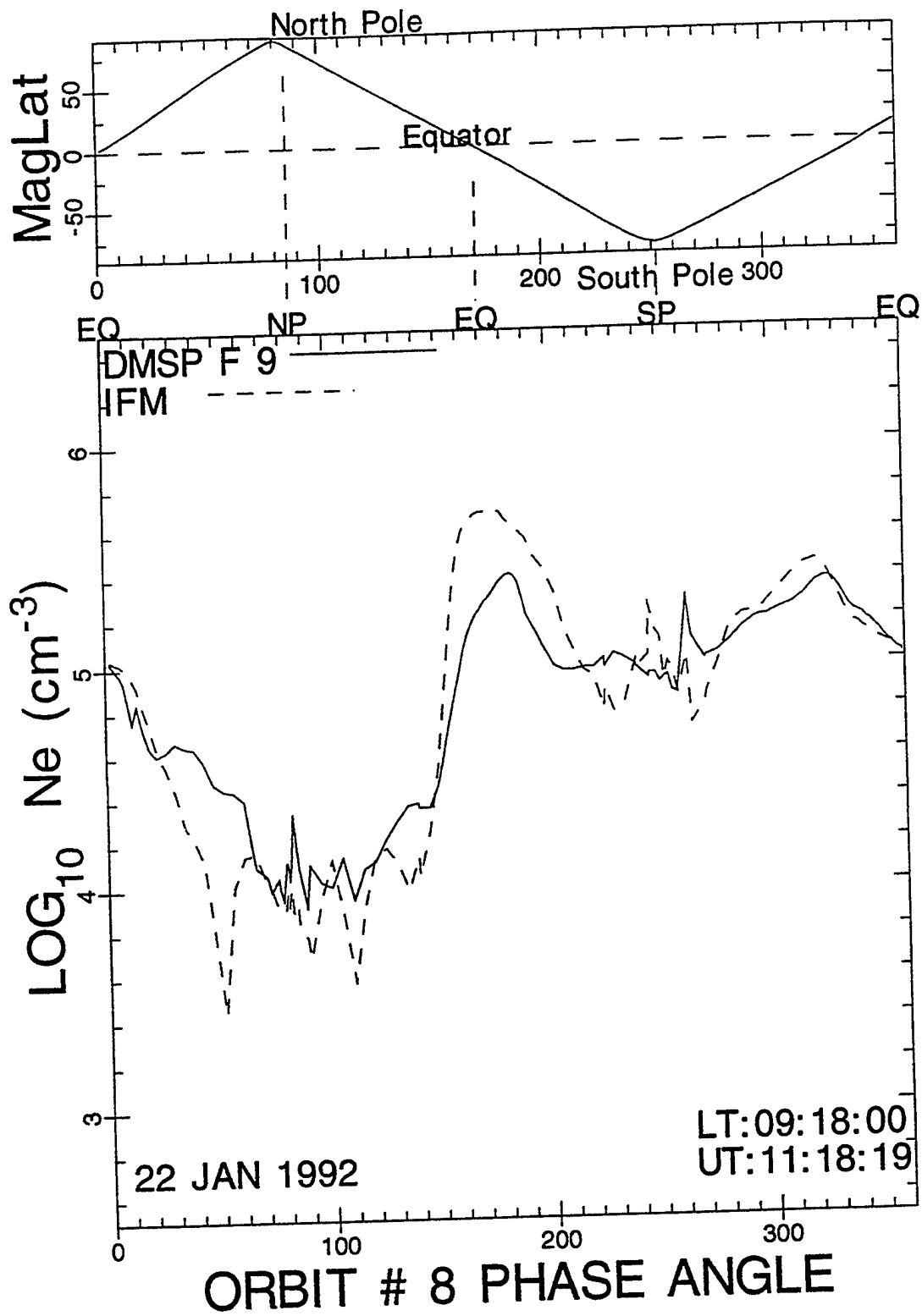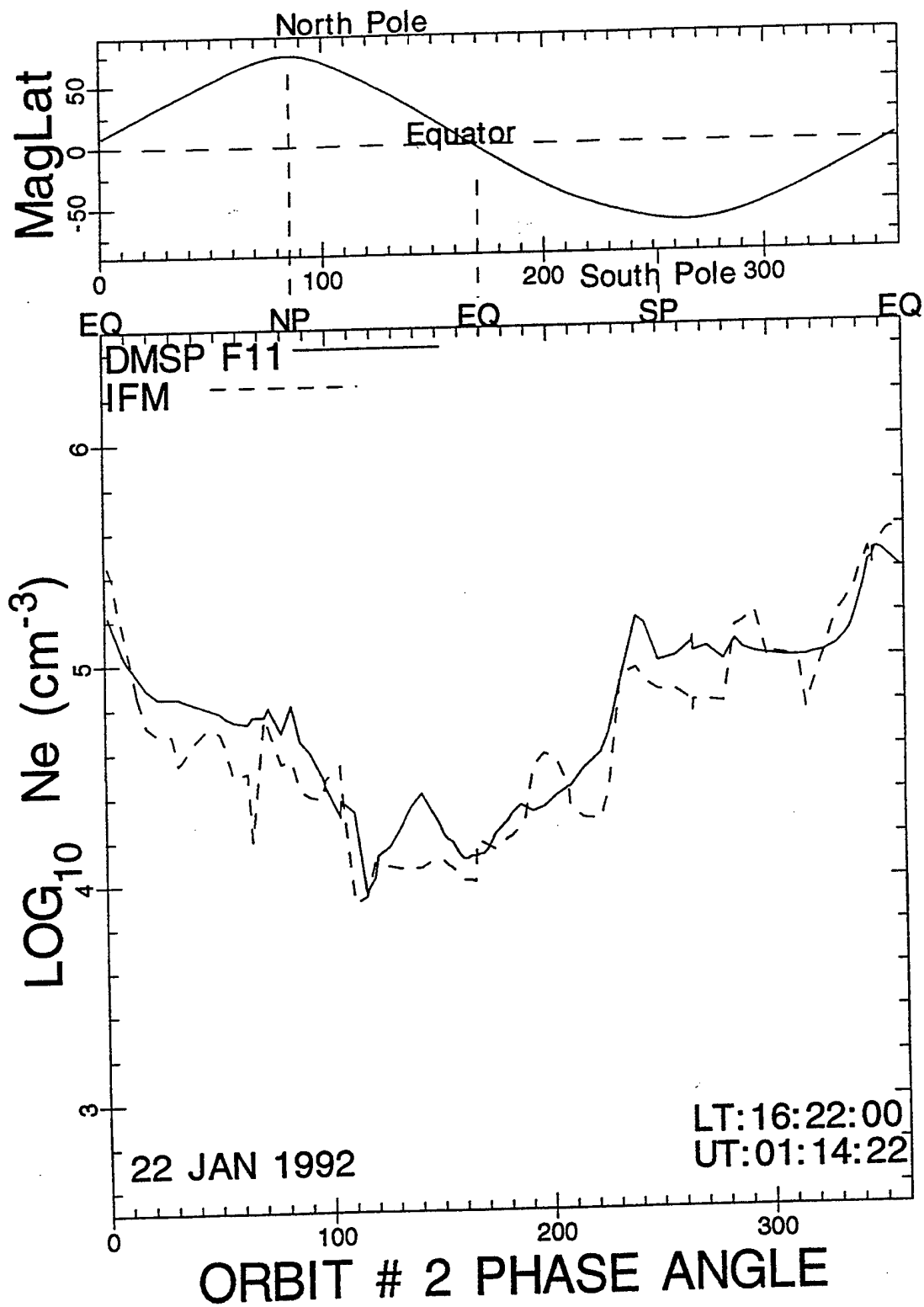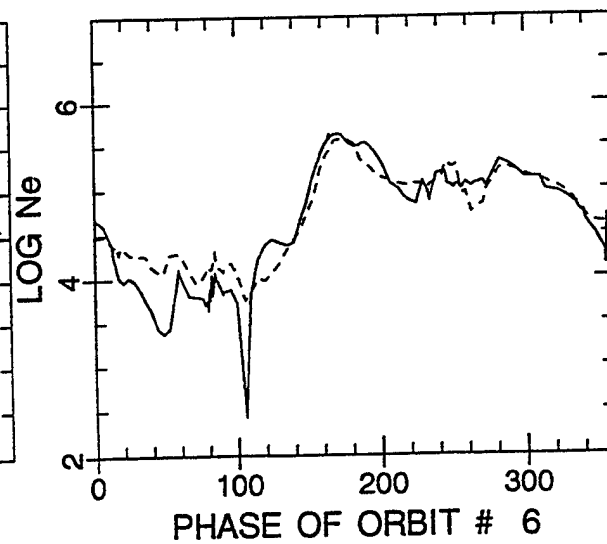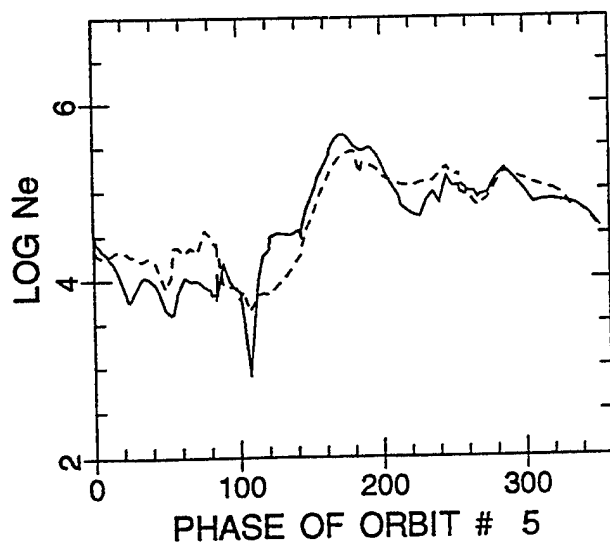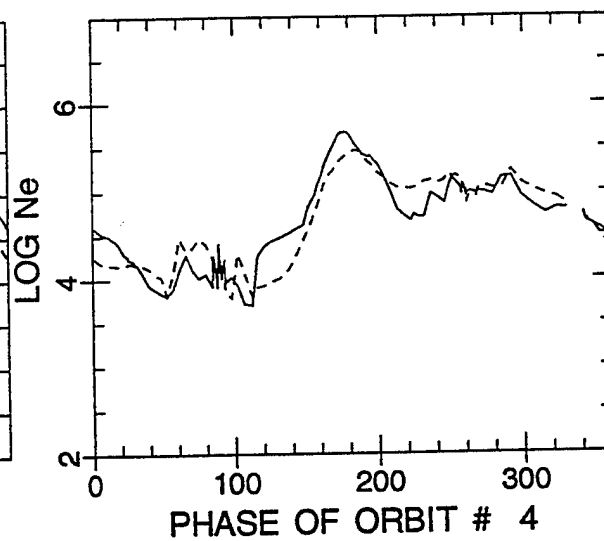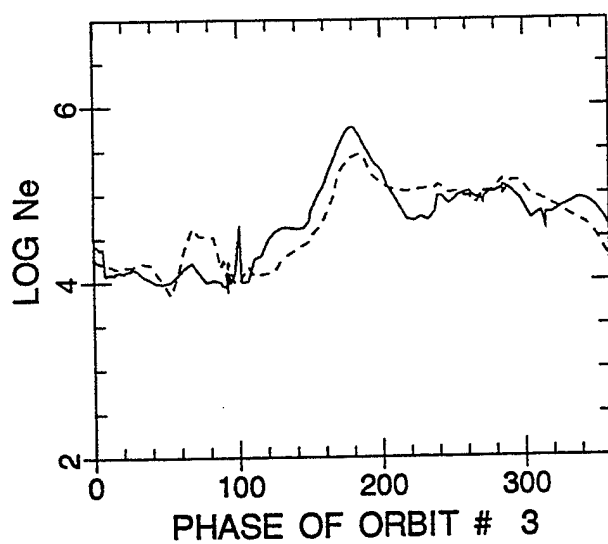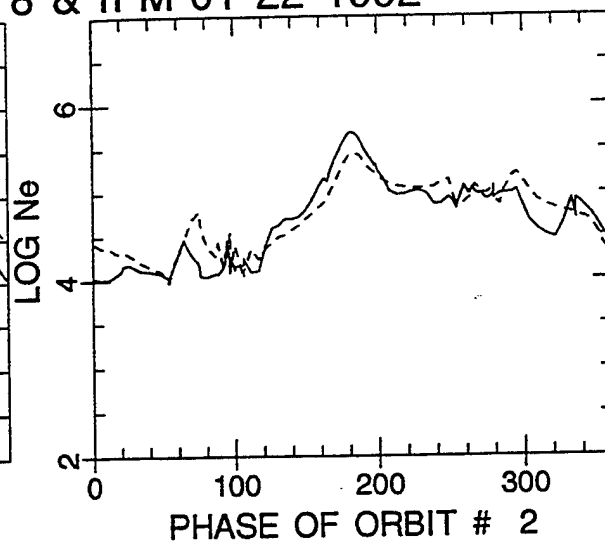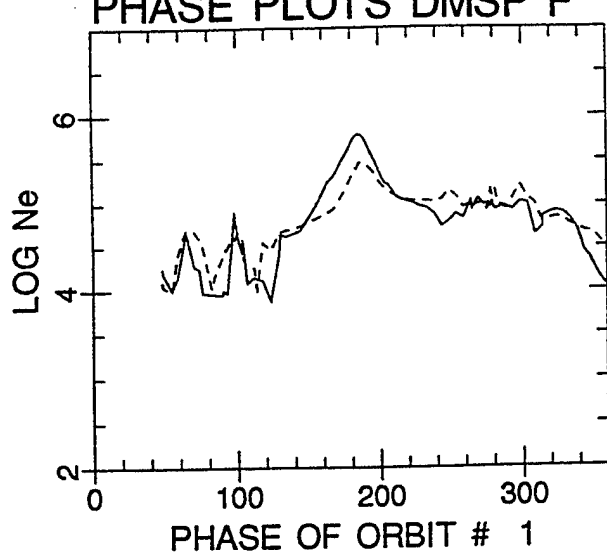
PHASE PLOTS DMSP F 8 & IFM 01 22 1992
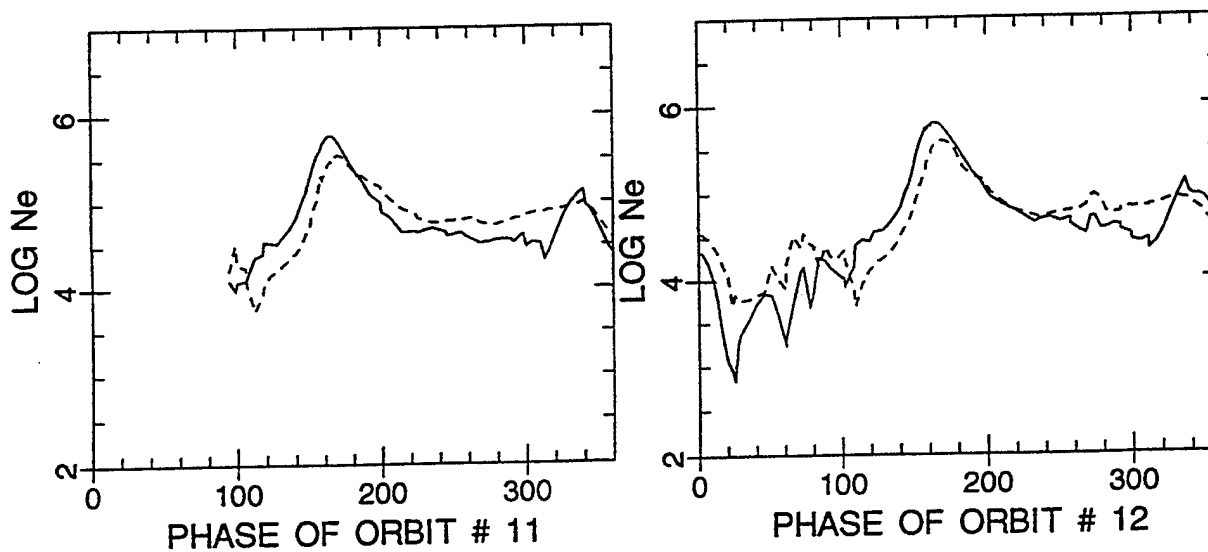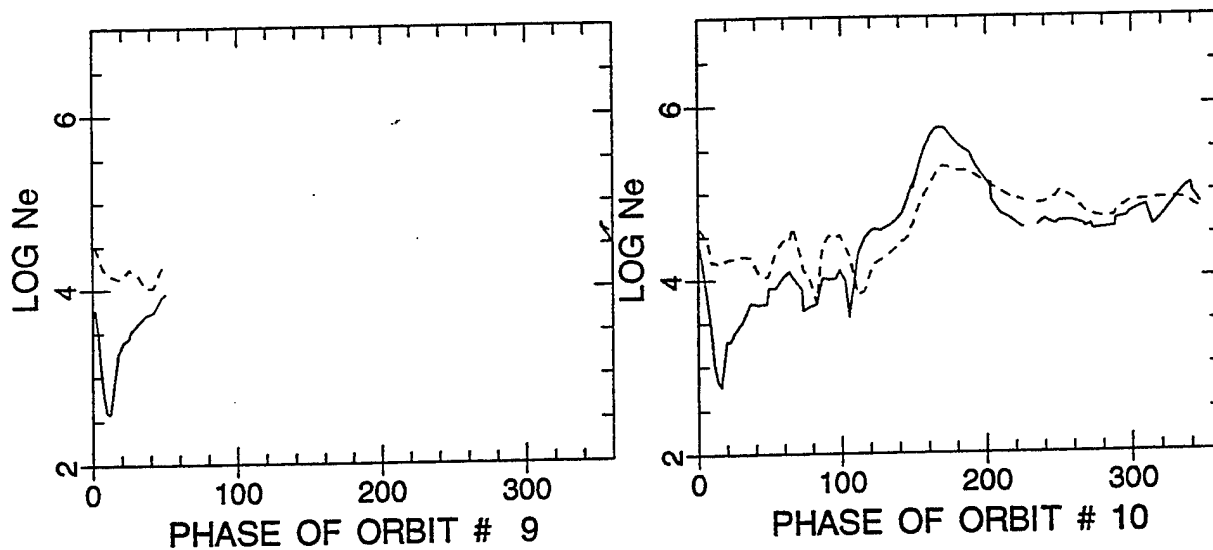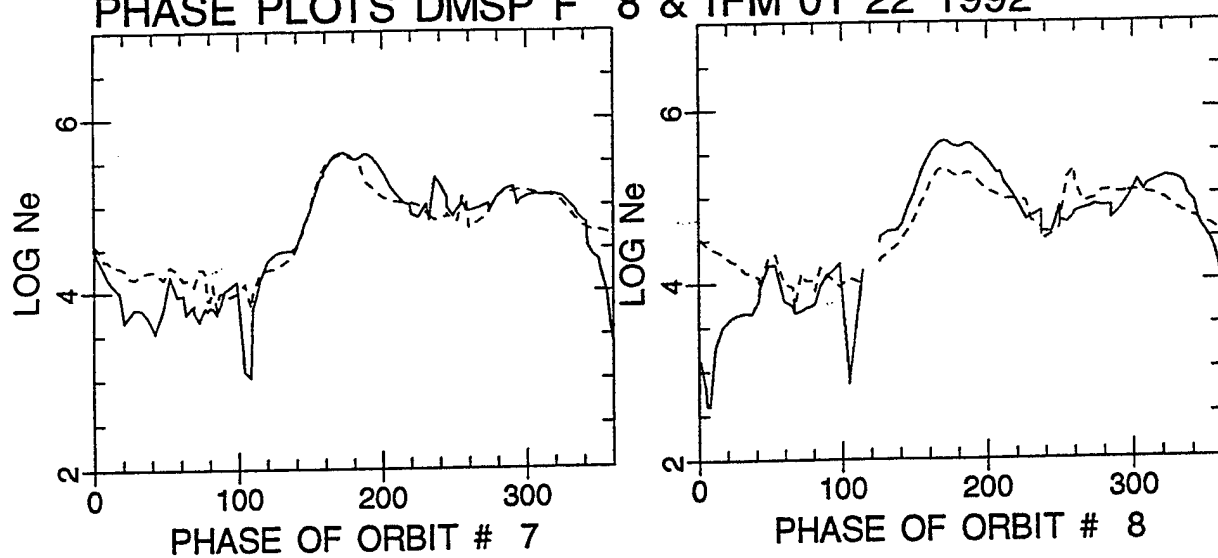
PHASE PLOTS DMSP F 8 & IFM 01 22 1992
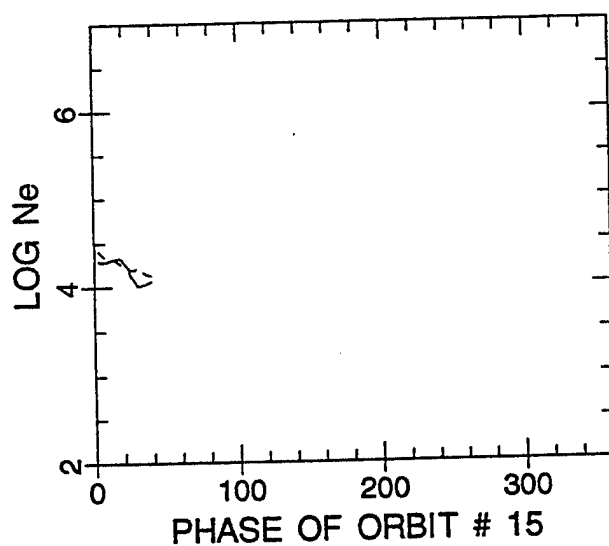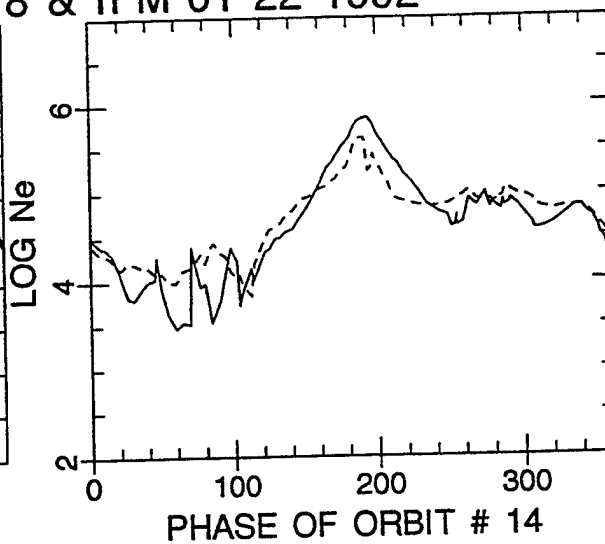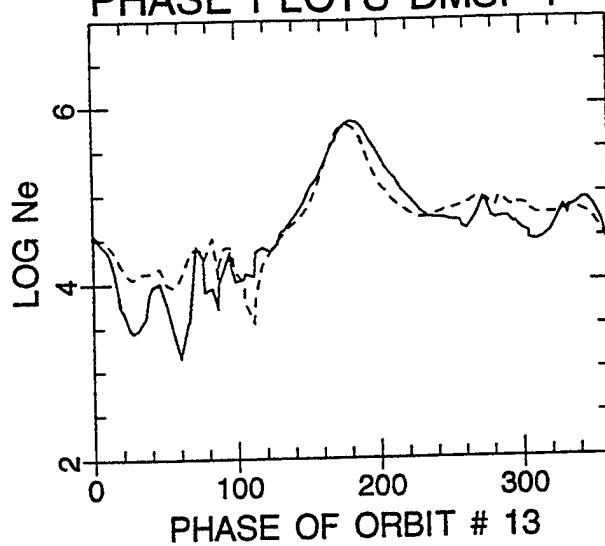
Southern Hemisphere (poleward of -50 deg)
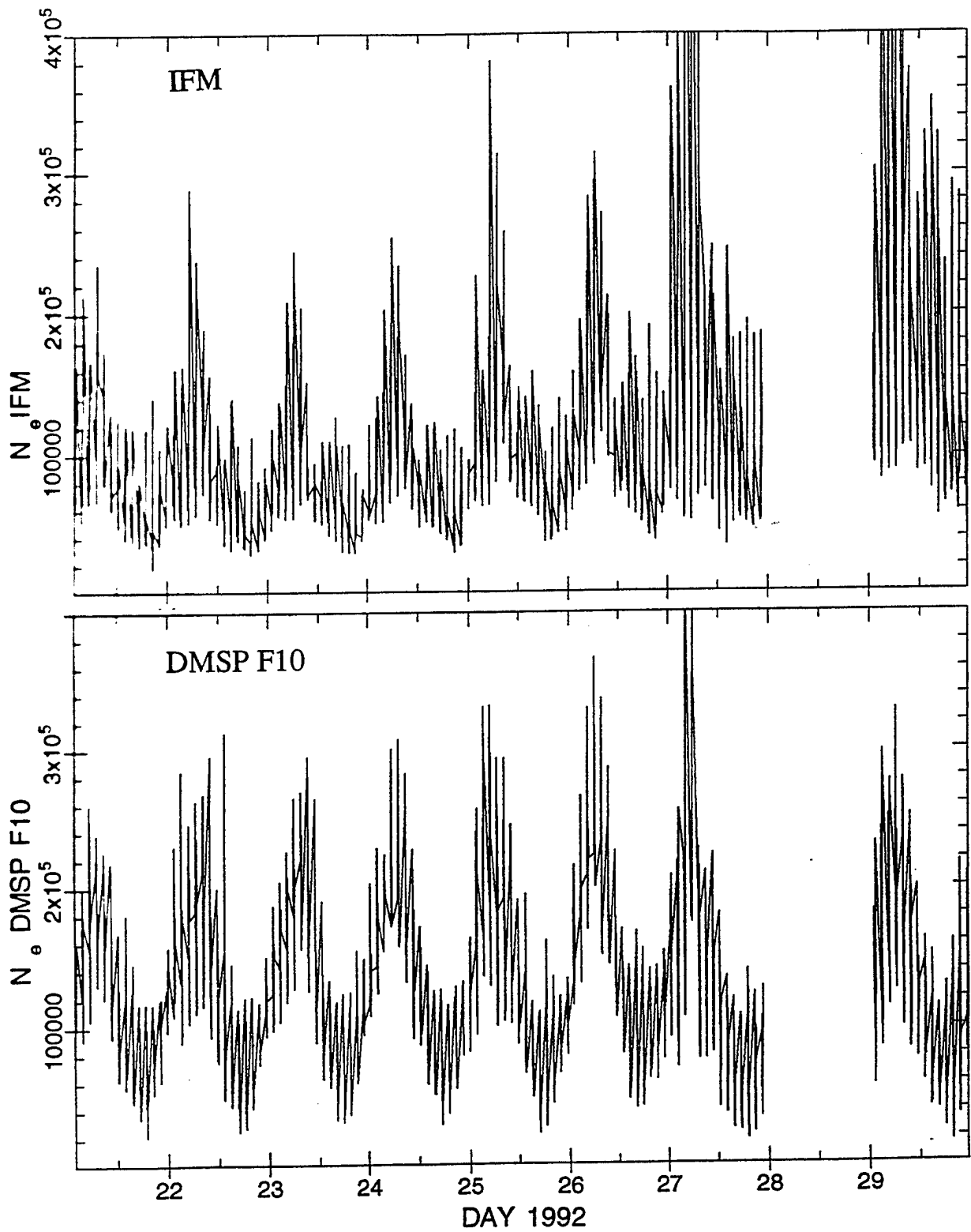
Southern Hemisphere (poleward of -50 deg)

IFM

orbital averaged data

N_e IFM

DMSP F10

N_e DMSP F10

DAY 1992

Northern Hemisphere (poleward of 50 deg)

54
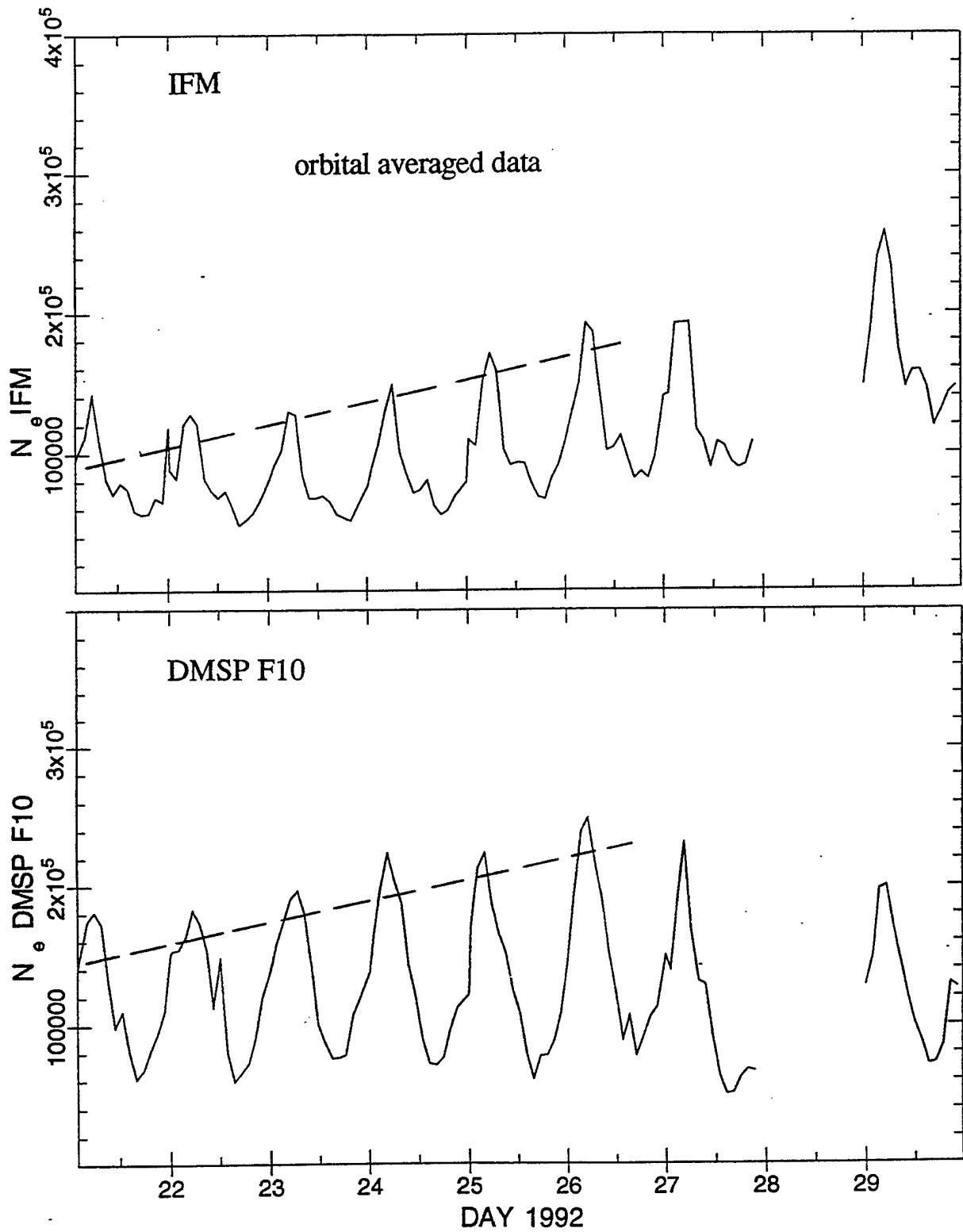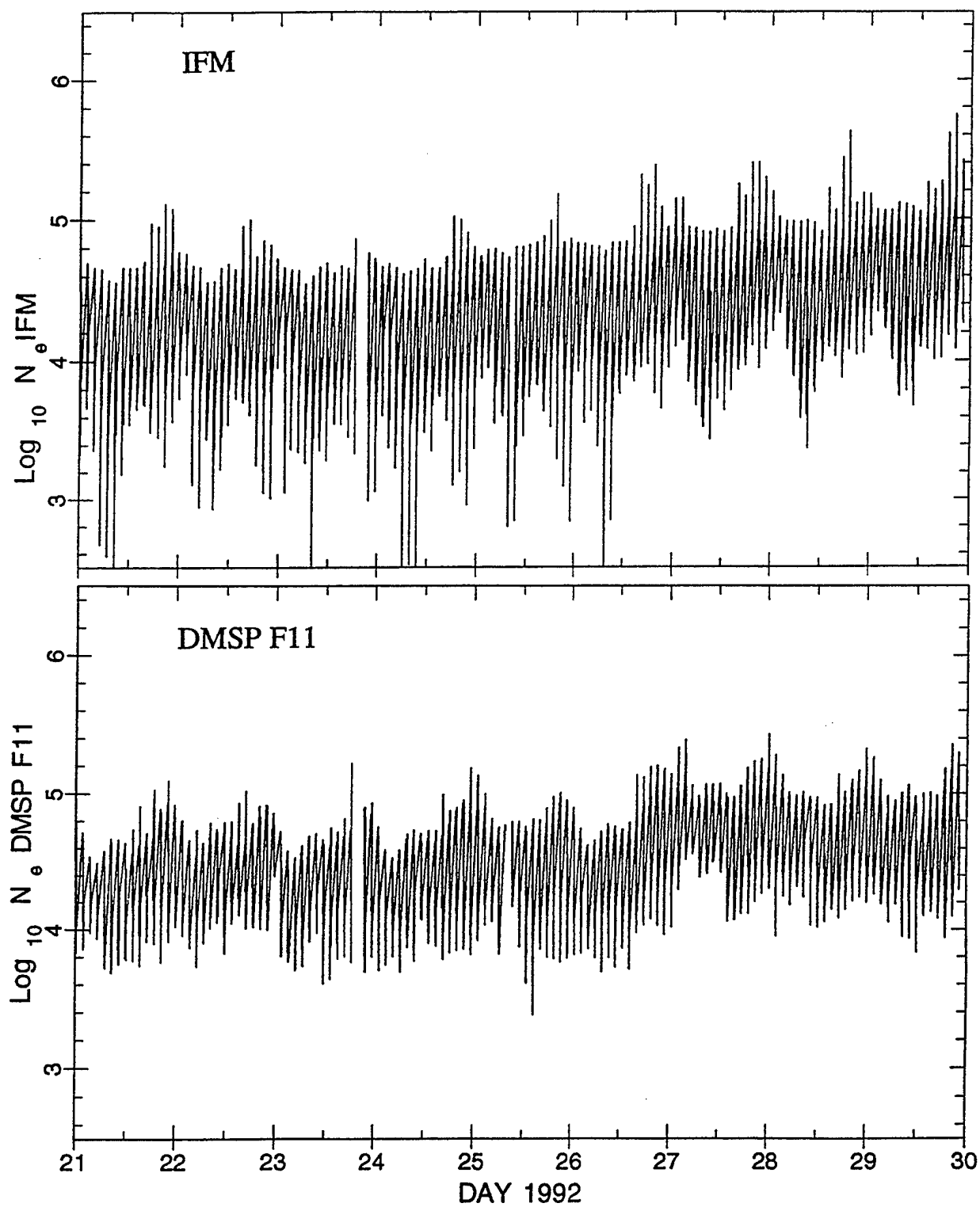
Northern Hemisphere (poleward of 50 deg)
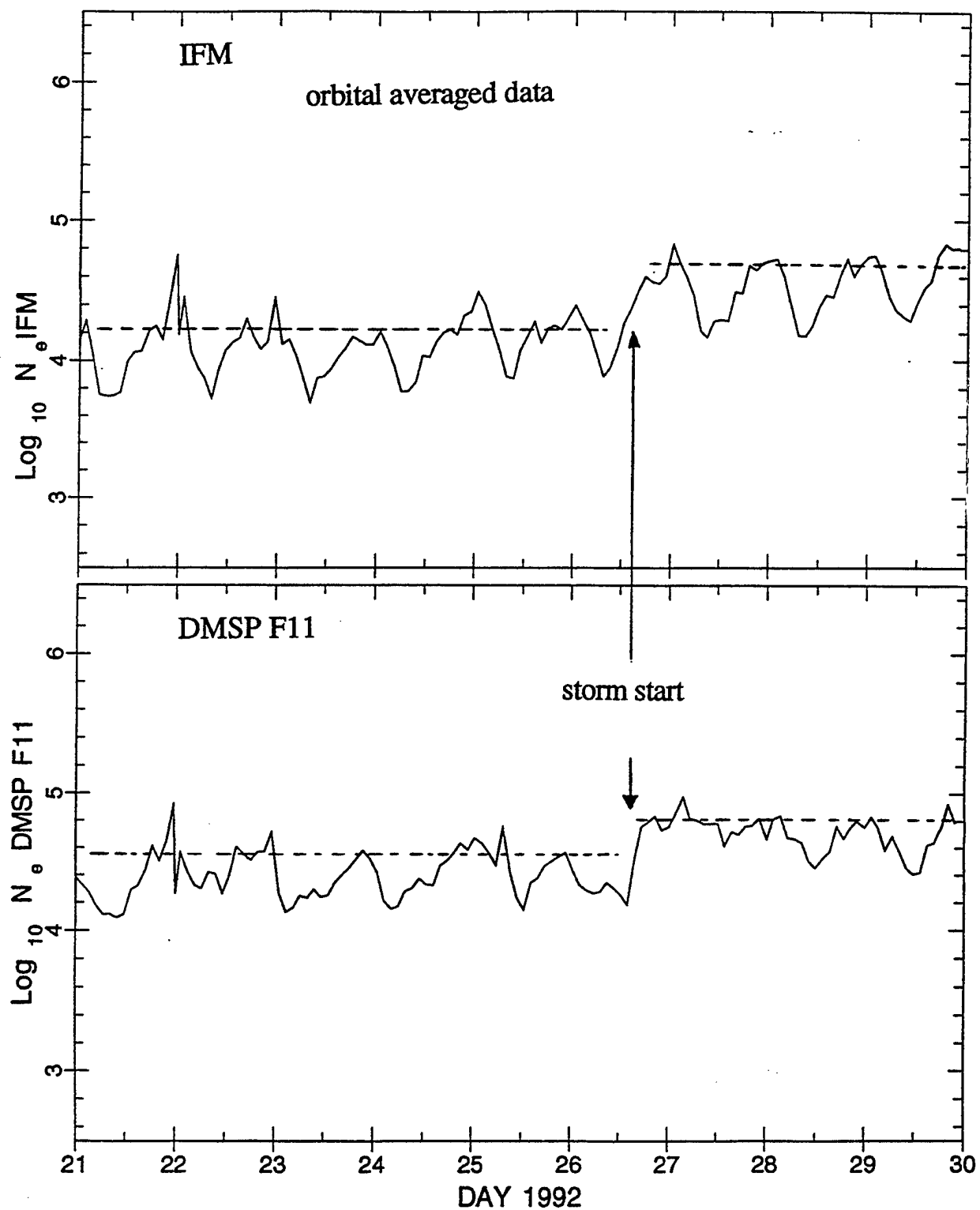
Entire Validation Period 1 N_e Comparison

- Compare all nine days (use linear and log_{10} plots) in the high latitude regions.

Linear Plots

- Southern hemisphere, summer, densities about $10^5 cm^{-3}$

  1) density shows about a factor of three orbital variation,
  2) also a factor of two "UT" daily variation, and
  3) an increase of 10's of % over 6 quiet days.

Log10 Plots

- Northern hemisphere, winter, densities about $2 \times 10^4 cm^{-3}$

  1) density shows about a factor of ten orbital variation,
  2) also a factor of 3 to 4 "UT" daily variation, and
  3) a storm related increase at about 1200UT on 26th.

- The phase of the UT daily variation is the same for the model and the observations. It is a combination of the satellite orbits drifting over a large polar region in the magnetic frame and an inherent ionospheric UT dependence.

DMSP - IFM Summary

- DMSP densities are on the average higher than IFM

- The difference range from 10 to 25%

- Orbital features are well modeled

- Equator density difference varies with UT

- IFM has deeper troughs, at certain UTs, than observed

- Boundaries of high latitude features correlate well

- The weak storm at 1200UT on 26 January 1992 is seen as an increase in density by DMSP and in the IFM simulation

- Mid latitude absolute densities are often different

Ionosonde - IFM comparison

- January 21-29, 1992 (9 days), These days were part of the January 1992 SELDADS data base obtained from NGDC, Ray Conkright.

- Five stations at roughly equal longitudes were compared

  1) Poitiers, France   {46 latitude, 0 longitude}
  2) Tomsk, Russia   {56, 85}
  3) Magadan, Russia   {60, 151}
  4) Eielson AFB, USA {74, 213}
  5) Wallops Is., USA {37, 285}

- Selected northern hemisphere midlatitudes

- Unfortunately, the Pacific sector was not well represented by ionosonde data. Used Eielson AFB which is in Alaska and hence is not midlatitudes.

- For this initial comparison have only used the F-region critical frequency, f_oF_2.

Wallops Island, USA (37N, 285E)

day (January, 1992)

Figure showing f_oF_2 (MHz) versus day (January, 1992) for three locations: Poitiers, France; Tomsk, Russia; and Magadan, Russia. Comparison of IFM (dashed) and observed (solid) values.
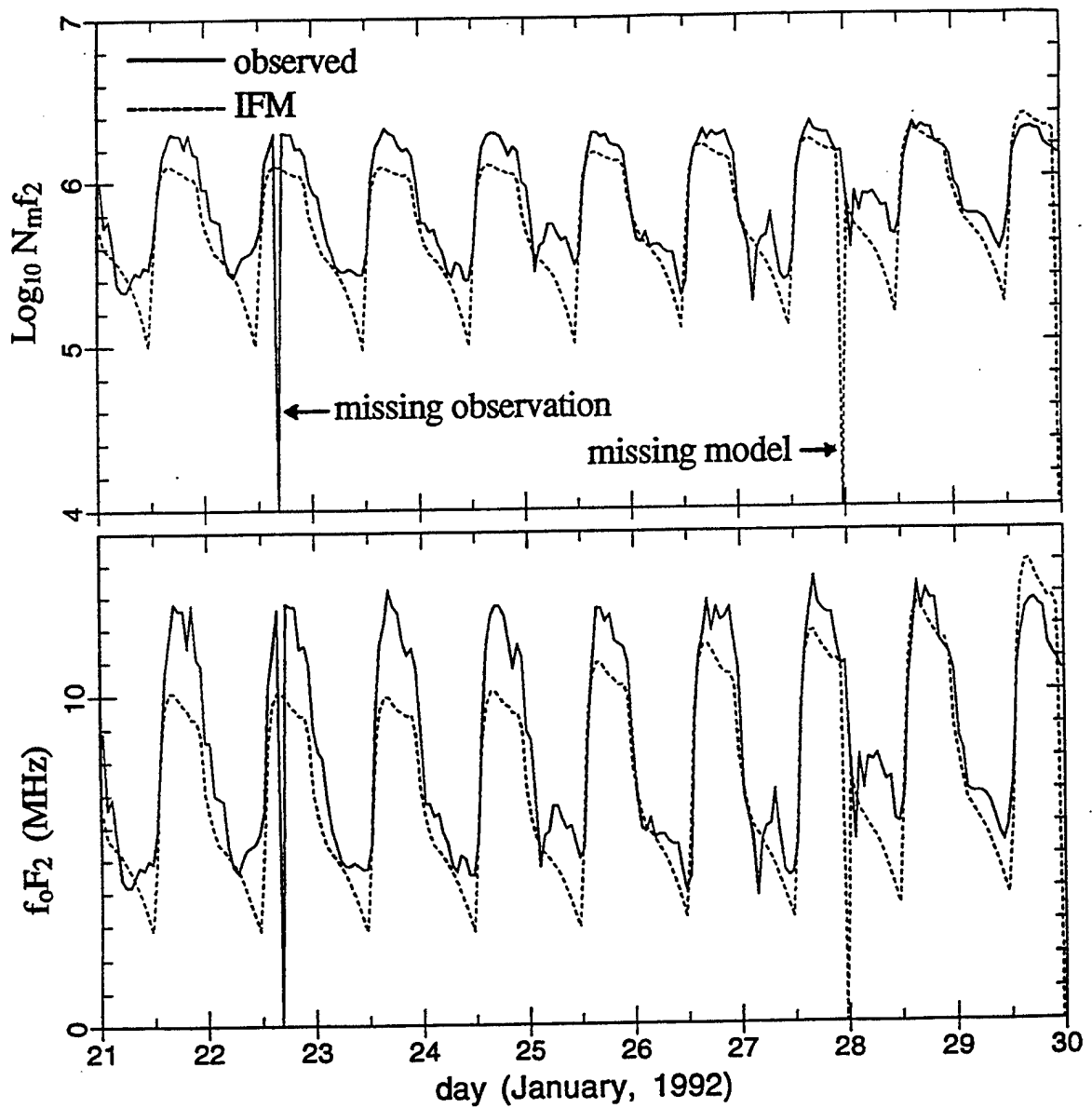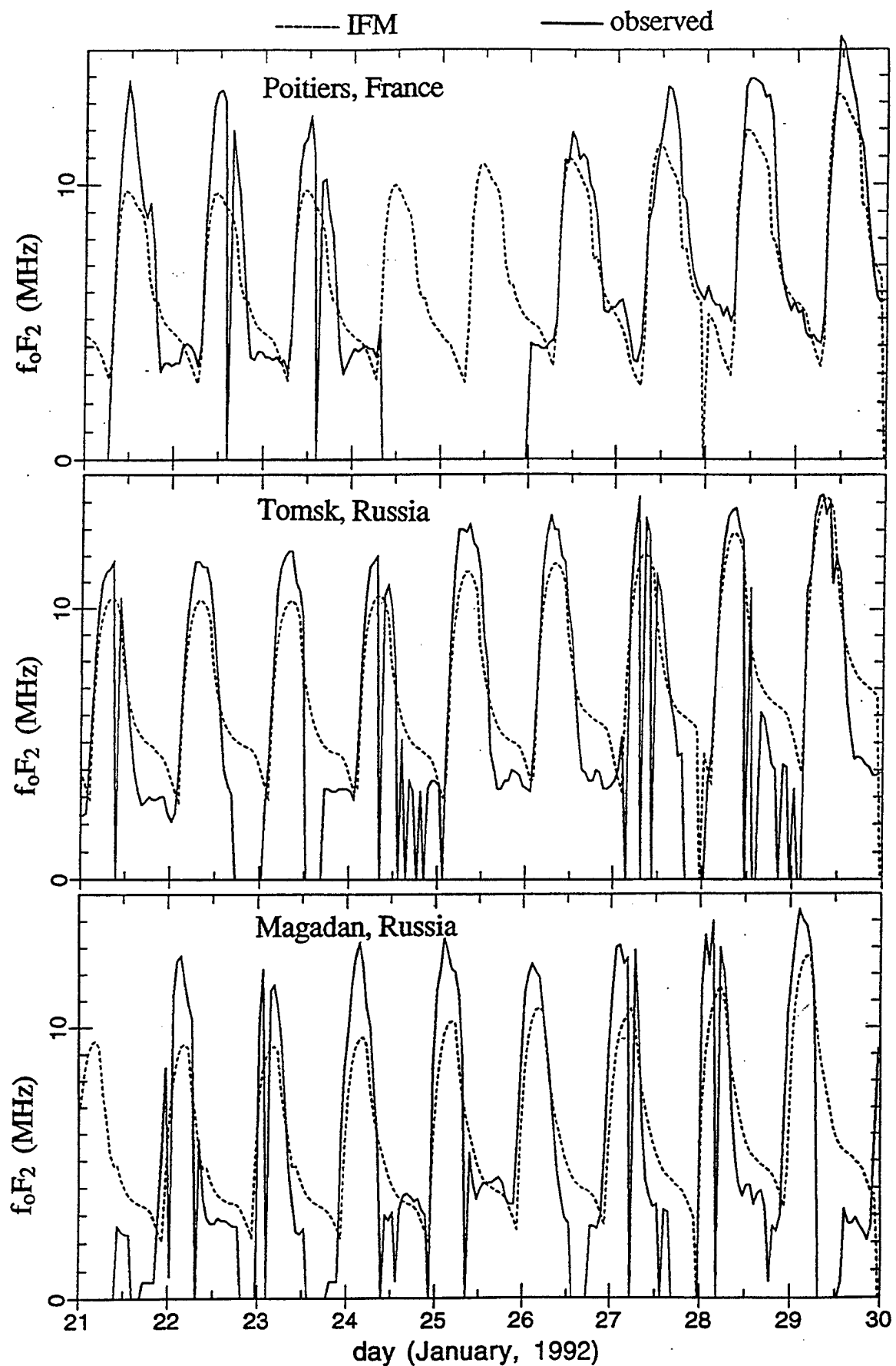
- Model f_oF_2 begins by being low, but towards the end of the 9 days has increased systematically to be about the same as observed.

- The F10.7 index varies markedly over the 9 day validation period.

F10.7initial	~160
F10.7final	~250
F10.7A	~215

- A special simulation to determine magnitude of this rate of change of F10.7 due to the MSIS neutral atmosphere used by the IFM was carried out.

Tomsk, Russia

observed

-------- IFM
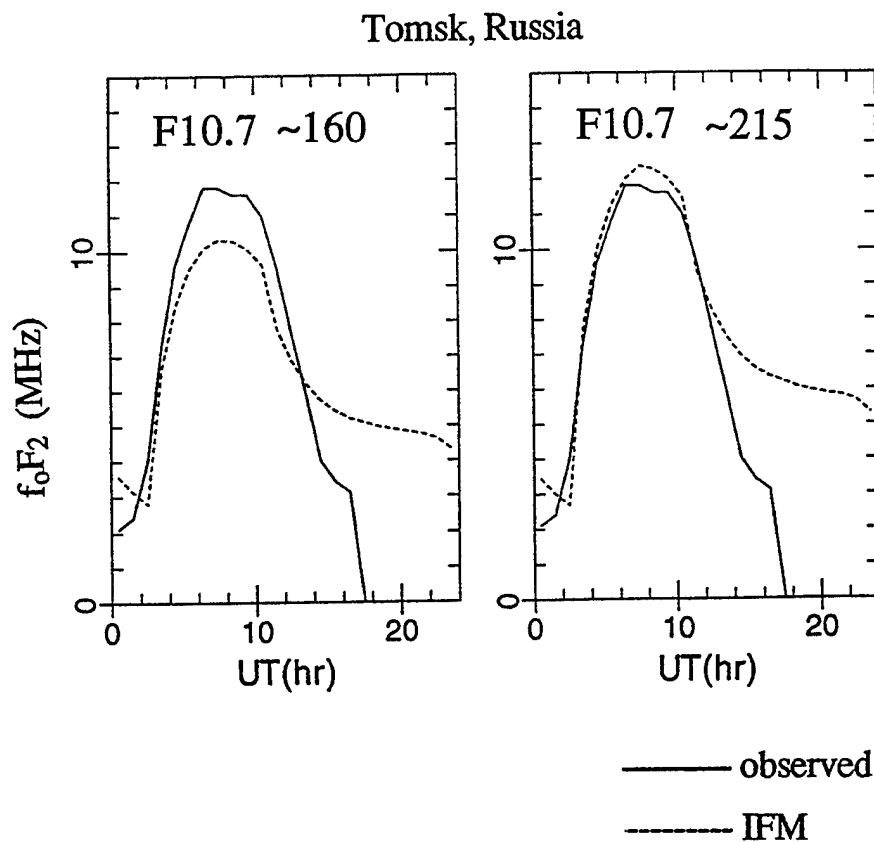
Eielson AFB, Alaska

(high latitude station at edge of terminator)
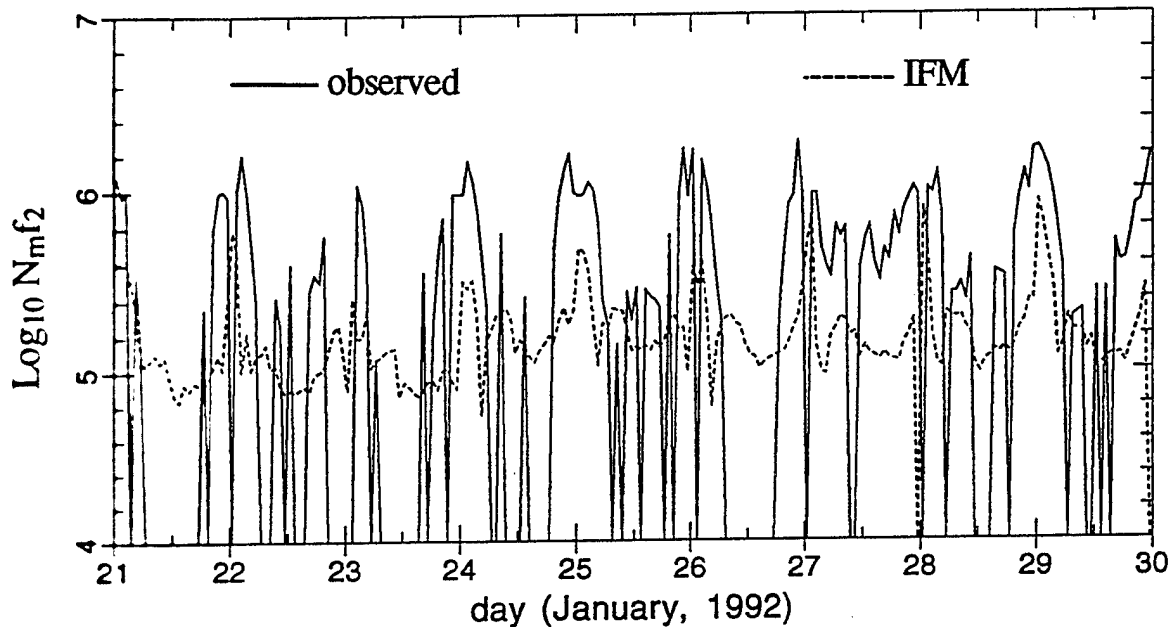
- Data is of poor quality, drop-outs occur every day and dominate the night sectors.

- Eielson AFB in Alaska is a high latitude station, whose location brings the station near the terminator at noon.

- Model (IFM) bin at this latitude has a latitudinal width of 5 degrees. Hence the trajectory used in the model could have been as much as 5 degrees poleward and hence could have missed the terminator region at noon.

Initial IFM Validation Summary

- IFM night density maintenance appears to be different from the observations.
  - a) In the IFM this is mainly a neutral wind dependent process.
  - b) While the observations show a distinct night-to-night variability, which includes increasing densities.

- The noon peak density is morphologically the same as observed, but the absolute density is lower at the begining of the 9 day period. This appears to be coupled to the rapid increase in the F10.7 index during the study.

- The IFM F10.7 dependence is mainly an MSIS neutral atmosphere climatology effect. A need exists to replace the MSIS model with a weather model.

- PL is developing such a thermospheric forecast model (TFM).

- The DMSP-IFM comparison also indicates that IFM densities are on the average low by 15 to 25%.

How does the IFM compare to IRI?

- Although not a required part of the validation, comparing with IRI does give a useful perspective on empirical/physical modeling.

- IRI does well at the equator at 840 km, but does not do so well at the peak region at the equator (Dr. David Anderson, PL, showed this during an earlier review meeting).

- At high latitudes IRI, during this validation period of 9 days, has the wrong morphology.

- There is little spatial structure in the high latitude IRI.

- Note: these are well known IRI problems, but the comparison does show the magnitude associated with the differences.

- The following three figures demonstrate this using data from DMSP F8, F9, and F10.

22 JAN 1992

LT: 06:18:00
UT: 06:34:49

ORBIT # 5 PHASE ANGLE

North Pole

MagLat

Equator

South Pole

EQ   NP   EQ   SP   EQ

DMSP F 9 ─────────
IFM   ─ ─ ─ ─
IRI   ─ ─ ─ ─

LOG_{10} Ne (cm^{-3})

LT: 09:18:00
UT: 11:18:19

22 JAN 1992

ORBIT # 8 PHASE ANGLE

North Pole

MagLat

Equator

50

0

-50

0   100   200   South Pole 300

EQ   NP   EQ   SP   EQ

DMSP F10 ——————
IFM   — — — —
IRI   - - - - - -

6

LOG₁₀ Ne (cm⁻³)

5

4

3

LT:20:12:00
UT:20:27:44

22 JAN 1992

0   100   200   300

ORBIT #14 PHASE ANGLE

67
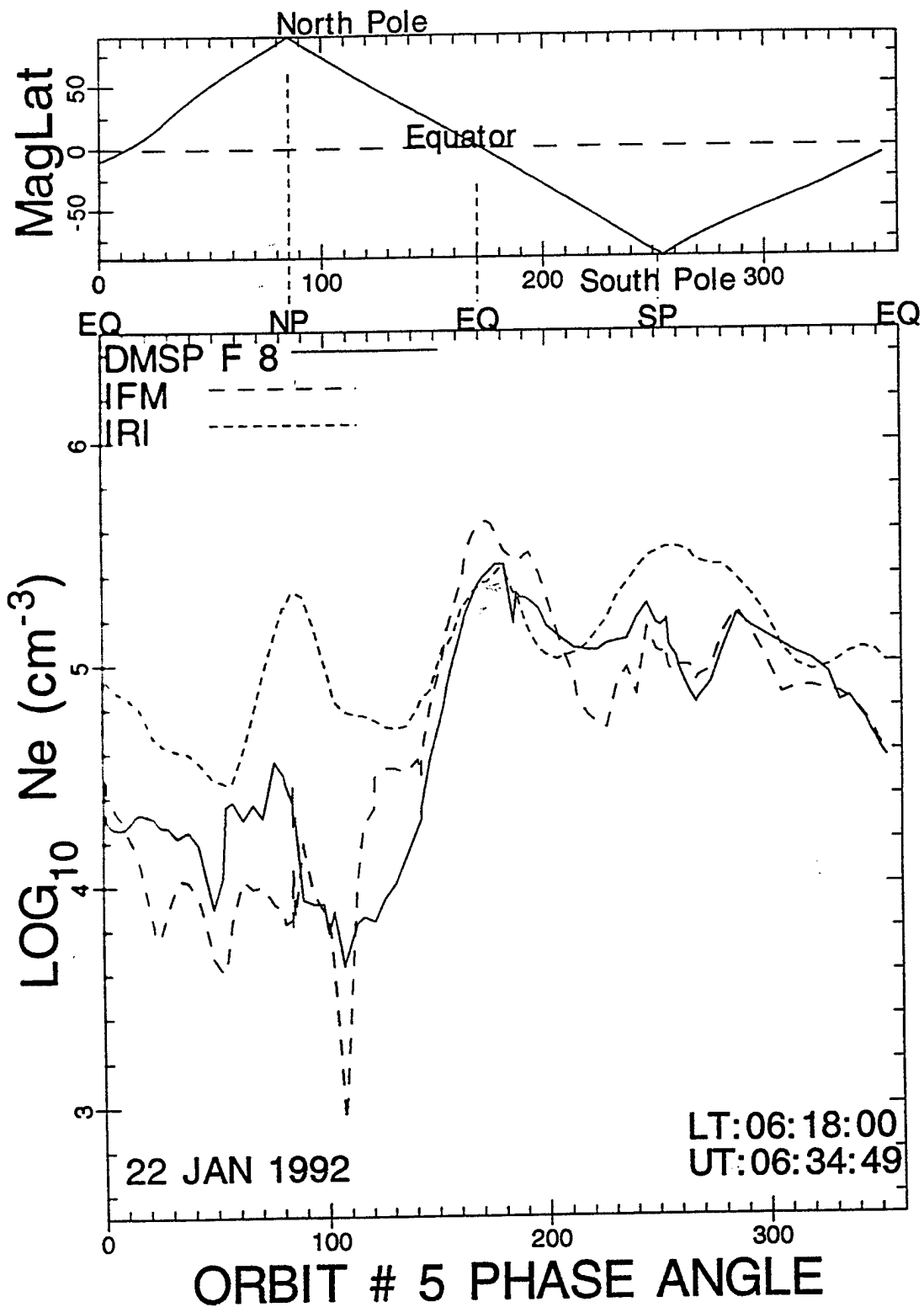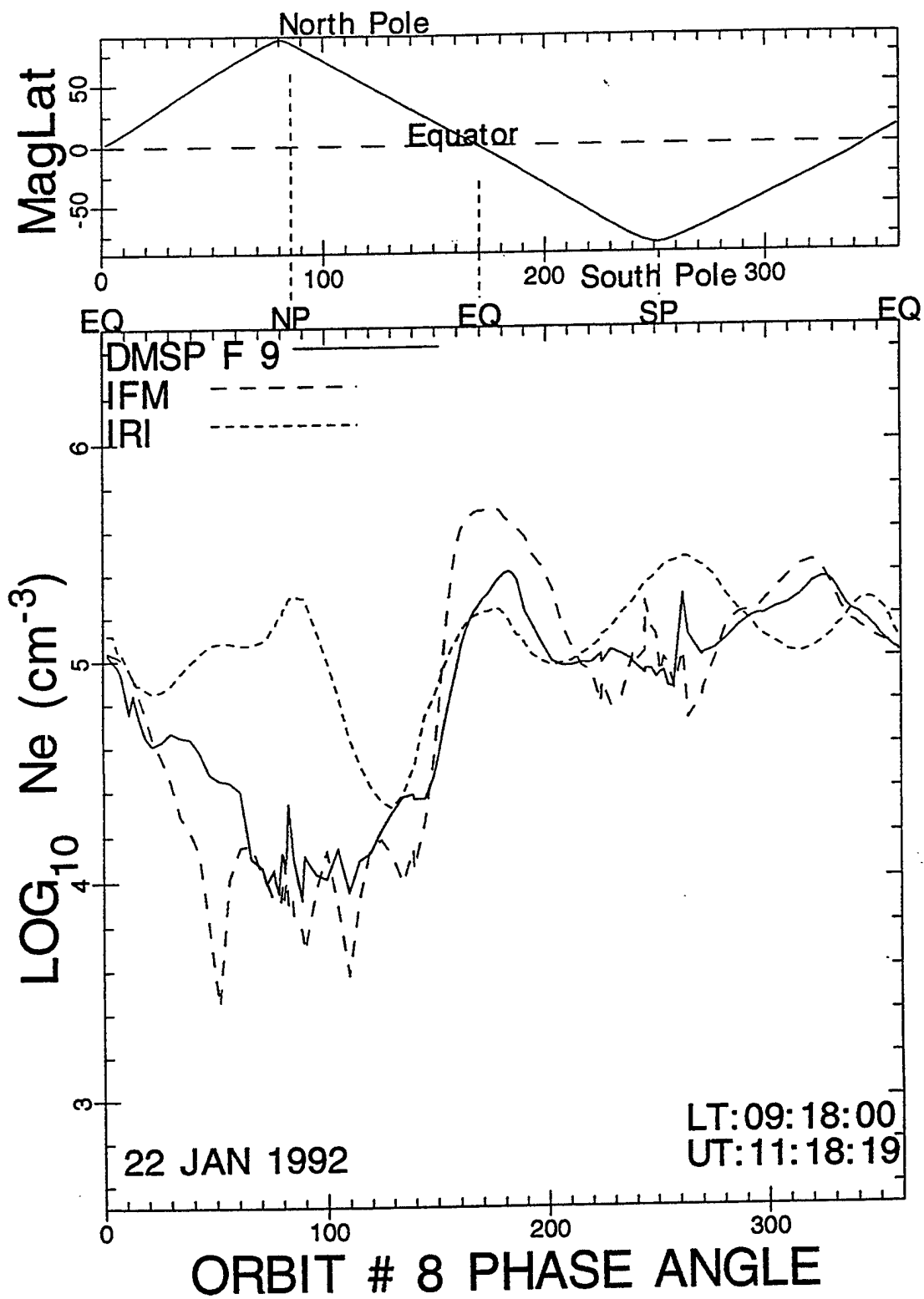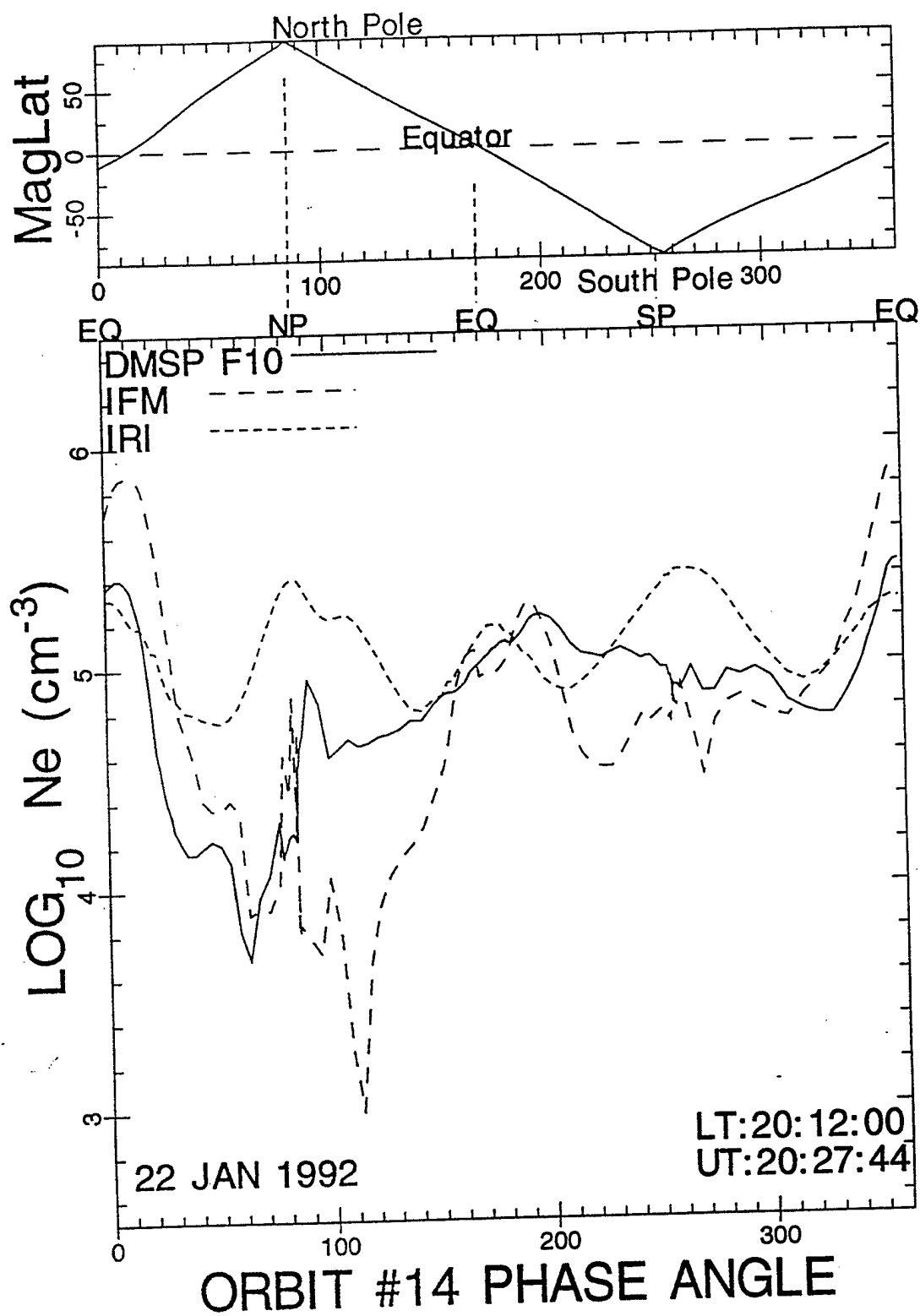
Ongoing Validation objectives

Continue Validation Period 1 analysis.
- Develop quantifiable objectives in the validation.

- Obtain information on the following:
  - DMSP SSIES ion temperature
  - DMSP SSIES ion composition
  - DMSP SSIES electron temperature

  These are critical in deciding if our suggested problem solutions are the correct ones.

- Analysis ionosonde data from the other stations. These are at lower latitudes as well as in the southern hemisphere.

Begin Validation Period 2 analysis
- The primary objectives are to confirm the Period 1 validation and to test the IFM during <u>more disturbed periods</u>.

- This second interval in February 1992 has a very disturbed period extending over 5 days.

- It is also a little closer to equinox.

Validation Issues
- As differences are encountered keep track of them.

- Using the observations establish the magnitude of the differences.

- Try to find the source of the problems, and suggest methods of avoiding the problems.

Validation Presented At

October 31, 1995
Models Review Meeting
Hughes STX, Colorado Springs

IFM -- E-Region Status

Comparison to ionosonde database showed some deficiencies in the IFM E region. Improvements were made to the dayside and nightside E region calculations.

- Updated absorption and ionization cross sections for E-region improvements in N_mE & H_mE.

- Recast nighttime ionization dependence to contain "solar angle dependence"

- Updated EUV-to-F10.7 dependencies for improved solar flux ionization.

- Compared against averaged, worldwide ionosonde data from years 1957-1975 and again for years 1976-1992.

- Worldwide ionosonde database is the NOAA-NGDC:

Ionospheric Digital Database
WORLDWIDE VERTICAL INCIDENCE PARAMETERS
CD-ROM DATASET

Ionospheric Digital Database
mid and low latitude stations
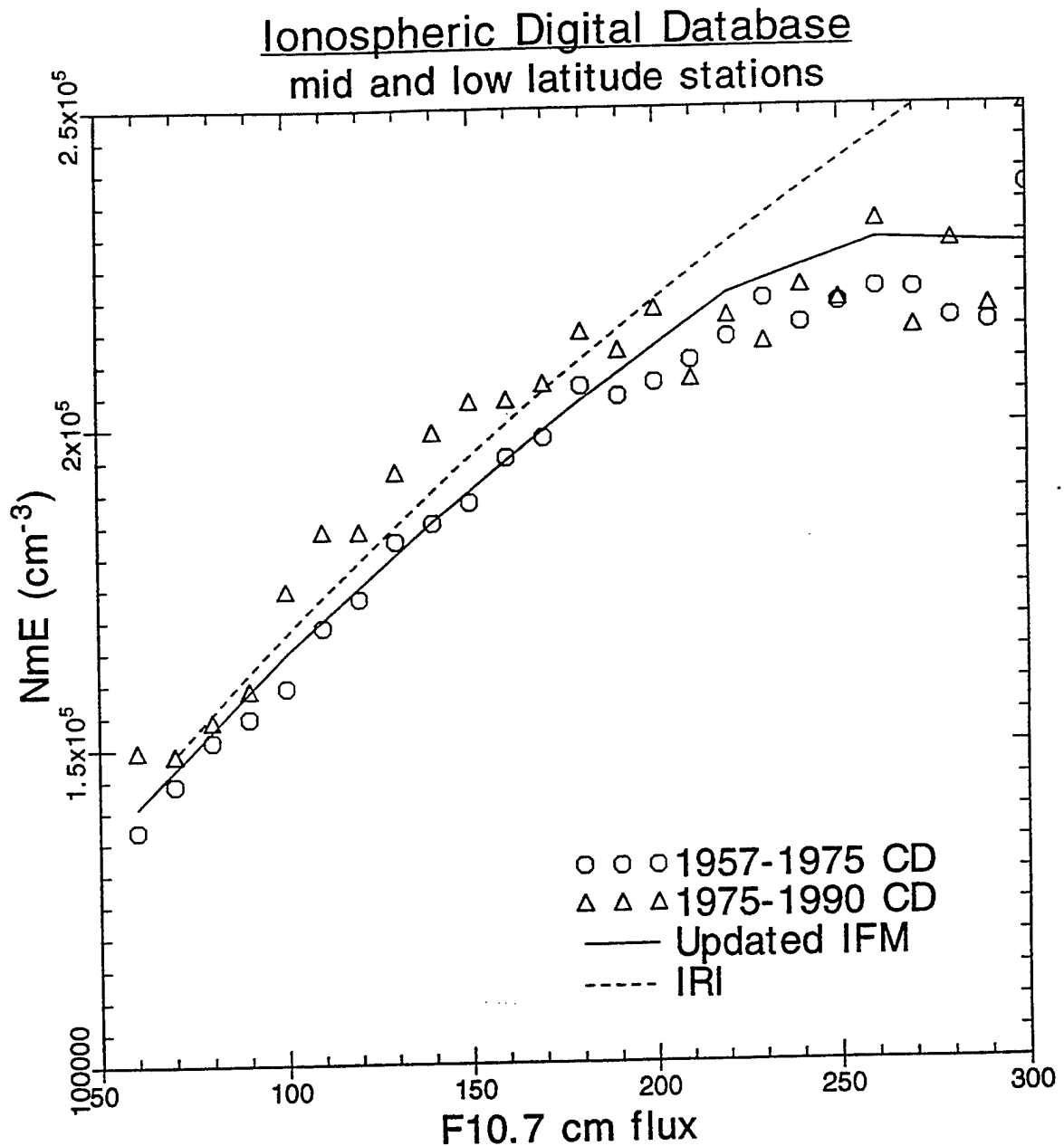
Data averaged in F10.7 Flux bins and solar angle bins. Above graph represents solar zenith ± 5 degrees.

The break in the graph at 240 represents the decoupling of F10.7 from EUV.

Ionospheric Digital Database
mid and low latitude stations
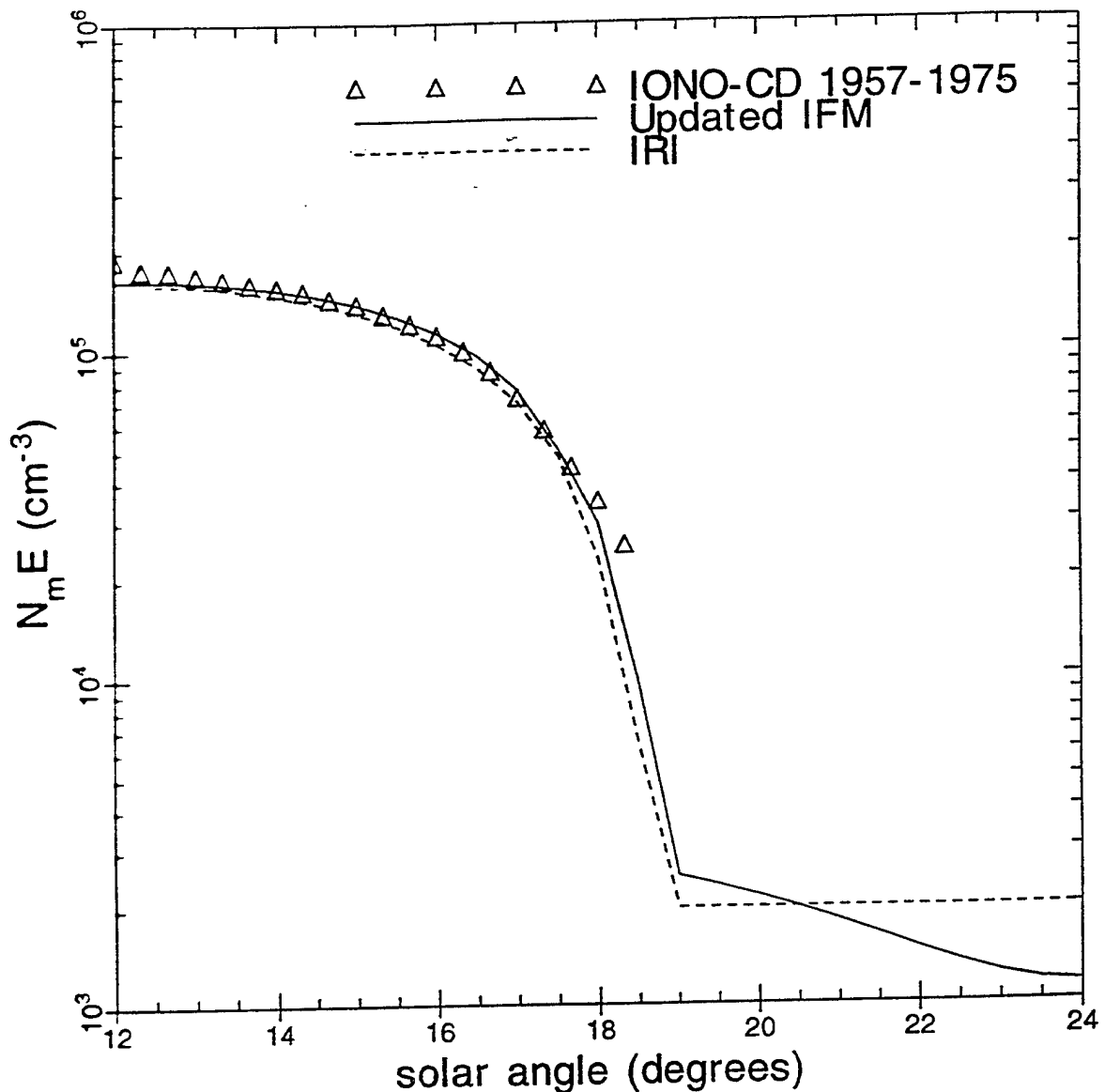
Ionospheric Digital Database NmE is averaged in solar angle bins for F10.7 =100. NmE is not consistently measured after sunset and is not useful for this comparison. The IFM NmE now matches the database and IRI values during the day. At night IFM NmE has a solar angle dependence with a local midnight minimum maintained by starlight and geocoronal emissions.

IFM vs IONOSPHERIC DIGITAL DATABASE
mid and low latitude stations
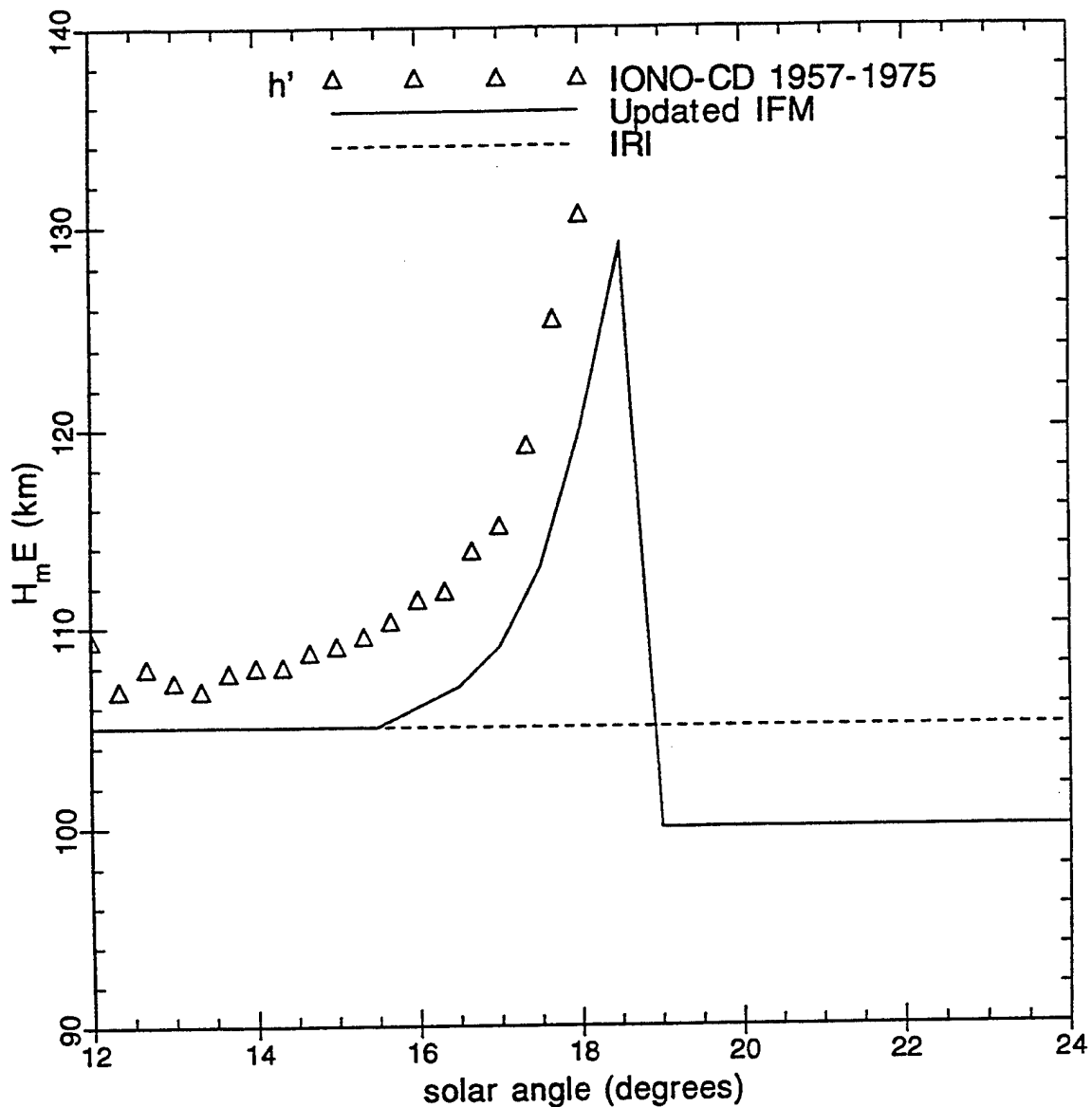
Ionospheric Digital Database virtual HmE is averaged in solar angle bins for F10.7 =100. With the increasing solar angle the E region should lift. The IFM HmE is actual height and should be lower than the virtual HmE.
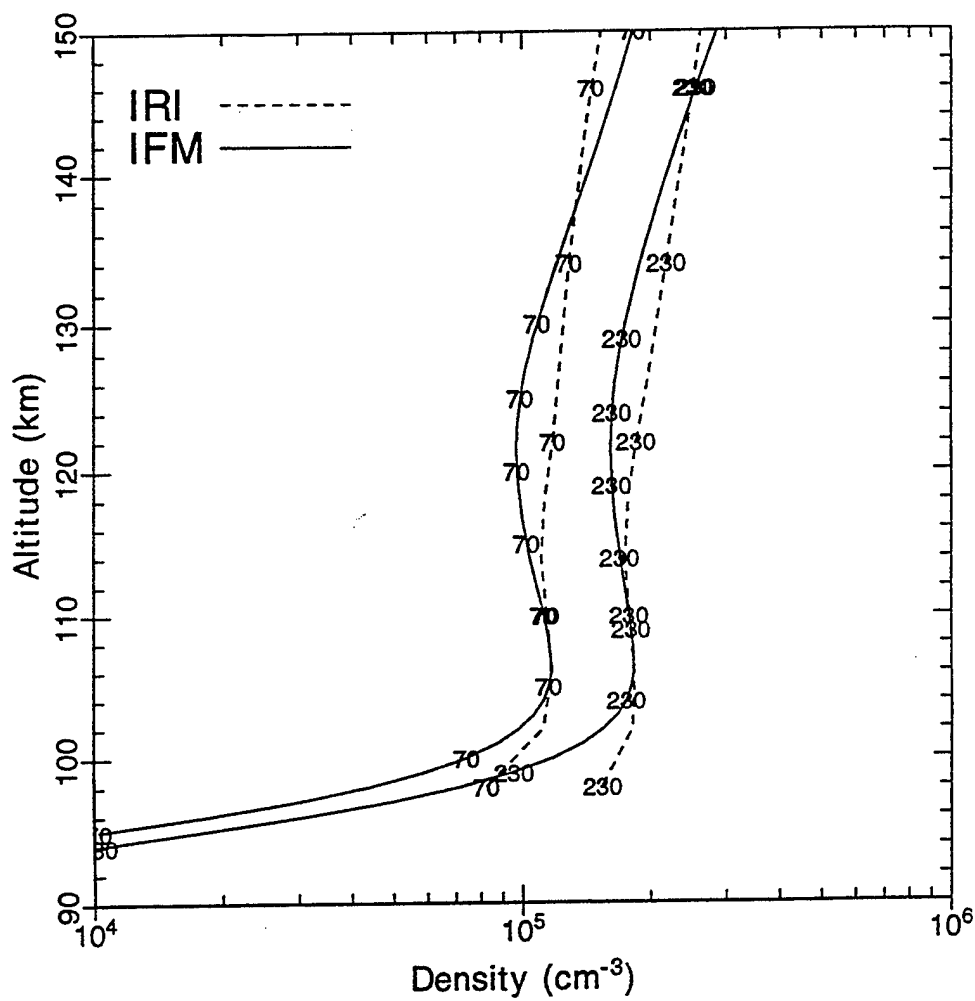
E Region Profiles from IFM and IRI for F10.7 cm = 70 and F10.7 cm = 230 at 45° Latitude, noon.

IFM Validation Status

The prior report focussed on Validation Period 1, 21-29 January 1992. Since that time we have extended the validation work to cover the second validation period.* Hence the presentation will be as follows:

- Validation Period 2, 11-21, February 1992.

- Geomagnetic Activity and Solar Conditions.

- Global f_oF_2 comparison of the IFM with the NGDC SELDADS data.

- Northern Midlatitude F-layer revisited.

- Global topside comparison using the DMSP SSIES observations and IFM.

- IFM E-region status. Validation based on a comparison with the NOAA-NGDC ionosonde data base. Already presented earlier in this report.

* Comparisons are also made with the International Reference Ionosphere.

75

VALIDATION PERIOD 2

- February 11-21, 1992 (11 days)

- Approaching Equinox in the Northern Hemisphere

- Quiet 6 days followed by 3 slightly disturbed days and 2 disturbed days.

- Data Sets Obtained

<u>DMSP SSIES</u> from Phillips Laboratory, Hanscom AFB supplied by Peter Sultan. Data from satellites F8, F9, F10, and F11 were available on each day during the study period. A total of 44 files (one per day and satellite) for the scintillation meter and another 44 for the drift meter were obtained. This corresponds to about 740 MBytes of data.

<u>Ionospheric Sounders</u> from NGDC supplied by Ray Conkright. The entire SELDADS data base for the month of February 1992 was supplied. This does include certain DISS sounders that were operational. A total of 43 stations, but only 24 have usable data.

<u>DMSP SSJ/4</u> from Phillips Laboratory, Hanscom AFB supplied by Fred Rich. Data from satellites F8, F9, F10, and F11 were available. Used to evaluate the empirical auroral precipitation model input to the IFM.

1992
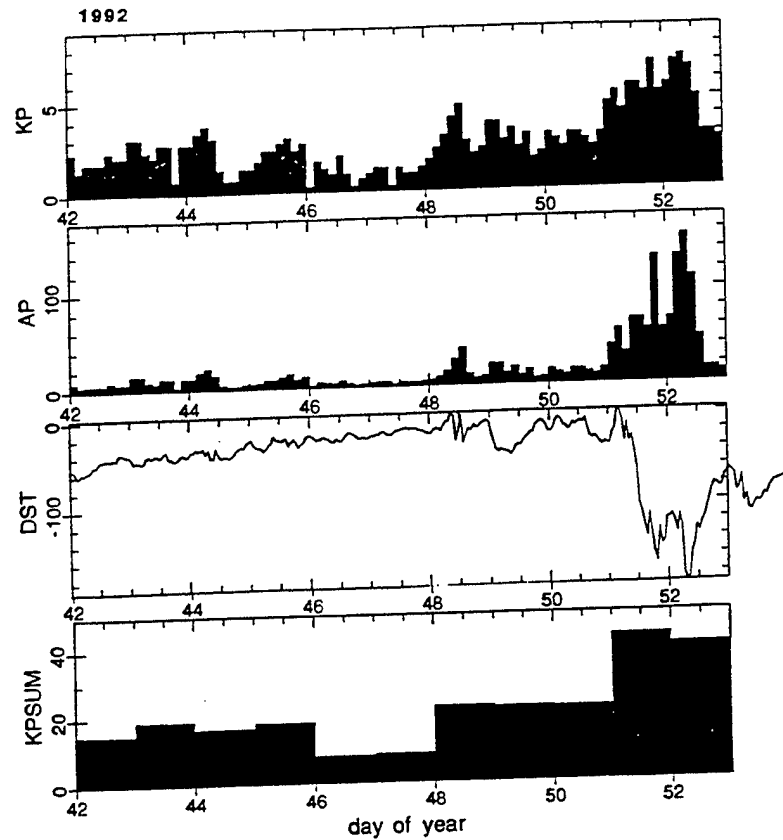
- Validation Period 2, starts on the 11th February (day 42).

- Kp averages about 1 for the first 6 days.

- ap averages about 5 for the first 6 days.

- Kp increases to about 3 on the 17 February and then to 5 on the 20 February.

- Dst drops by over 150 on the 20 February.

- The last 2 days are disturbed geomagnetically.

- Kp averages about 5 for the last 2 days.

77

1992
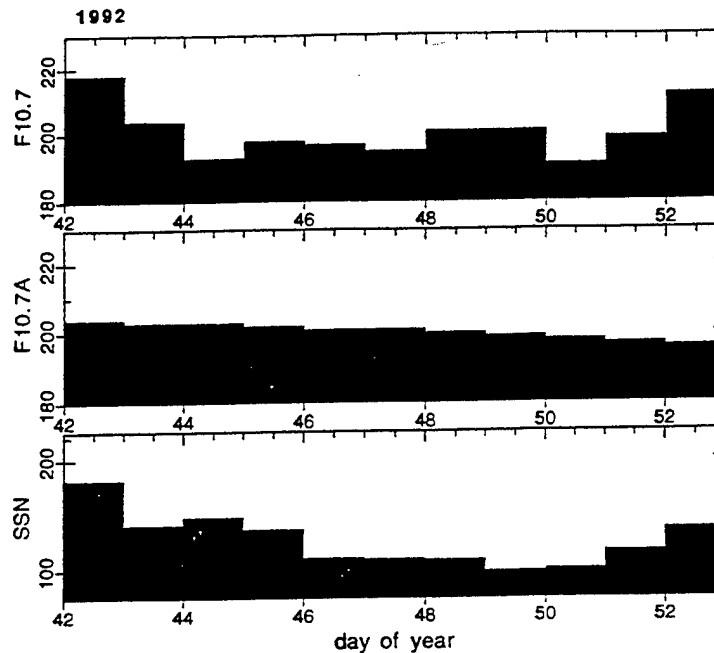
- Validation Period 2, starts on the 11 February (day 42).

- F10.7 is relatively constant at 195 units.

- The sunspot number reflects the solar maximum conditions.

- Unlike Validation Period 1, this period has very little solar variability as measured by the F10.7 radio proxy index.

Global Ionosonde Data Base

- The NOAA SELDADS ionosonde data base for the month of February 1992 was obtained from Ray Conkright at NGDC.

- Of the 43 ionosondes in this global data set 23 had usable data during the second validation period.

- These stations can be roughly grouped as follows:

    Southern hemisphere   1 station
    Equatorial regions   5 stations
    Northern mid latitudes 11 stations
    Northern high latitudes 6 stations

- These stations, their geographic latitude and longitude, and identifier codes are listed on the following table. These same stations are shown on the world map using their respective identifier codes.

- No data are available from the following key regions:

    Central America
    South America
    Africa
    Antarctica
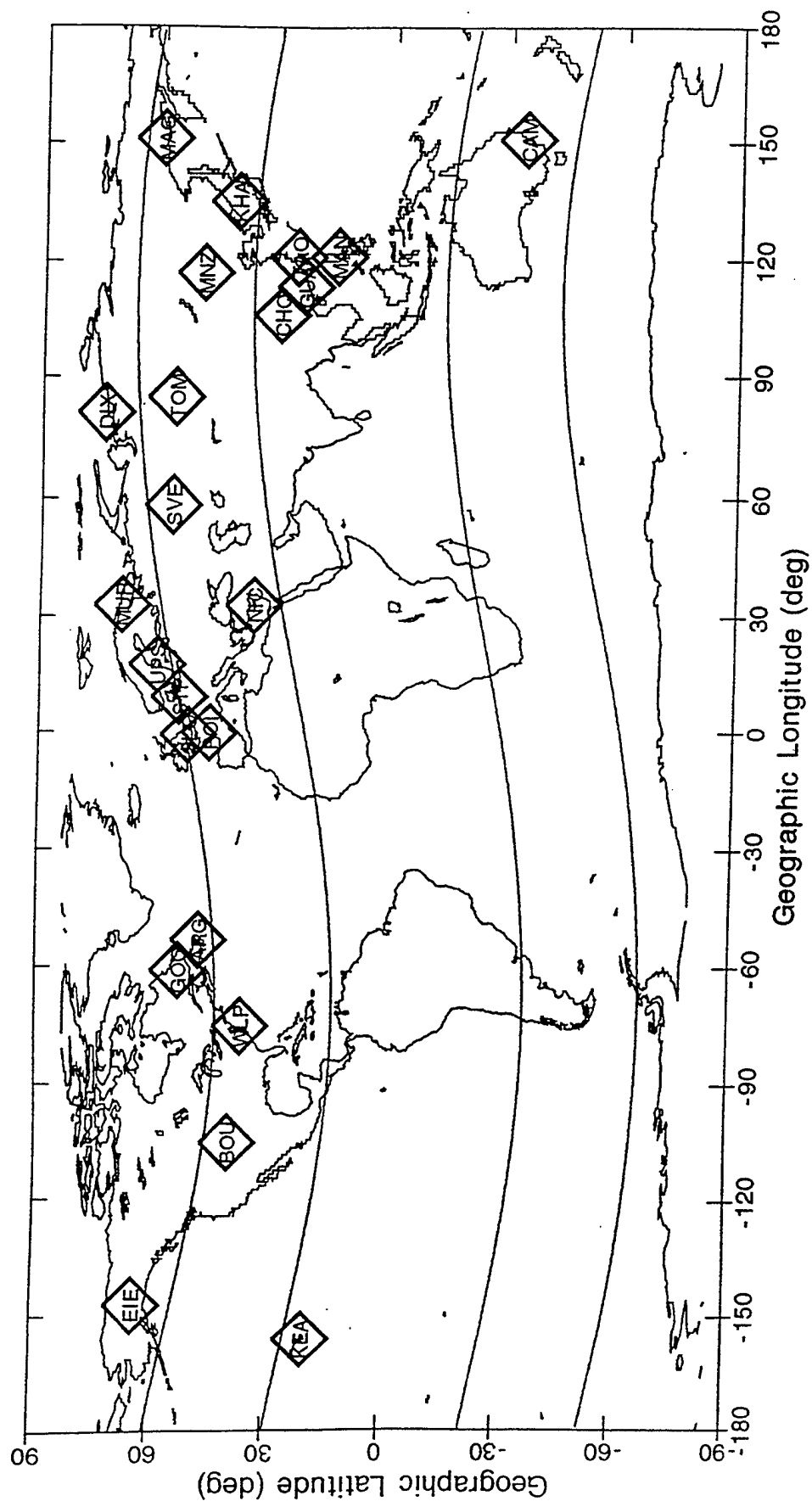
One southern hemisphere station (near equinox); Camden, Australia

One station almost on magnetic equator; Manila, Philippines

Magnetic dipole constant latitude lines drawn at ± 25° and at ± 55°

NOAA SELDADS IONOSONDE STATIONS USED
FOR VALIDATION PERIOD 2

station	country	Identifier code	geographic latitude	geographic longitude	magnetic latitude
Argentia	Canada	ARG	48.0	307.0	58.8
Boulder	USA	BOU	40.0	255.0	48.9
Camden	Australia	CAM	-34.0	151.0	-42.2
Chongqinq	China	CHQ	29.0	106.0	17.6
Dixon	Russia	DIX	74.0	81.0	63.5
Eielson AFB	USA	EIE	74.0	213.0	64.2
Goose Bay	Canada	GOO	53.3	299.2	64.5
Guangzhou	China	GUA	23.1	113.4	11.7
Keakawapu	Hawaii	KEA	20.0	204.0	20.3
Khabarousk	Russia	KHA	40.5*	135.1	30.0
Magadan	Russia	MAG	60.0	151.0	50.7
Manila	Philippines	MAN	14.6	121.1	3.4
Manzhouli	China	MNZ	49.0	117.0	37.7
Murmansk	Russia	MUR	69.0	33.0	64.1
Nicosia	Cyprus	NIC	35.0	33.0	31.8
Poitiers	France	POI	46.0	0.0	48.8
Slough	UK	SLO	51.5	359.4	54.2
St. Peter_Ording	Denmark	STP	54.0	9.3	54.6
Sverdlousk	Russia	SVE	56.4	58.6	48.5
Taoyuan	Taiwan	TAO	25.0	121.0	13.8
Tomsk	Russia	TOM	56.0	85.0	45.5
Uppsala	Finland	UPS	59.8	17.6	58.4
Wallops Is.	USA	WLP	37.0	285.0	48.3

* Latitude is probably in error

81

CAMDEN, AUSTRALIA (CAM)

IFM is the dashed line

Latitude= -34.0°   Longitude= 151.0°

day (February, 1992)
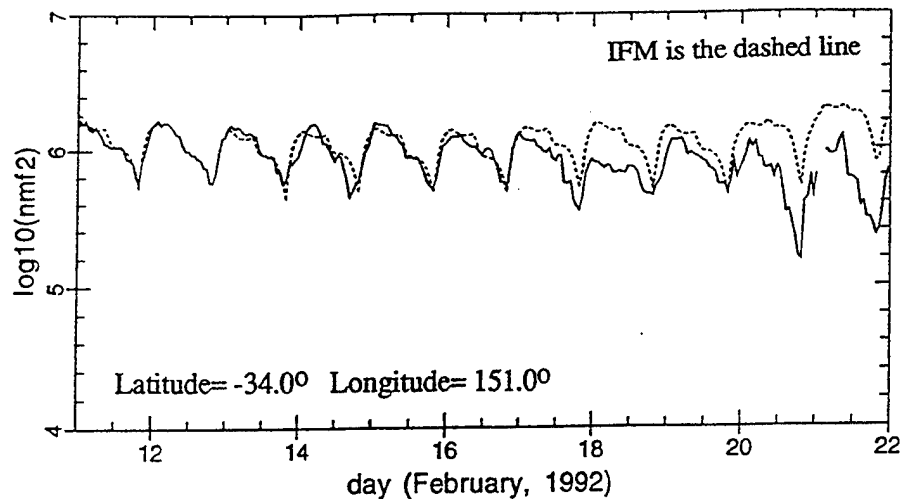
- During 6 Quiet Days Agreement Excellent
- On 18th Kp increase, marked decrease in observed density
- On 20th and 21st, Kp reaches 5 and IFM predicts an increase

MANILA, PHILIPPINES   (MAN)

IFM is the dashed line

Latitude= 14.6°   Longitude= 121.1°

day (February, 1992)
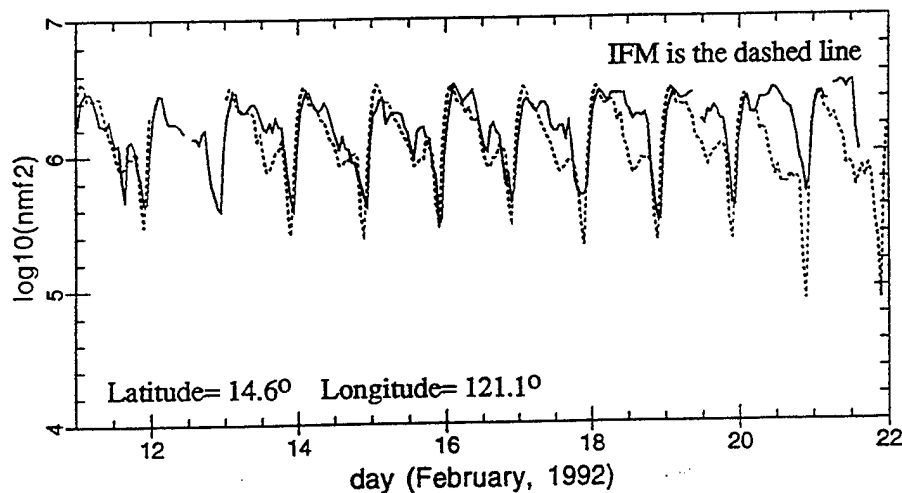
- During 6 quiet days IFM durnal variation agrees with observations
- From 17th onwards observations show an increasing late afternoon-evening enhancement, this is not modeled.
- Overall the absolute agreement is very good

82

TAOYUAN, TAIWAN   (TAO)

IFM is the dashed line

Latitude= 25.0°   Longitude= 121.0°E

day (February, 1992)
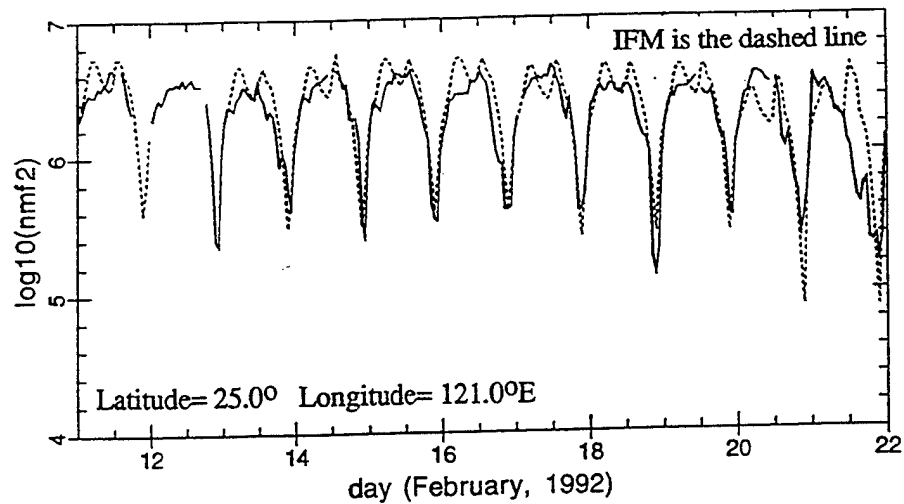
- Dynamic ranges agree.
- But IFM day-afternoon structure is different
- Again indicative of the input electric field being inconsistent with conditions on these days.

GUANGZHOU, CHINA   (GUA)

IFM is the dashed line

Latitude= 23.1°   Longitude= 113.4°E

day (February, 1992)
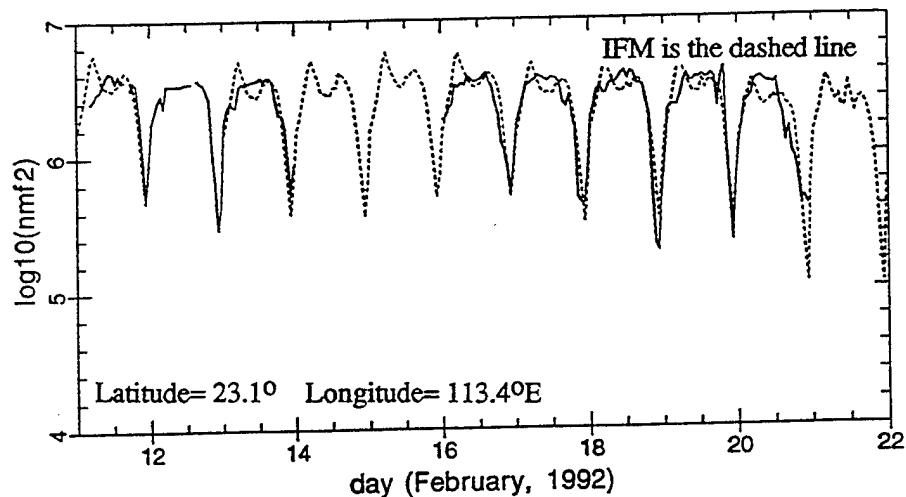
- This station is only 7.5° in longitude and 1.9° in latitude from the TAO station.
- Model indicates differences in day-evening N_mf_2 between stations.
- Observation differences between these two close stations.

KEAKAWAPU, HAWAII (KEA)
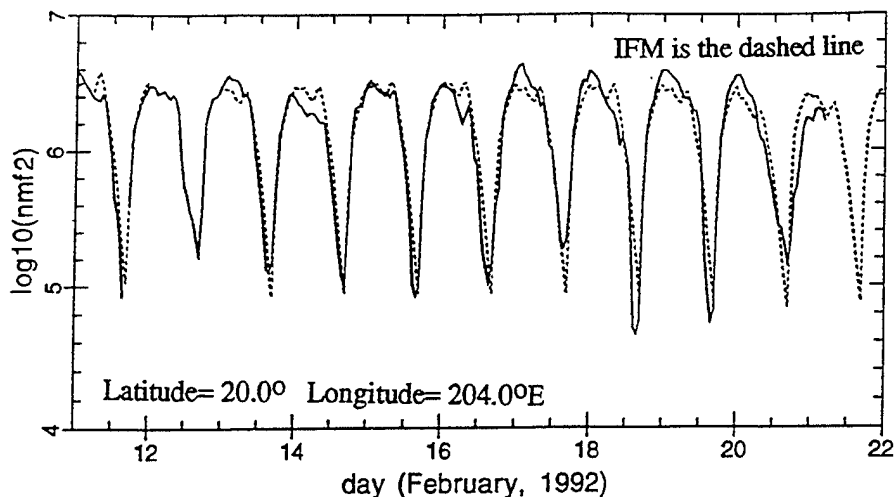
- Northern equatorial location.
- During quiet days observe significant variability.
- Model dynamic range is consistent with observations.

CHONGQUING, CHINA (CHQ)
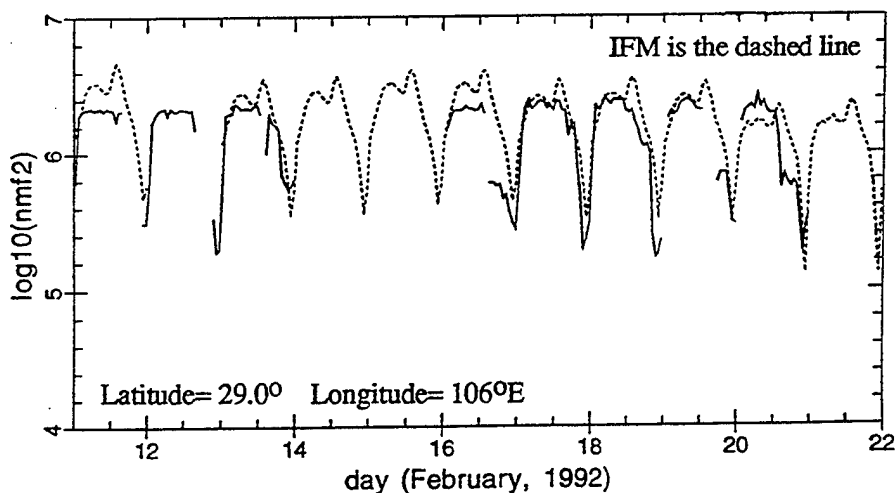
- Northern equatorial location.
- Model has a late afternoon signature not observed.
- This signature results from input electric field structure.

84

Mid Latitudes Revisited

The first validation focussed on ionosondes at mid-latitudes. At these latitudes it was found that the IFM densities where often low in the noon sector.

- At Mid-latitudes the dayside F-region is very sensitive on the neutral wind.

- In the IFM the neutral wind is obtained from the Hedin 1990 wind model.

- The effect of a poleward wind on the dayside is to drive plasma downwards along the magnetic field.

- This downward drift reduces the F-region peak density.

- The two following pages show the effect of reducing the dayside Hedin wind by 50%, and reducing the dayside wind to zero.

- The first plot is for Wallops Island. At this location the reduced wind yields enhanced densities. These are in better agreement with the observations.

- This is followed by examples from Sverdlousk and Magadan which are both in Russia. At these locations the reduced wind improves the agreement with observations, but not to the same degree as at Wallops Island.

station code: WLP

latitude= 37.0 longitude= 285.00

Wallops Is., USA

IFM is the dashed line

Full HEDIN wind

0.5 dayside HEDIN wind

Zero dayside wind

14 February 1992

14 February 1992

14 February 1992
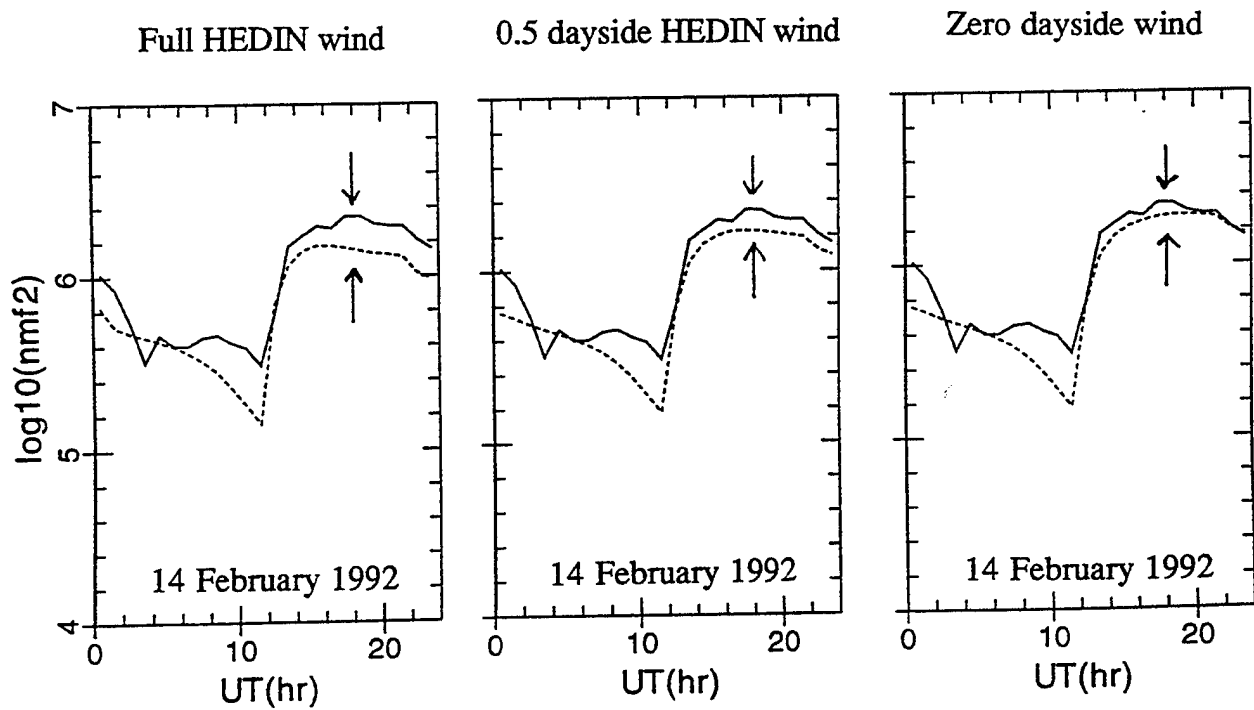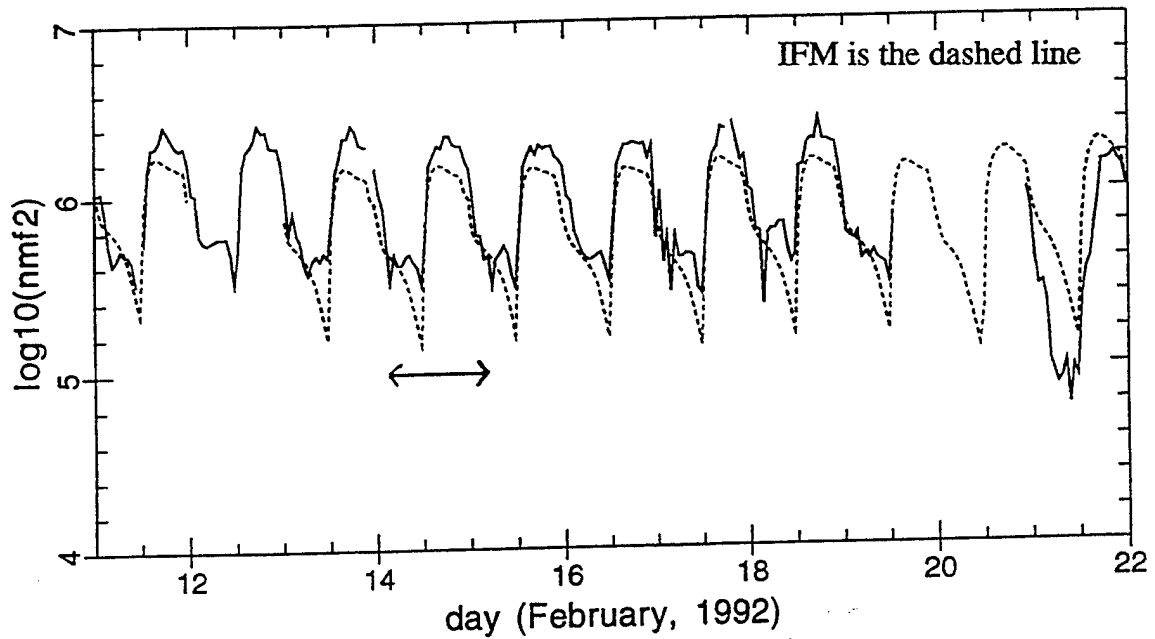
Sverdlousk, Russia   latitude= 56.4 longitude= 58.60

Full HEDIN wind   **0.5 dayside HEDIN wind**   **Zero dayside wind**

IFM is the dashed line

14 February 1992   14 February 1992   14 February 1992

UT(hr)   UT(hr)   UT(hr)

log10(nmf2)
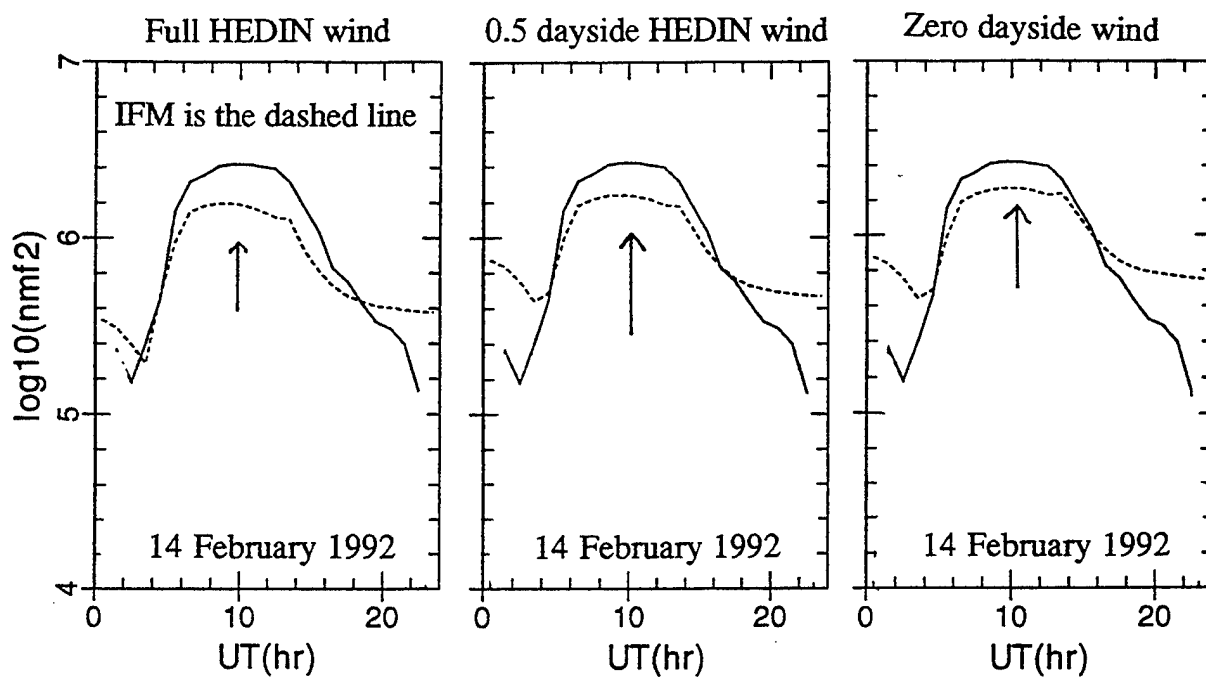
Magadan, Russia   latitude= 60.0 longitude= 151.00

Full HEDIN wind   **0.5 dayside HEDIN wind**   **Zero dayside wind**

IFM is the dashed line

14 February 1992   14 February 1992   14 February 1992

UT(hr)   UT(hr)   UT(hr)

log10(nmf2)
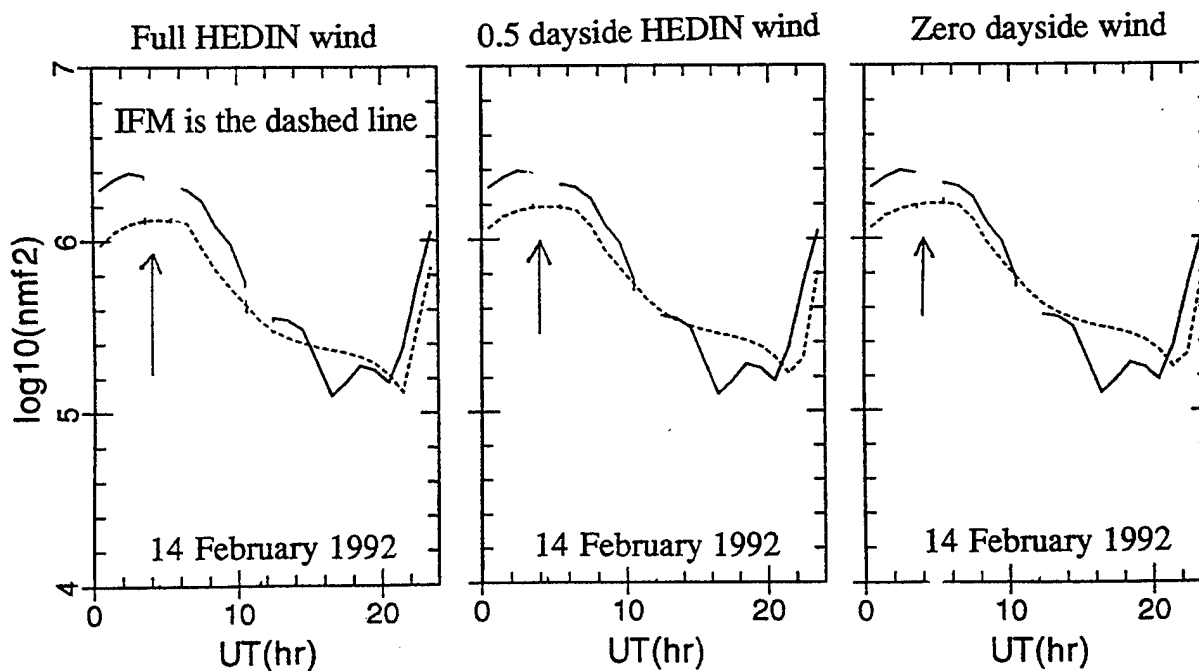
Global Topside DMSP-IFM Comparisons

- Data from DMSP F8, F9, F10, and F11 satellites were used

- Each satellite had in-situ plasma density measurements from the SSIES instrument.

- Density was sampled every second, hence a total of 3.8×10^6 observations were used in this validation 2 study.

  o The presentation used color overview plots to compare DMSP and IFM.

  o The following pages in this report provide detailed single orbit or fixed orbit phase angle-11 day plots.

- Comparisons with the International Reference Ionosphere (IRI) model are also made to emphasize the present state of ionospheric forecasting.
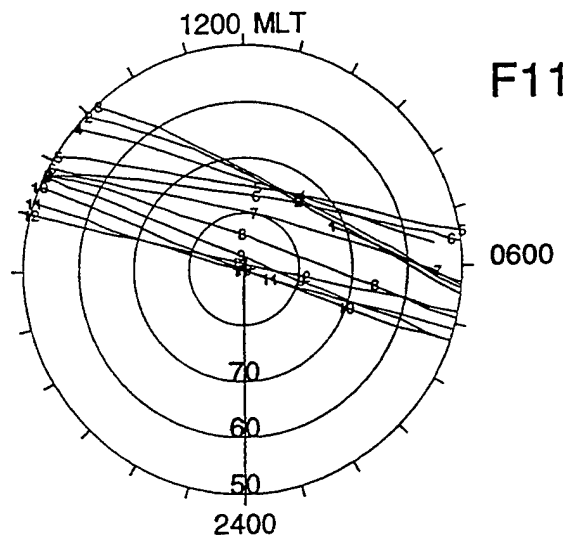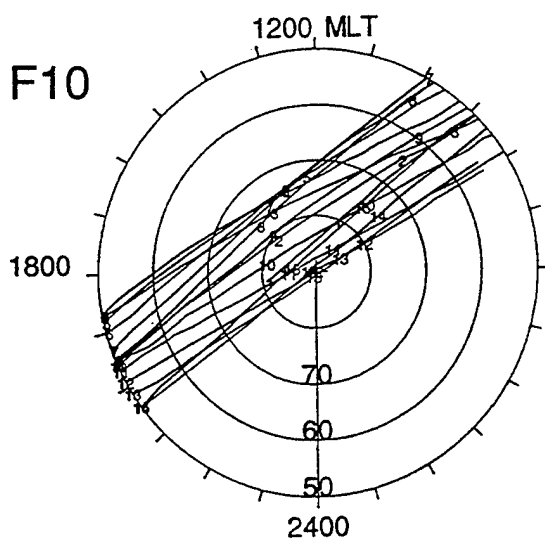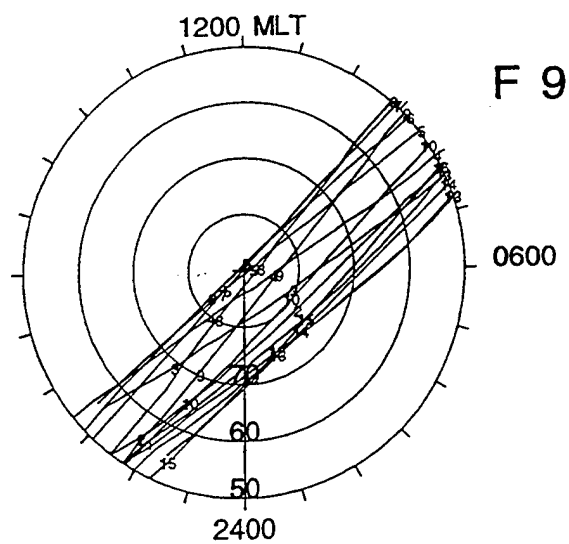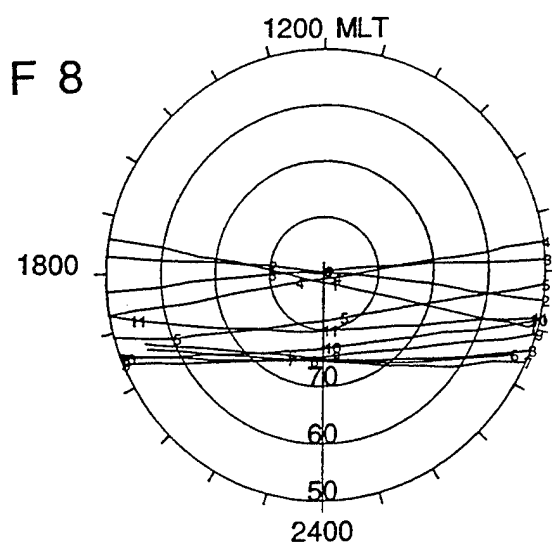
F 8

1200 MLT

1800

2400

F 9

1200 MLT

0600

2400

F10

1200 MLT

1800

2400

F11

1200 MLT

0600

2400

- DMSP northern hemisphere orbits (labeled sequentially 1 through 15) for 24 hours during validation period 2.

- DMSP southern hemisphere orbits (labeled sequentially 1 through 15) for 24 hours during validation period 2.

IFM and DMSP densities at phase=100 of F8
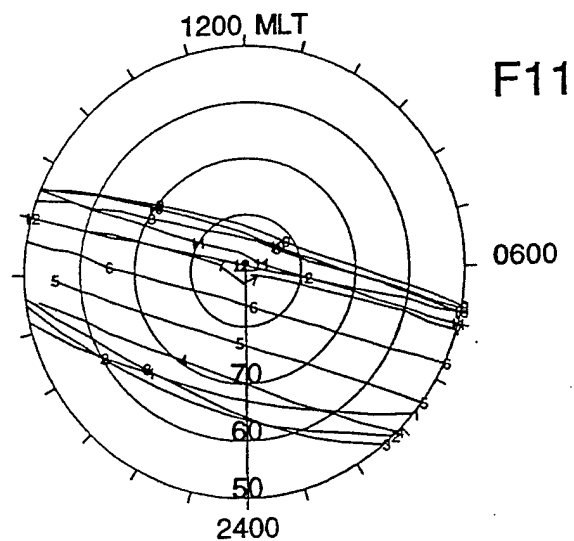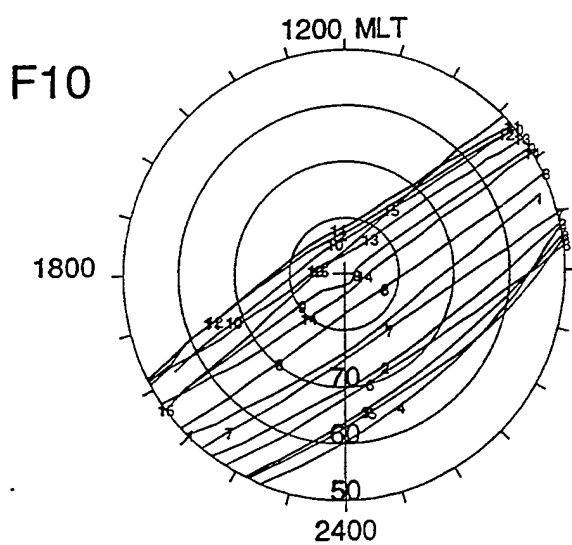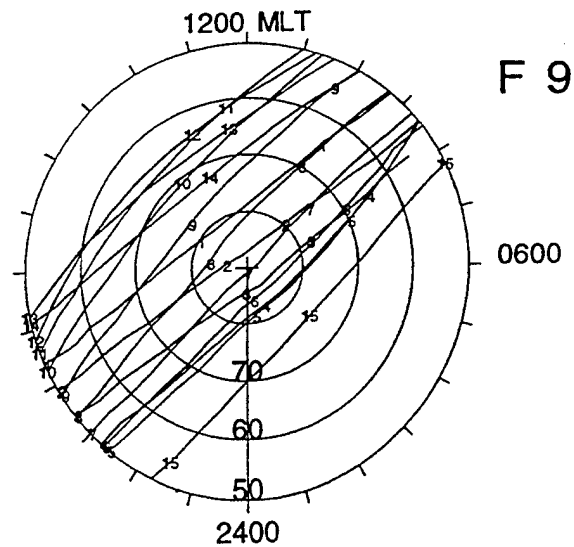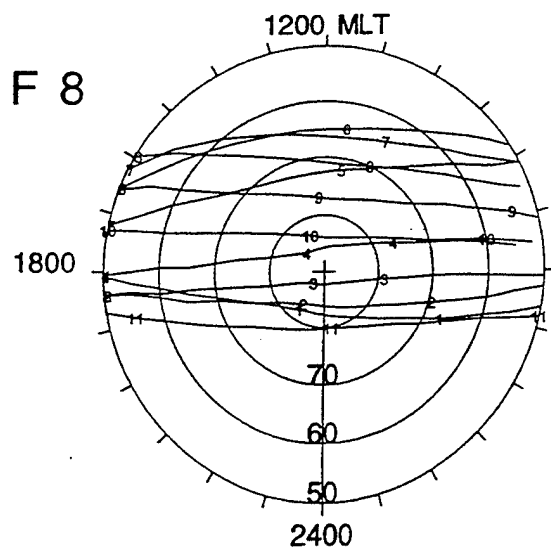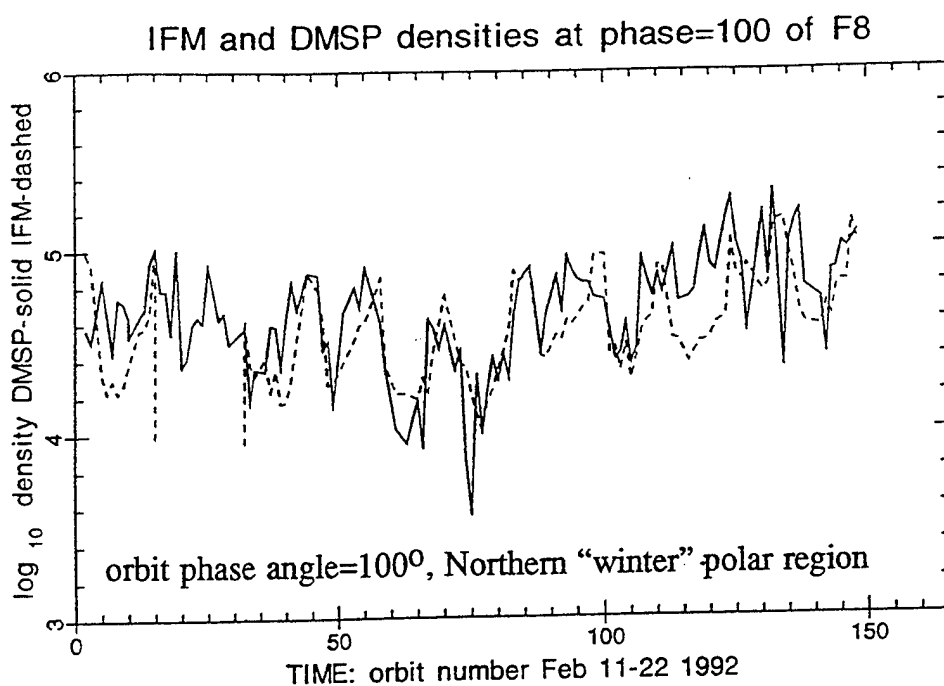
DMSP
F8

- Observations (solid line) and IFM densities agree well.
- Lowest densities occur on quiet day prior to disturbances.
- Highest densities occur during the Kp=5 disturbance at end of period.

IFM and DMSP densities at phase=280 of F8
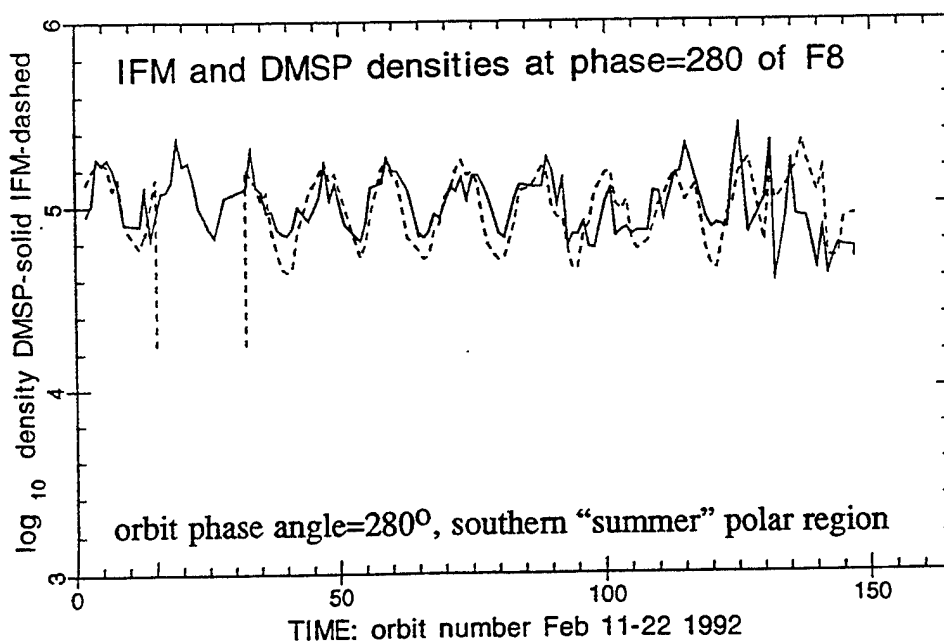
DMSP
F8

- Observations and IFM same dynamic range
- Smaller diurnal variability than in winter
- negligible storm dependencies.

IFM and DMSP densities at phase=160 of F8

orbit phase angle=160°, 1800 LT equatorial region

TIME: orbit number Feb 11-22 1992

DMSP
F8
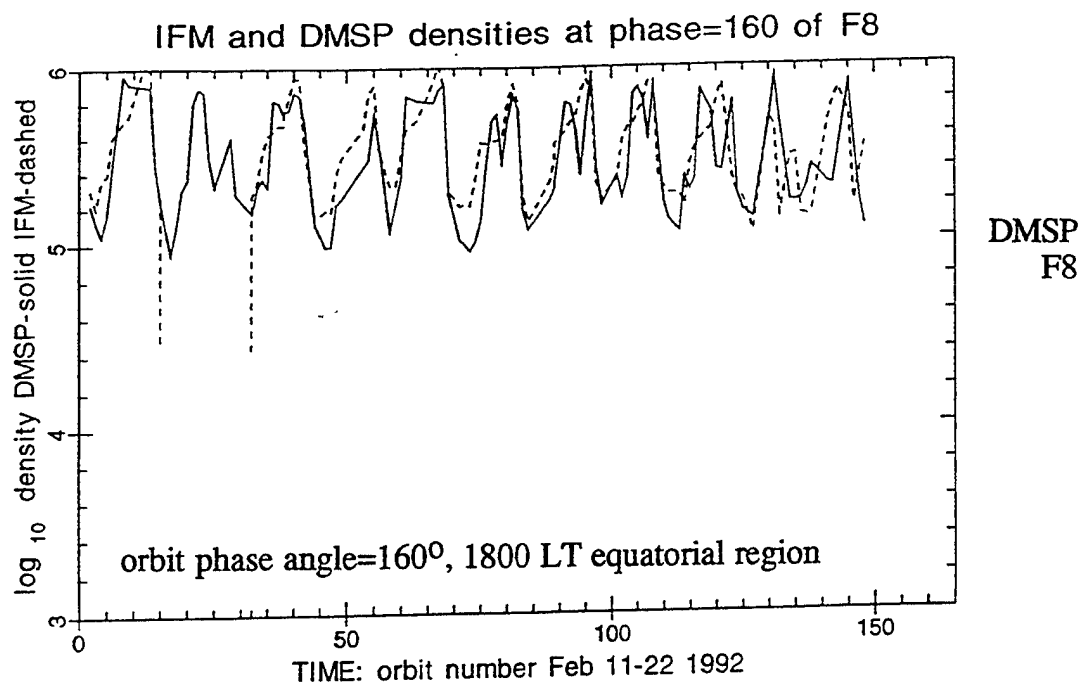
- Observation and model show almost an order of magnitude diurnal variation
- Agreement is very good, phase relationship is good.
- negligible storm effect.

IFM and DMSP densities at phase=350 of F8

orbit phase angle=350°, 0600LT equatorial region

TIME: orbit number Feb 11-22 1992
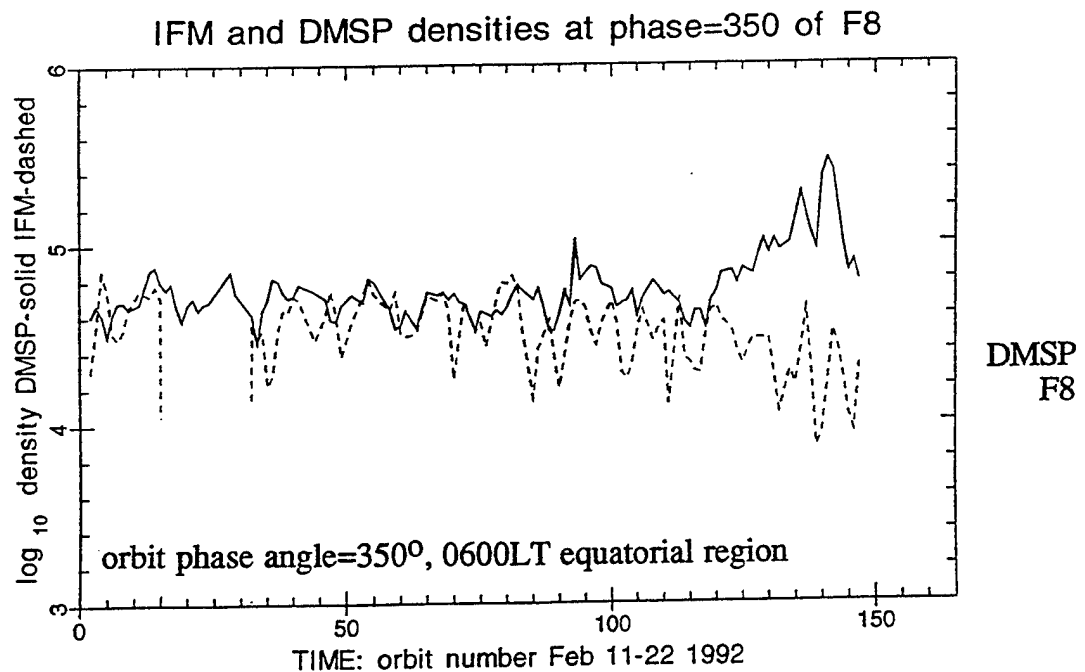
DMSP
F8

- Pre drawn diurnal variability is negligible.
- Agreement good till Kp=5 storm (last 2 days)
- model decreases while observation increases.

IFM and DMSP densities at phase=120 of F9

DMSP
F9

orbit phase angle=120°, evening northern midlatitude

TIME: orbit number Feb 11-22 1992
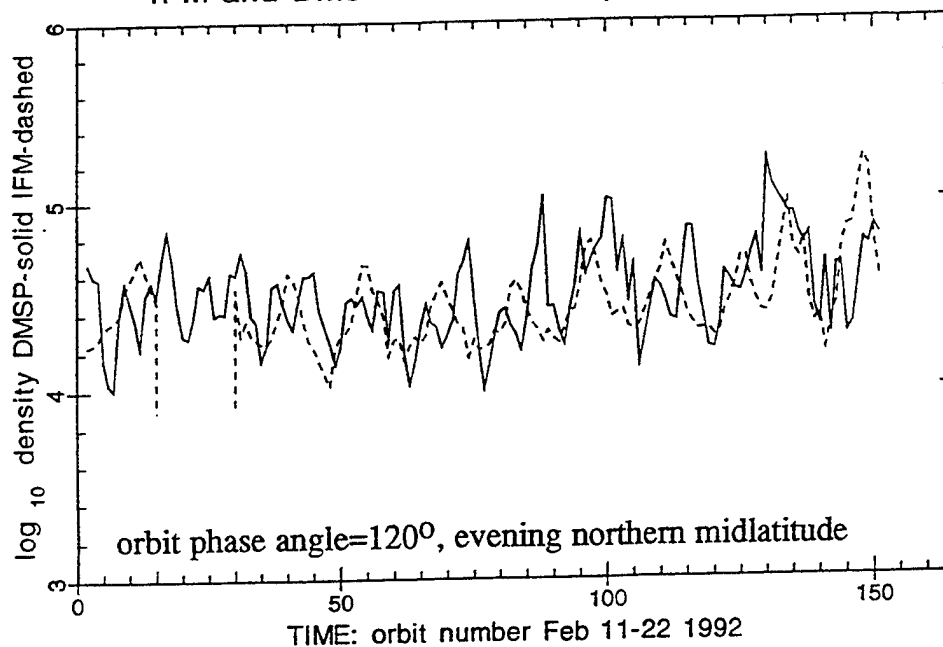
- Dynamic range similar
- Complex diurnal structures
- storm enhanced on last 30 orbits

IFM and DMSP densities at phase=150 of F9

DMSP
F9

orbit phase angle=150°, evening northern equatorial region

TIME: orbit number Feb 11-22 1992
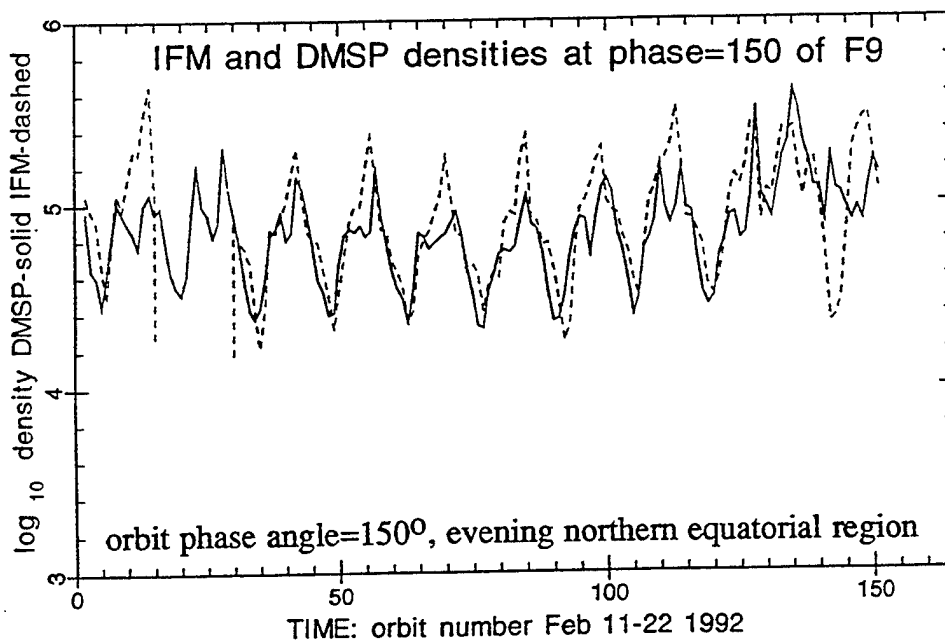
- Dynamic range is very similar
- Complex diurnal structures well reproduced
- Similarities in the storm enhancements.

93

IFM and DMSP densities at phase=30 of F10

orbit phase angle=30°, dawn northern mid latitude

TIME: orbit number Feb 11-22 1992
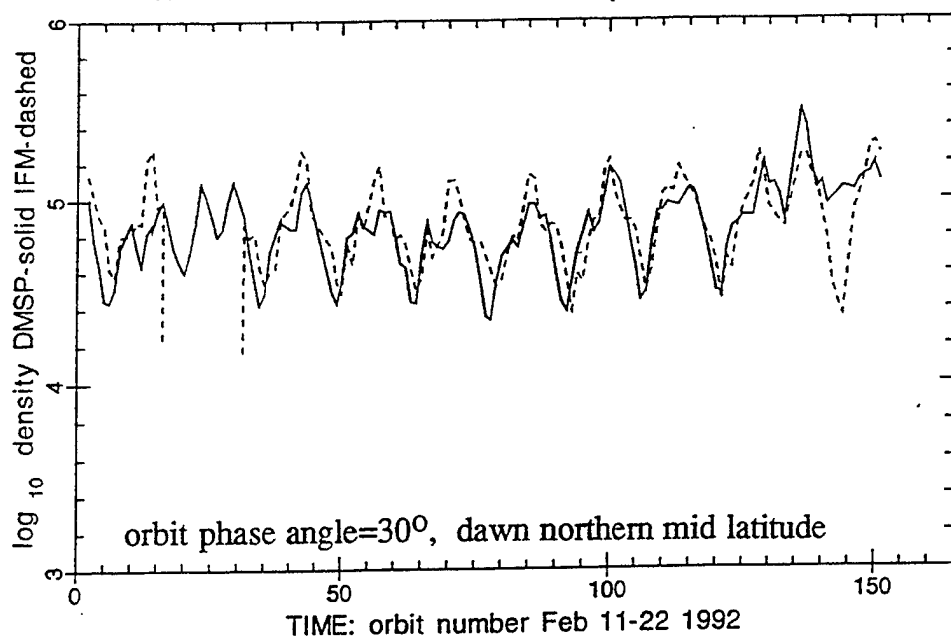
DMSP
F10

- Diurnal variations agree well
- Storm at end is present

IFM and DMSP densities at phase=310 of F10

orbit phase angle=310°, dawn southern midlatitudes

TIME: orbit number Feb 11-22 1992
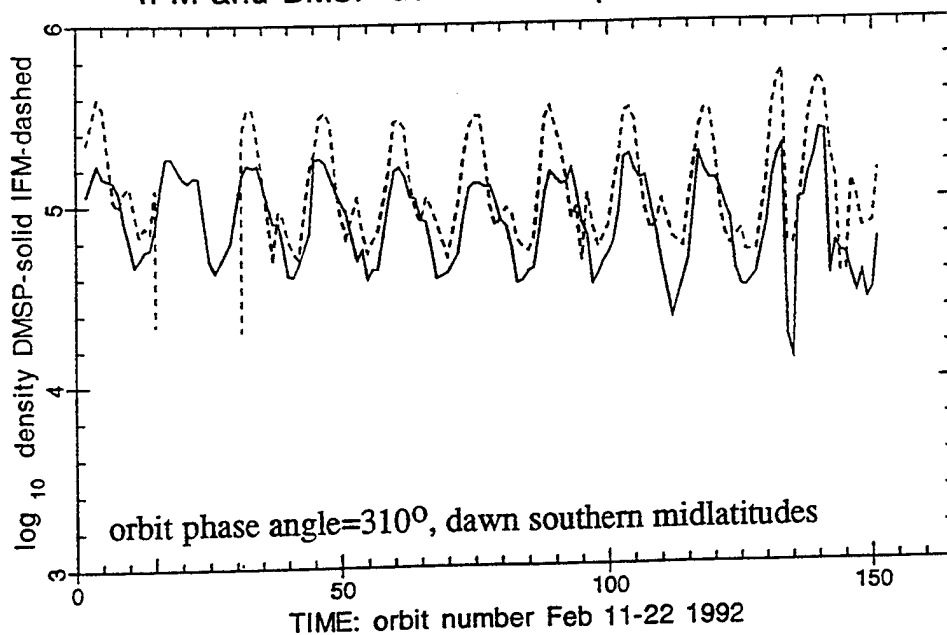
DMSP
F10

- IFM maximum density too high
- Storm effect at end has similar morphology

94

IFM and DMSP densities at phase=200 of F11

DMSP F11

orbit phase angle=200°, dawn "summer" equatorial

TIME: orbit number Feb 11-22 1992
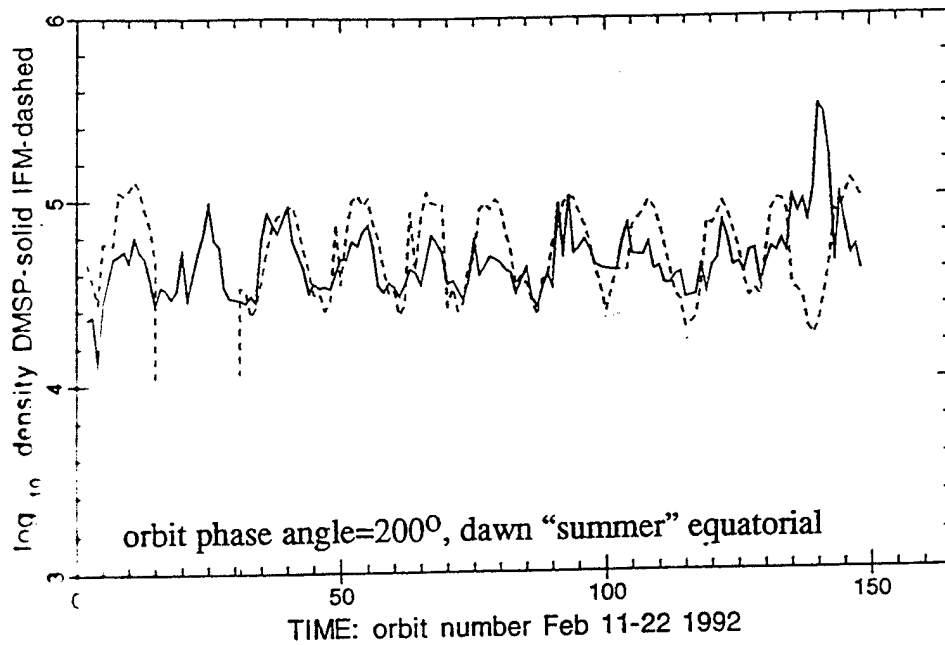
- Observations indicate weak diurnal variation
- IFM models a well defined diurnal variation
- Storm at end is different

IFM and DMSP densities at phase=220 of F11

DMSP F11

orbit phase angle=220°, dawn "summer" midlatitude

TIME: orbit number Feb 11-22 1992
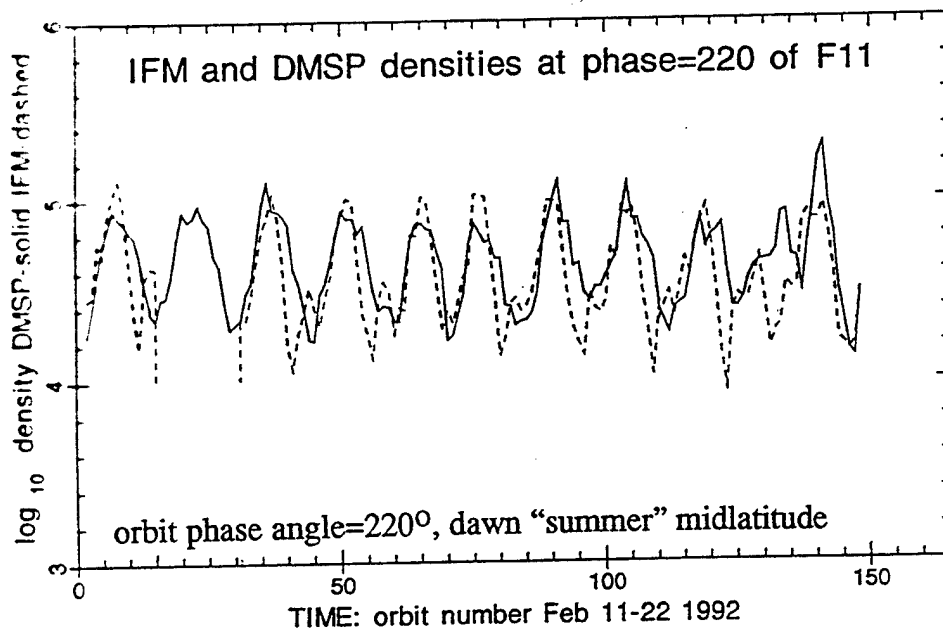
- 20° change in latitude, well defined diurnal modulation
- dynamic ranges agree well
- better storm agreement as well

95

North Pole

MagLat

Equator

0   100   200 South Pole 300

EQ   NP   EQ   SP   EQ

DMSP F 8 ——————
IFM   — — — —
IRI   - - - - -

LOG$_{10}$ Ne (cm^{-3})

LT:05:42:00
UT:01:31:24

12 FEB 1992

0   100   200   300
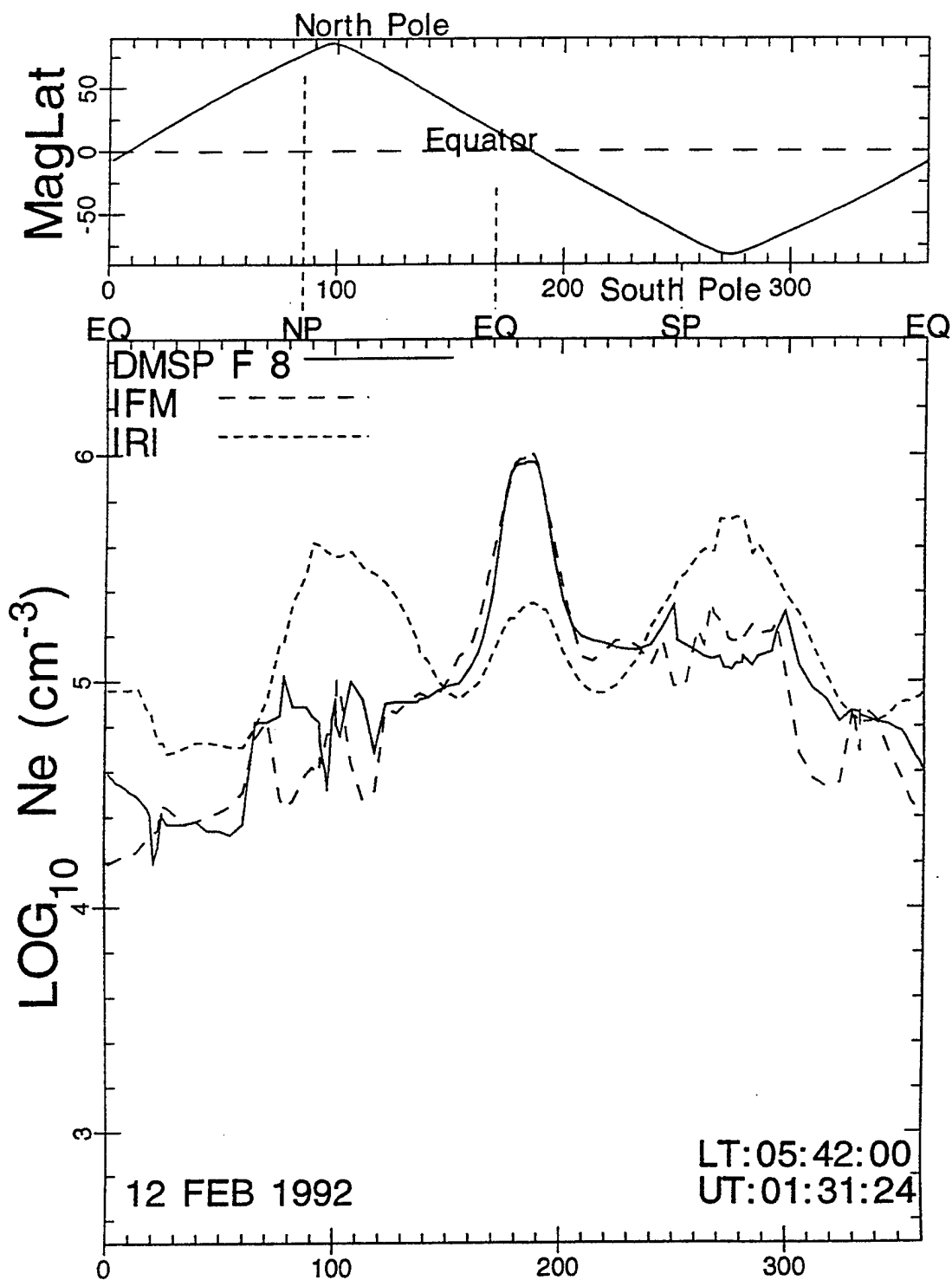
ORBIT # 2 PHASE ANGLE

- IFM and DMSP both show structure in polar regions.
- IRI polar densities are too large
- IFM and DMSP have good agreement at the equators

96

North Pole

MagLat

Equator

South Pole

EQ   NP   EQ   SP   EQ

DMSP F 9 ————
IFM   — — — —
IRI   - - - - - -

LOG_{10} Ne (cm^{-3})

LT:08:44:00
UT:21:49:39

13 FEB 1992
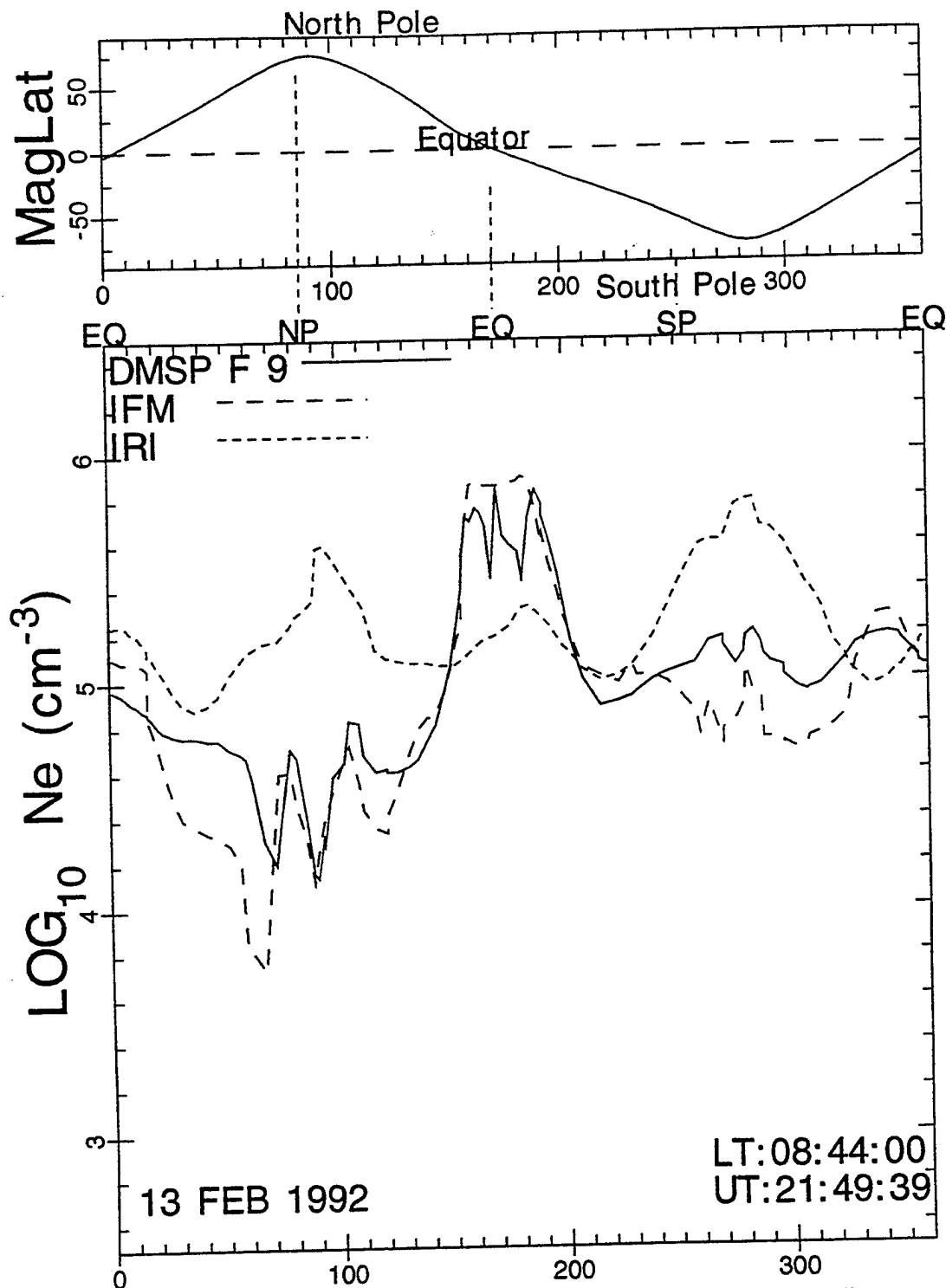
ORBIT #14 PHASE ANGLE

- Northern polar structure is the same for IFM and DMSP
- IRI polar densities are too large
- IFM and DMSP have good agreement at the equators

97
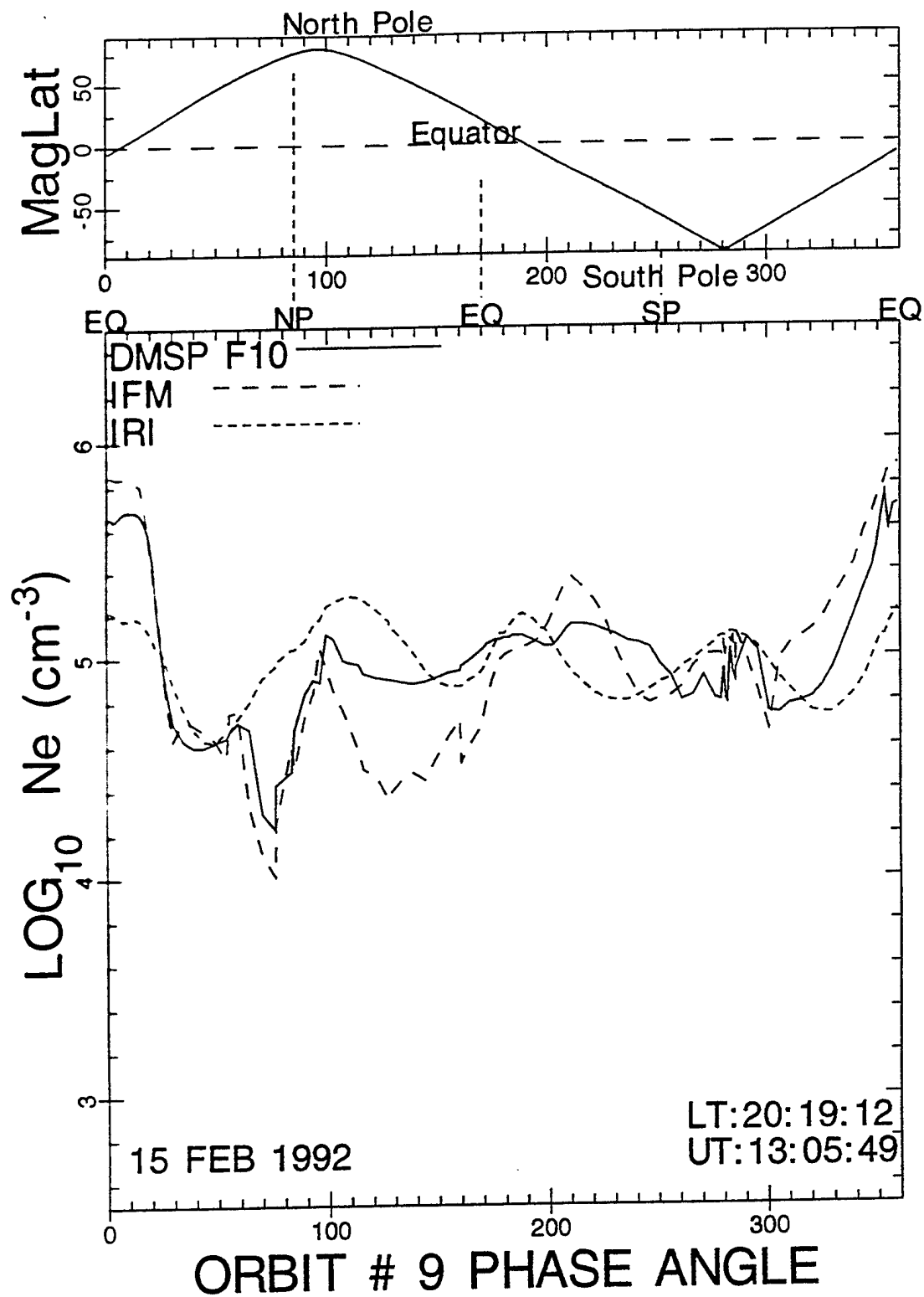
- Polar structure is the same for IFM and DMSP
- IRI polar densities are almost comparable to DMSP
- IFM is low in the winter mid-latitudes, morning sector

North Pole

MagLat

Equator

South Pole

EQ   NP   EQ   SP   EQ

DMSP F11 ————
IFM   – – – –
IRI   - - - - -

LOG_{10} N_e (cm^{-3})

LT:16:30:00
UT:00:50:09

17 FEB 1992
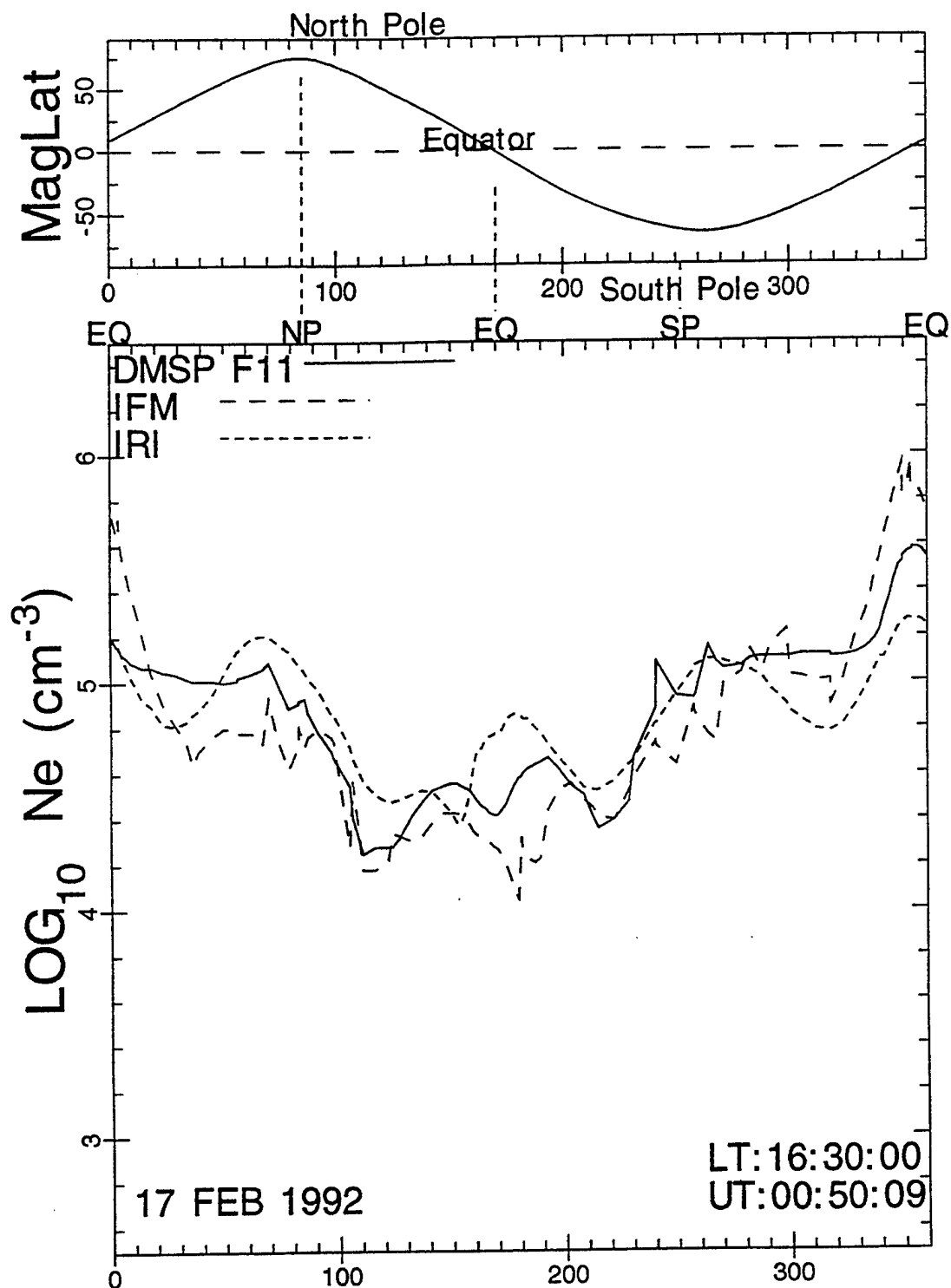
ORBIT # 2 PHASE ANGLE

- Both IFM and DMSP show a double humped equatorial region, phase angles from 150 to 210 degrees.
- IRI orbital variation is similar to that of DSMP and IFM.

VALIDATION DATA BASE

- Should include winter-equinox-summer.
  Should include storm and quiet geomagnetic conditions.
  Solar cycle is difficult, but many instruments were running
  during the last solar maximum.

- Need: a) DISS and other ionospheric soundings.
          b) DMSP and other magnetospheric inputs.

- From December 1991 through April 2, 1992 there were 4
  DMSP satellites; F8, F9, F10, and F11.
  (Then there were 3 through August 2, 94; F8, F10, F11).

- Quiet periods
December 5-9, 1991	4 days
January 21-26, 1992	6 days
February 11-16, 1992	6 days
April 9-14, 1992	6 days

- Disturbed periods
February 17-21, 1992	5 days(major storm)
January 27-29, 1992	3 days(moderately disturbed)
April, 15-16, 1992	2 days(isolated disturbance)

- Prioritization of combined periods

1. January 21-29, 1992	9 days
2. February 11-21, 1992	11 days
3. April 9-16, 1992	8 days
4. December 5-9, 1992	4 days

- These are subsets of the 5 month long data base requested
in IFM quarterly presentation on 2 February, 1994.

Ongoing Validation Objectives

Continue Validation Periods 1 and 2.

- Obtain information on the following:
  DMSP SSIES ion temperature
  DMSP SSIES ion composition
  DMSP SSIES electron temperature
  These are critical in deciding if our suggested problem solutions are the correct ones.

Begin Validation Period 3

- The second interval in February 1992 has a very disturbed period extending over 5 days, while periods 1 and 3 have only small disturbances. Need to compare results.

- Now northern hemisphere is closer to summer.

- Large offset of poles in southern (winter) hemisphere should produce different results than in northern hemisphere.

Validation Issues

- As differences are encountered keep track of them.

- Using the observations establish the magnitude of the differences.

- Try to find the source of the problems, and suggest methods of avoiding the problems.

101

Validation Presented At

March 13, 1996
Models Review Meeting
Boulder, Colorado

IFM Validation #1

The southern hemisphere 0600 UT phenomenon described as a "cliff" or "ledge".

Duncan [1962] and Piggot and Shapley [1962] reported that at midnight around 0600 UT their southern hemisphere ionosonde observations showed a repeatable high f_of2 density at latitudes equatorward of about 70° and at 70° this density dropped to lower values. This sharp cliff or ledge was not present in other longitude sectors at midnight.

Hopkins [1973] using Ariel 3 in-situ plasma and D. Eccles et al [1973] using ISIS-1 topside sounder data verified this feature and produced crude UT plots as well as season averaged snapshots. These clearly show the midnight-0600 UT density enhancements.

IFM reproduces this ionospheric feature.
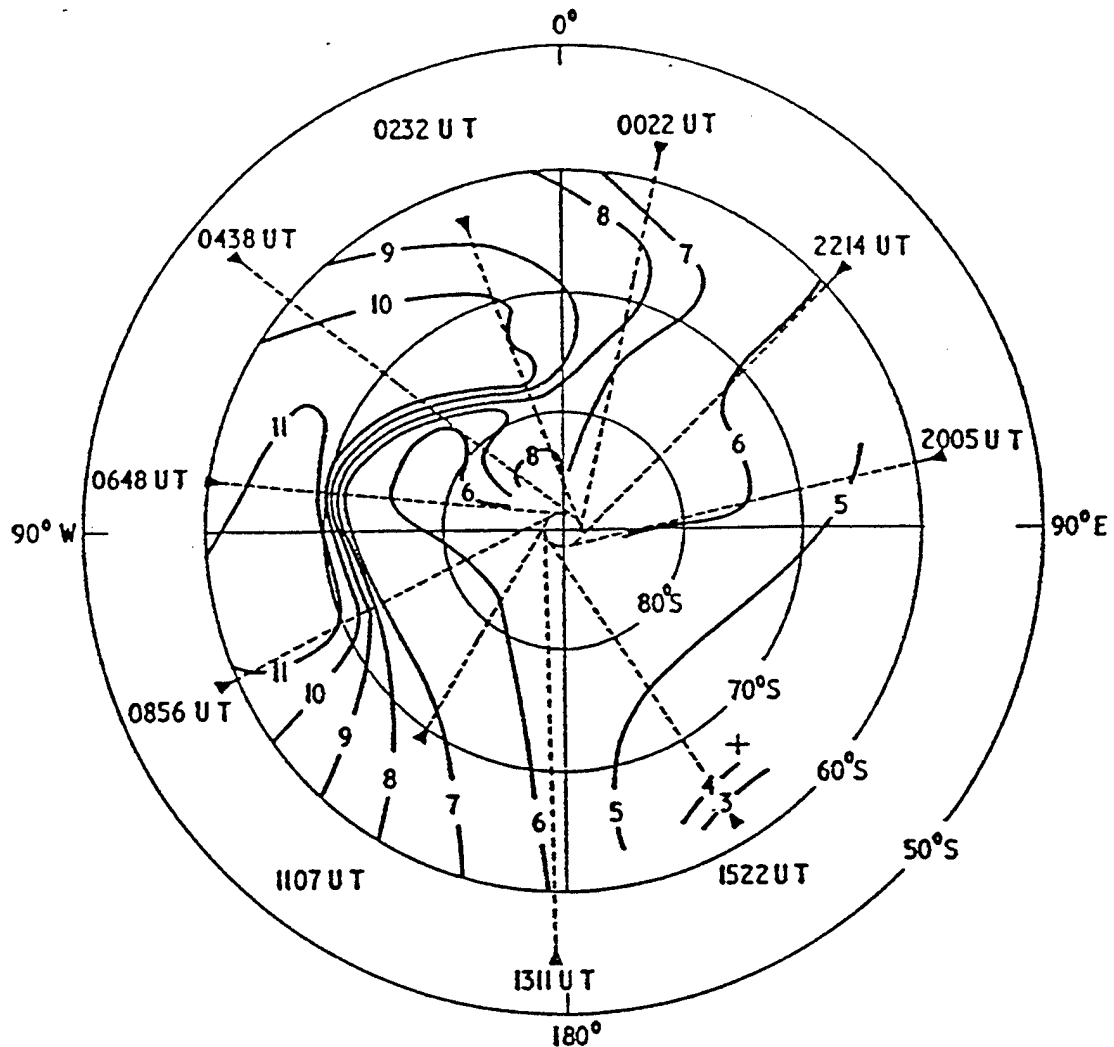
Fig. 1. Contour 'map' of f_oF2 values (MHz) for times near 02 LMT. The data were obtained from consecutive southbound passes (broken lines) of ISIS-1 between 2005 UT on 21 November and 1522 UT on 22 November 1969. The position of the magnetic dip pole (67°S, 141°E) is indicated by a cross.

Space Environment Corporation
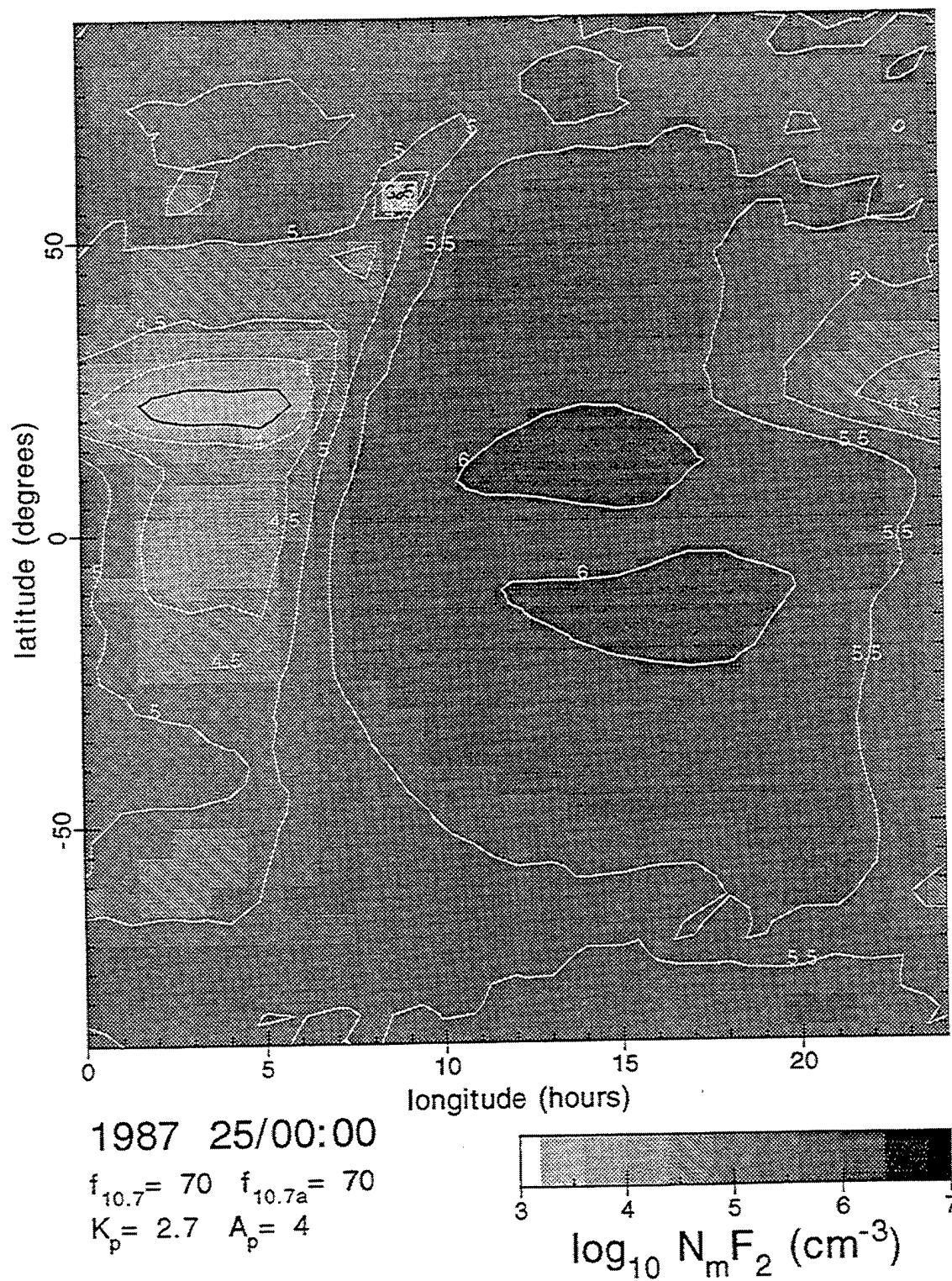
latitude (degrees)

longitude (hours)

1987 25/00:00

$f_{10.7} = 70$ $f_{10.7a} = 70$
$K_p = 2.7$ $A_p = 4$

$\log_{10} N_m F_2$ (cm^{-3})

Model = IFM V2.0 (25 December 1995)

Grid = geomagnetic local time

00:00UT
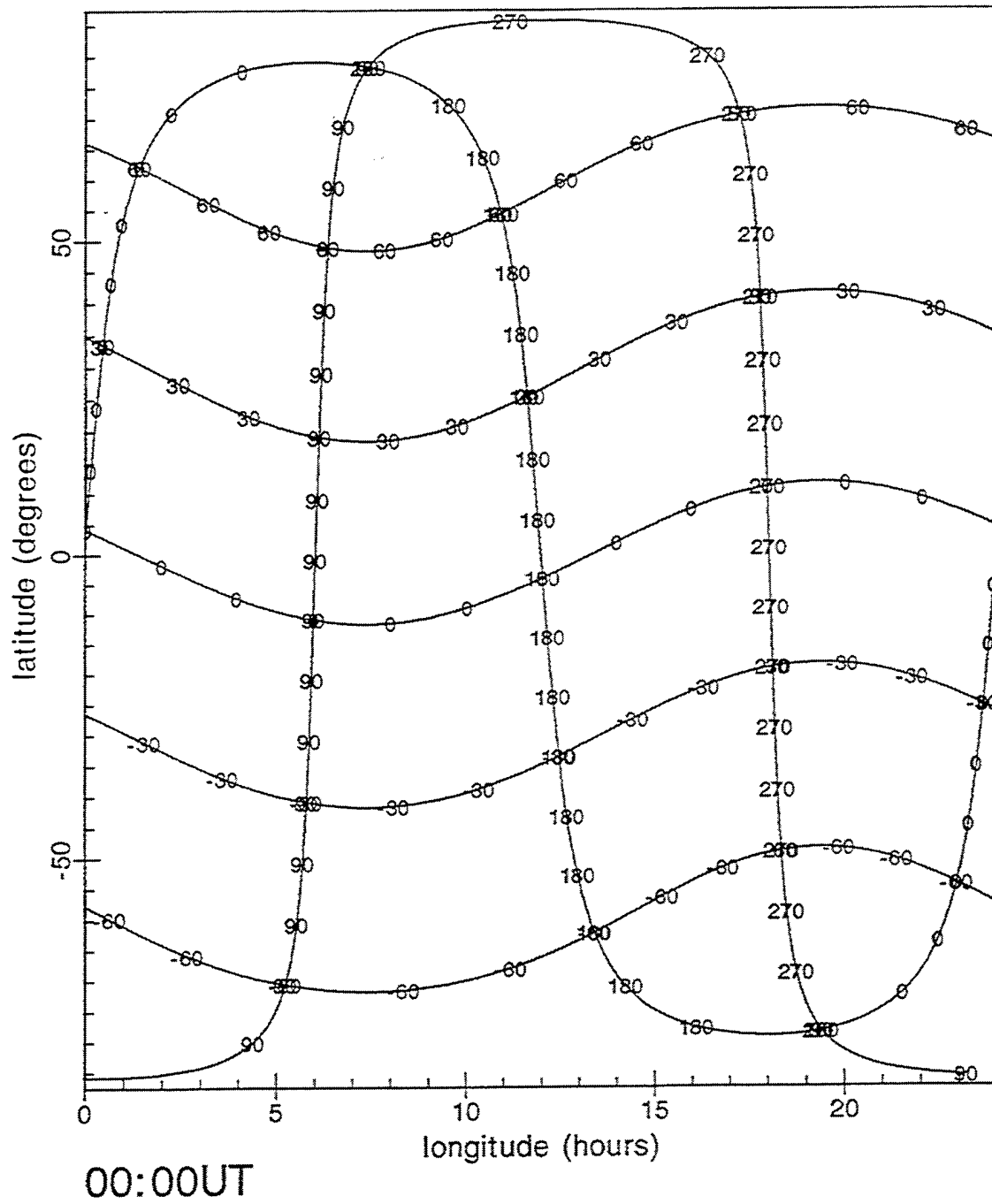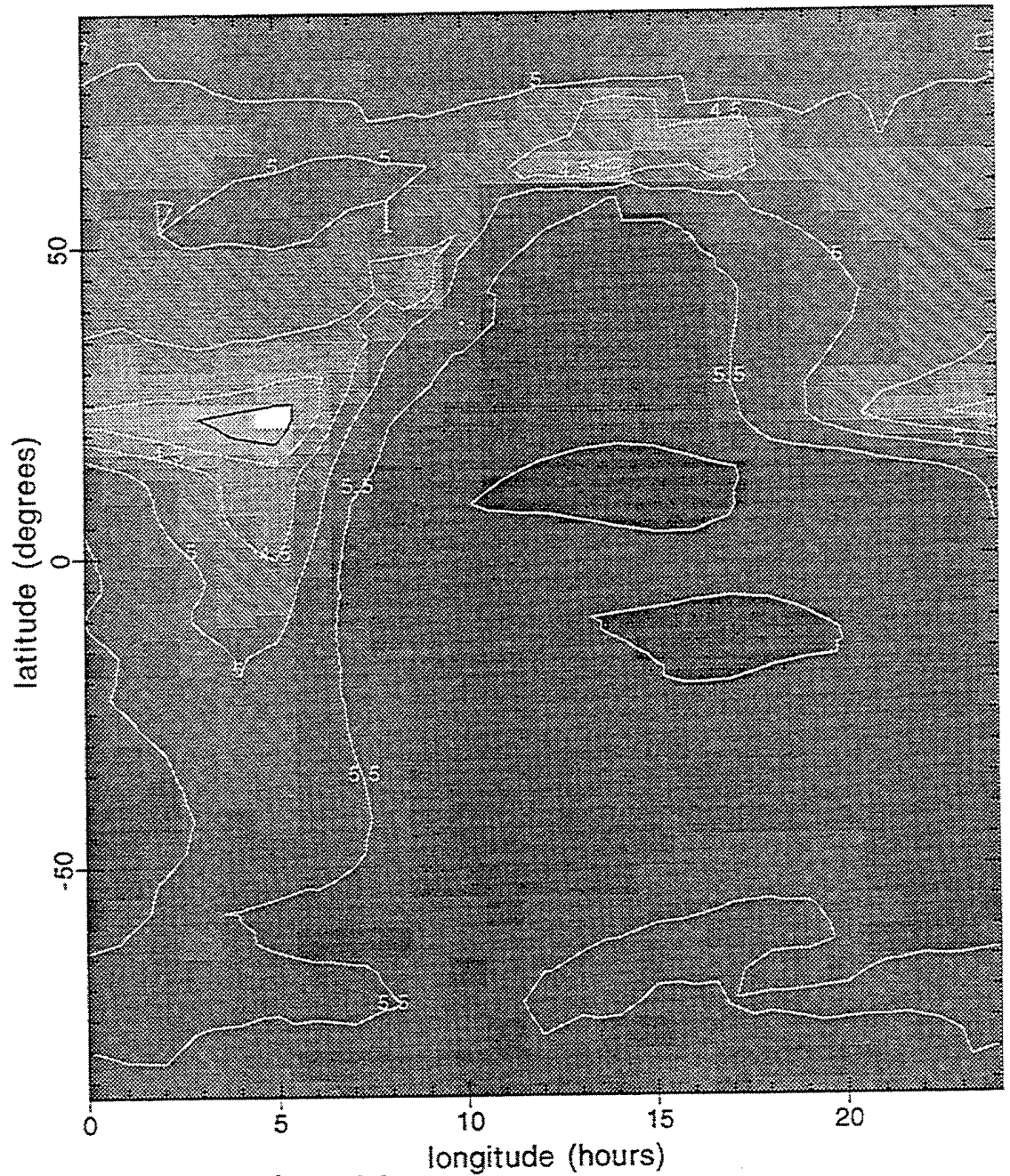
Space Environment Corporation

1987 25/06:00

$f_{10.7}$= 70 $f_{10.7a}$= 70
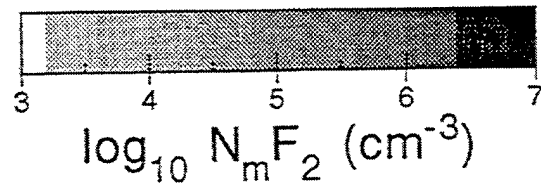
K_p= 0.7 A_p= 4

$\log_{10} N_m F_2$ (cm^{-3})

Model = IFM V2.0 (25 December 1995)

Grid = geomagnetic local time
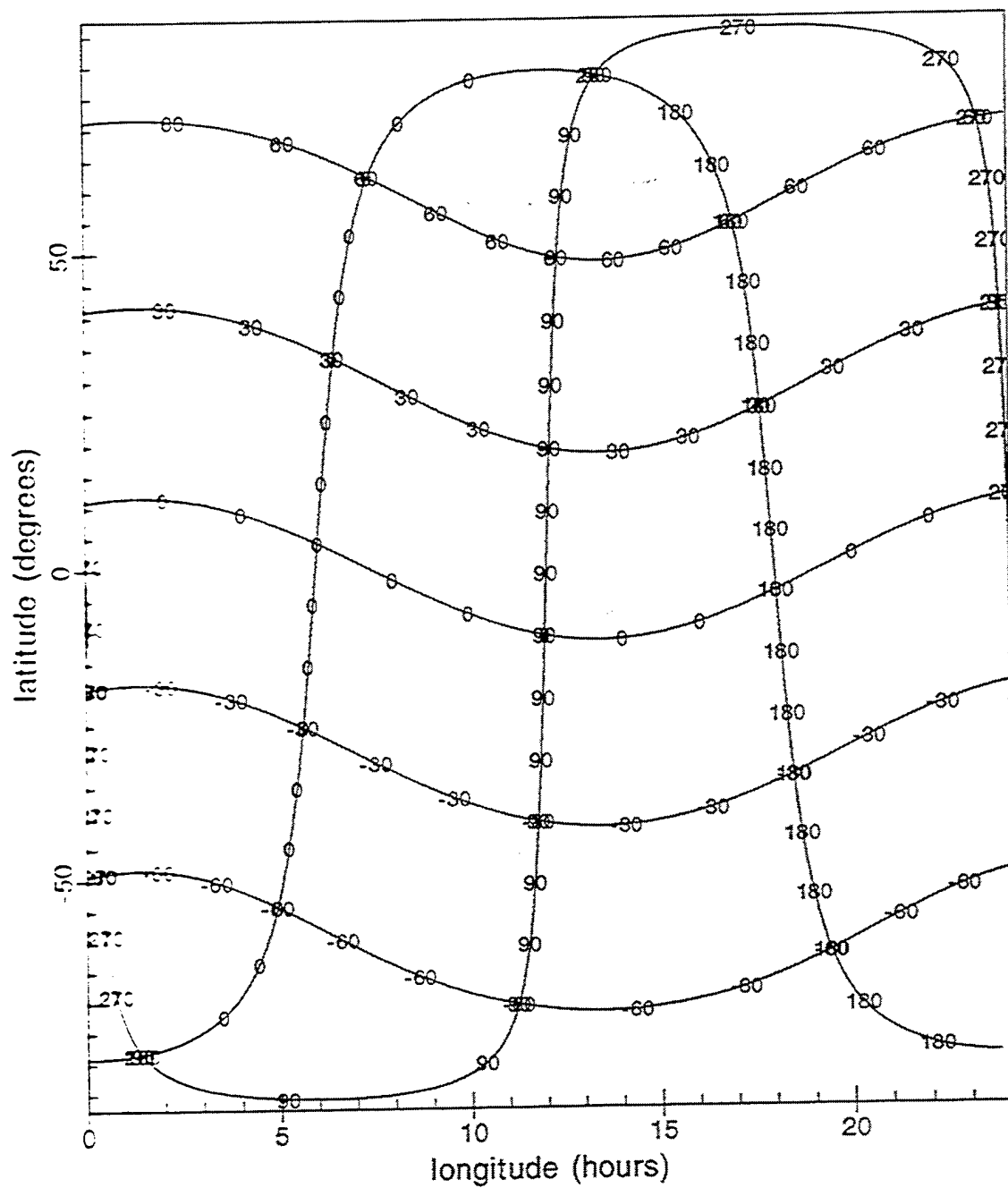
06:00UT

Space Environment Corporation
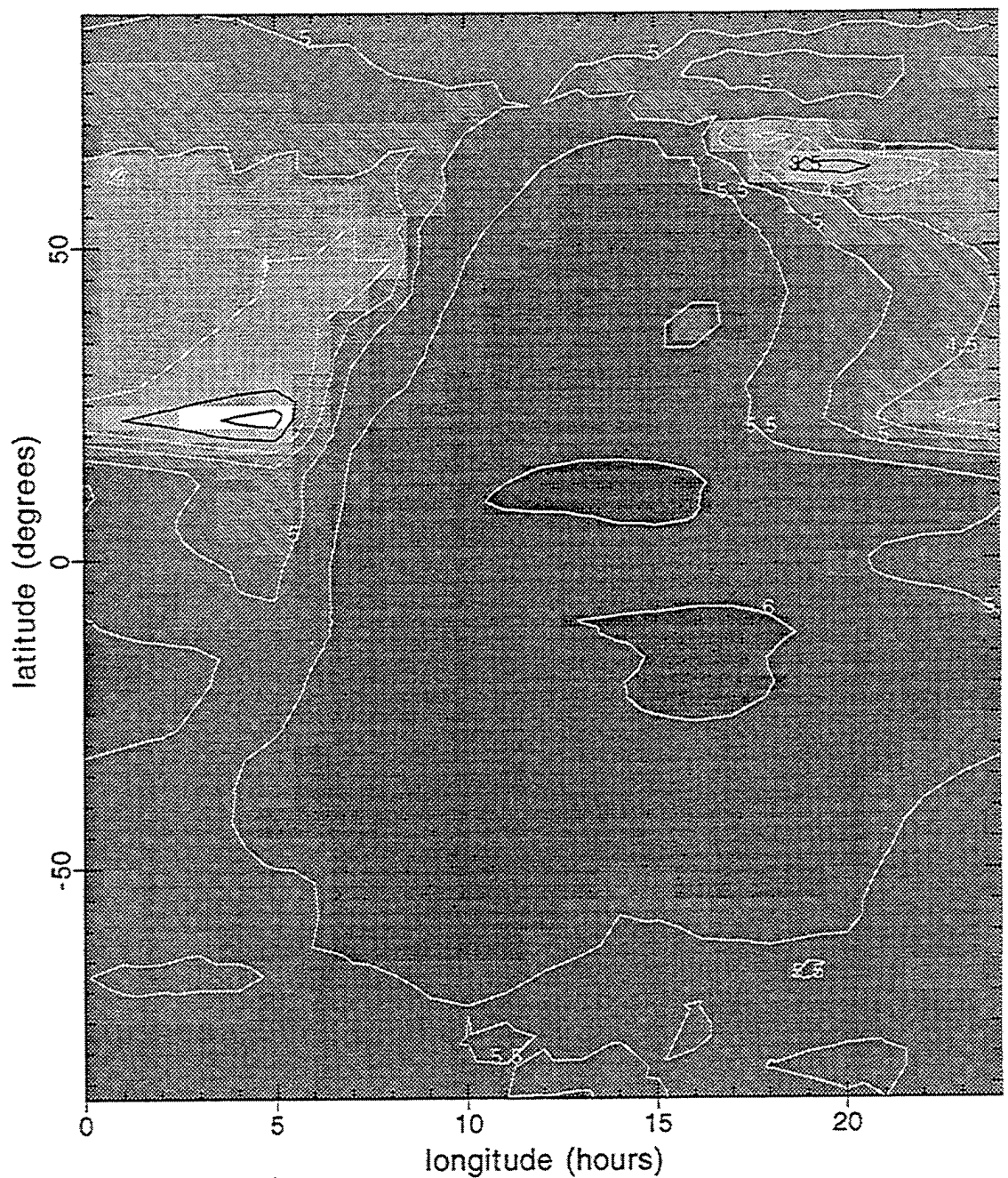
1987 25/12:00

$f_{10.7} = 70$ $f_{10.7a} = 70$

$K_p = 1.3$ $A_p = 4$

$\log_{10} N_mF_2$ (cm^{-3})

Model = IFM V2.0 (25 December 1995)

Grid = geomagnetic local time

12:00UT

Space Environment Corporation

1987 25/18:00

$f_{10.7} = 70$ $f_{10.7a} = 70$

$K_p = 0.3$ $A_p = 4$

$\log_{10} N_m F_2$ (cm^{-3})

Model = IFM V2.0 (25 December 1995)

Grid = geomagnetic local time

18:00UT
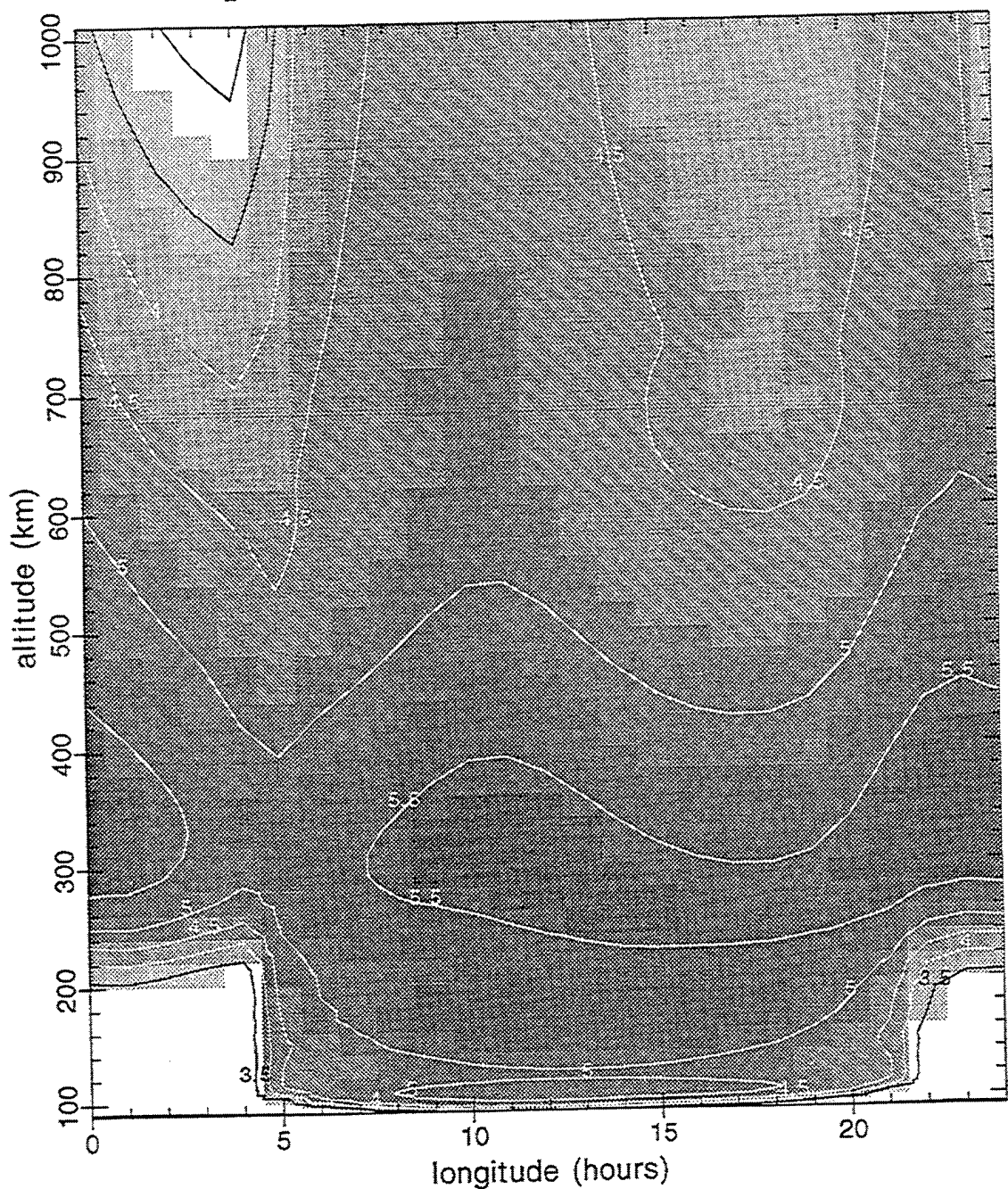
1987 25/06:00

$f_{10.7}$= 70 $f_{10.7a}$= 70

K_p= 0.7 A_p= 4

latitude = -47.5

Model = IFM V2.0 (25 December 1995)

Grid = geomagnetic local time

$\log_{10} N_E$ (cm^{-3})
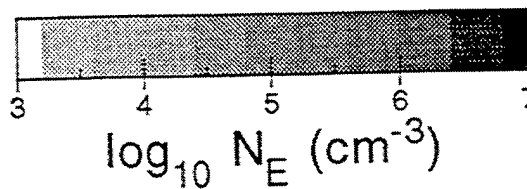
Validation IFM #2

The famous recent tether flight of the Space Shuttle carried in-situ plasma instrumentation. To date the IFM validation has been from topside DMSP or ionosonde (fixed location) observation. The opportunity to compare IFM with IRI and observations is valuable, especially since the shuttle altitude is about 300 km and low inclination.

- Although the mission had notorious complications data was still acquired.

- IFM predictions for Ne were made in advance.

- IRI predictions were also made.

- At 300 km there are "ionospheric" structural differences not predicted by IRI.

- By in large IFM and IRI are in agreement with the gross durinal-orbital Ne variations.

- TEC however is different. The IFM produces small total TEC values in the Appleton Anomaly.

NOTE: NASA has impounded all the shuttle data sets. We need to wait for these data to be released before producing a statement of comparison.

Space Environment Corporation
Log(Ne) at 300 Km
Feb 24, 1996 -- IRI Forecast

115

Space Environment Corporation
Log(Ne) at 300 Km
Feb 24, 1996 -- IFM Forecast

Log(Ne) at 300 Km
Feb 24, 1996 -- IFM Forecast
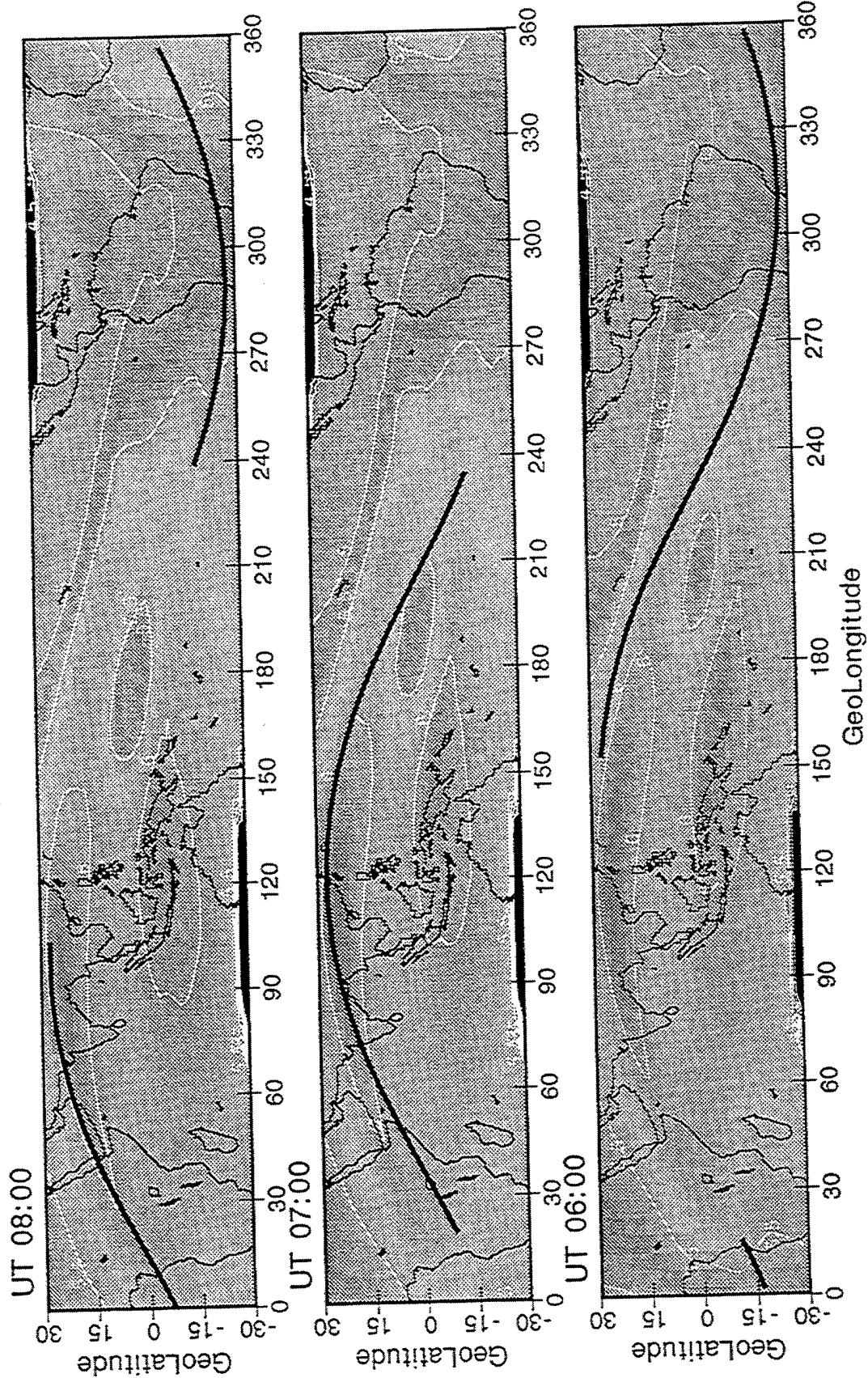
Space Environment Corporation

Feb 24, 1996   1st Ascending Node: 106
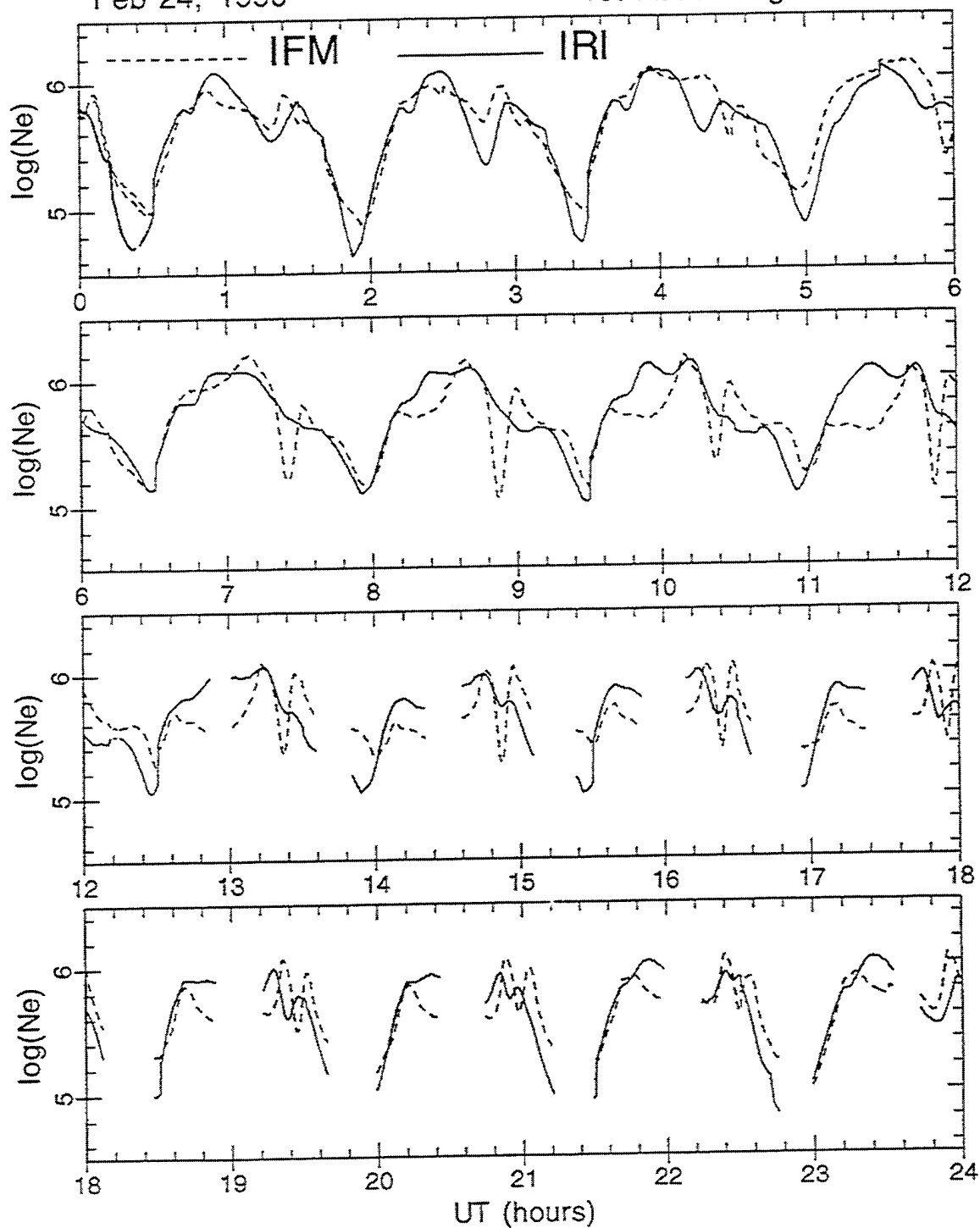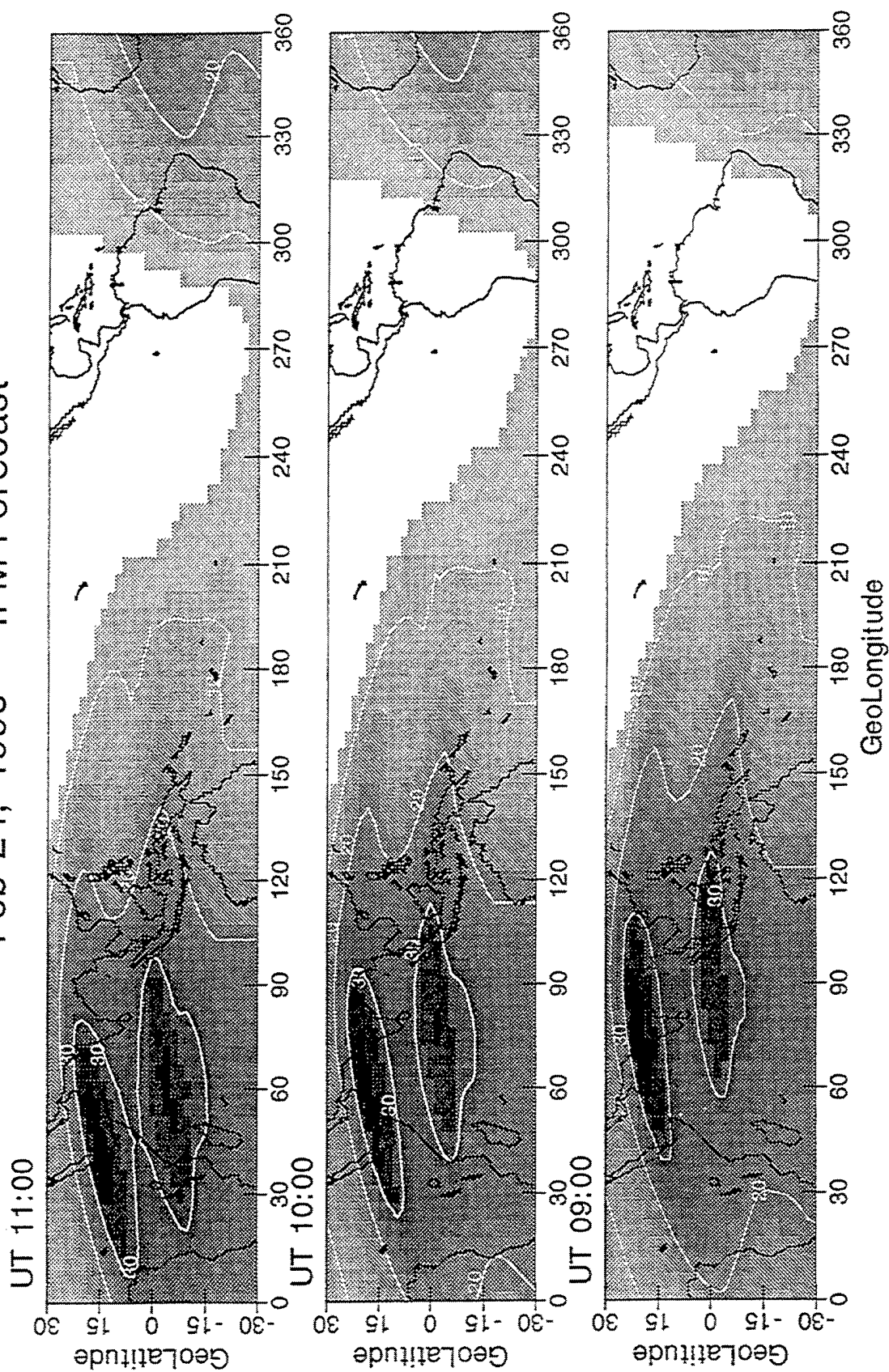
TEC
Feb 25, 1996 -- IFM Forecast
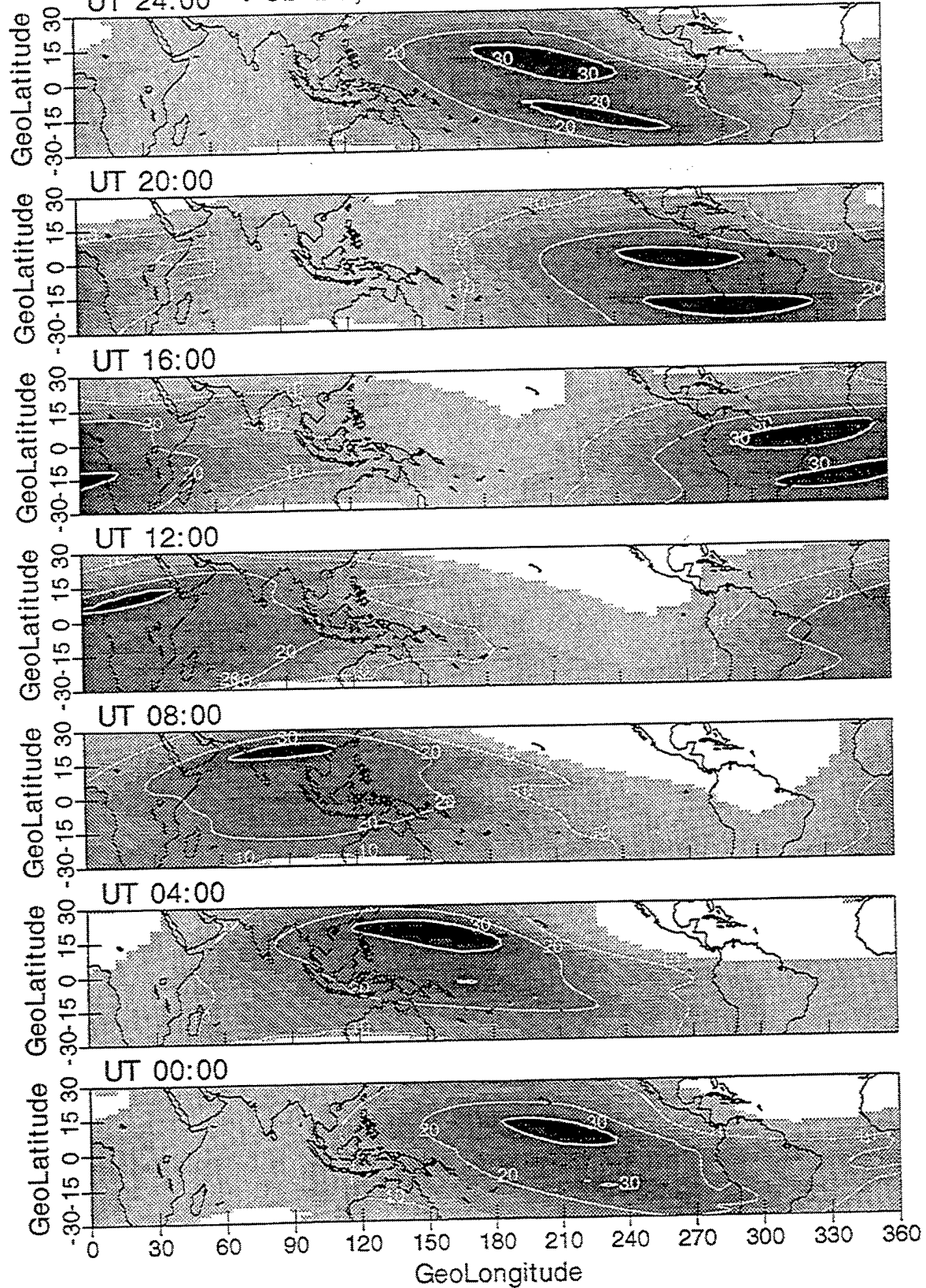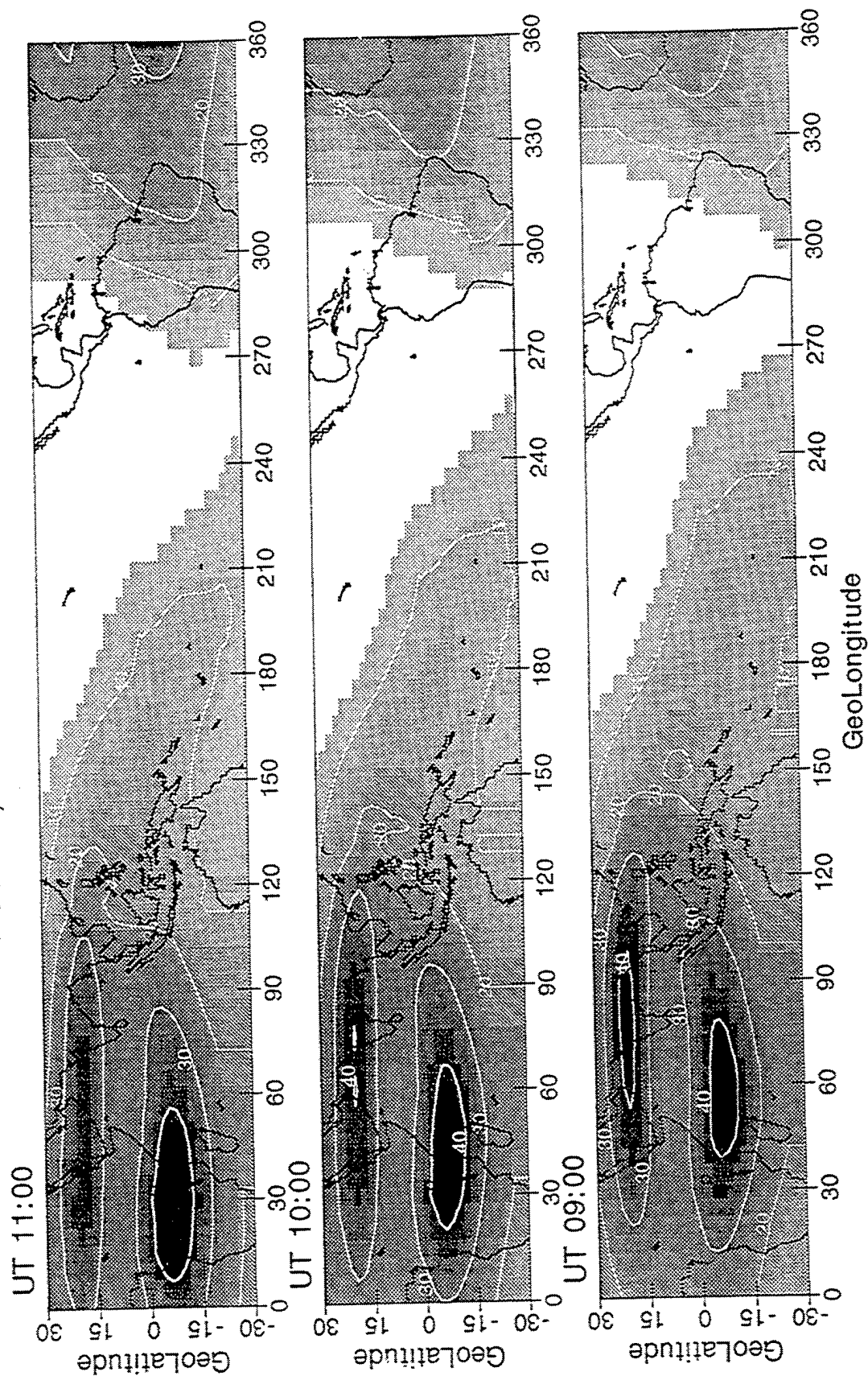
Space Environment Corporation
TEC
Feb 24, 1996 -- IFM Forecast
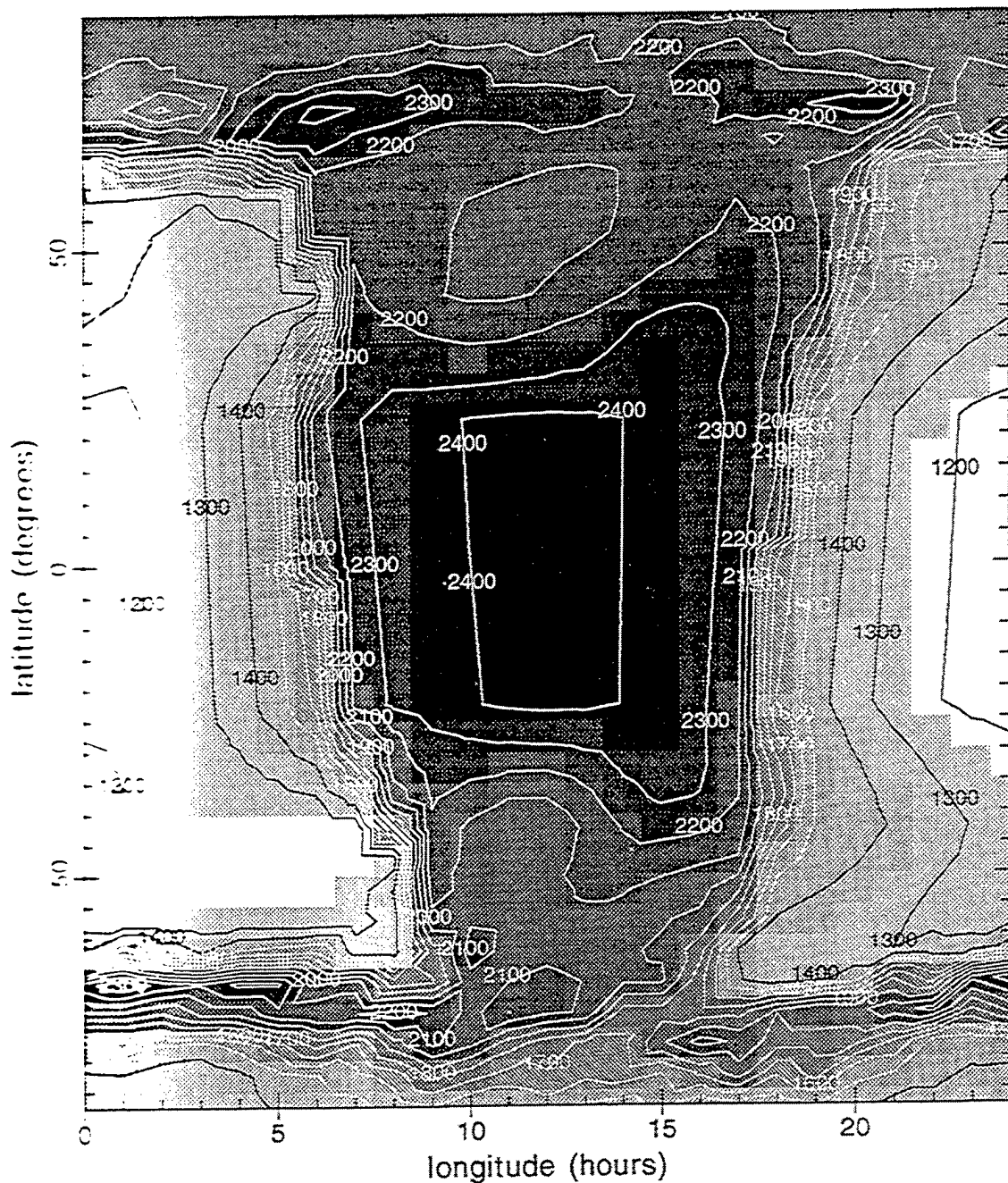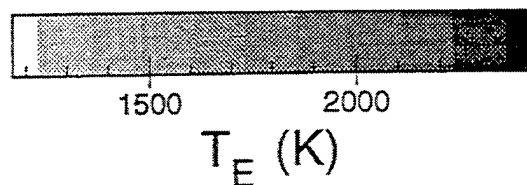
Space Environment Corporation
TEC
Feb 24, 1996 -- IRI Forecast

1991 88/18:00

$f_{10.7}$= 250 $f_{10.7a}$= 250

K_p= 0.7 A_p= 4

altitude = 790

Model = IFM V2.0 (10 July 1995)

Grid = geomagnetic local time
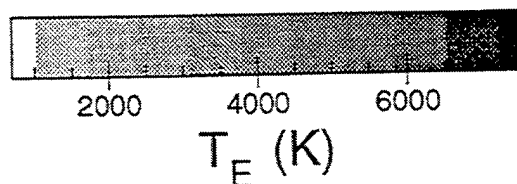
T_E (K)

Space Environment Corporation
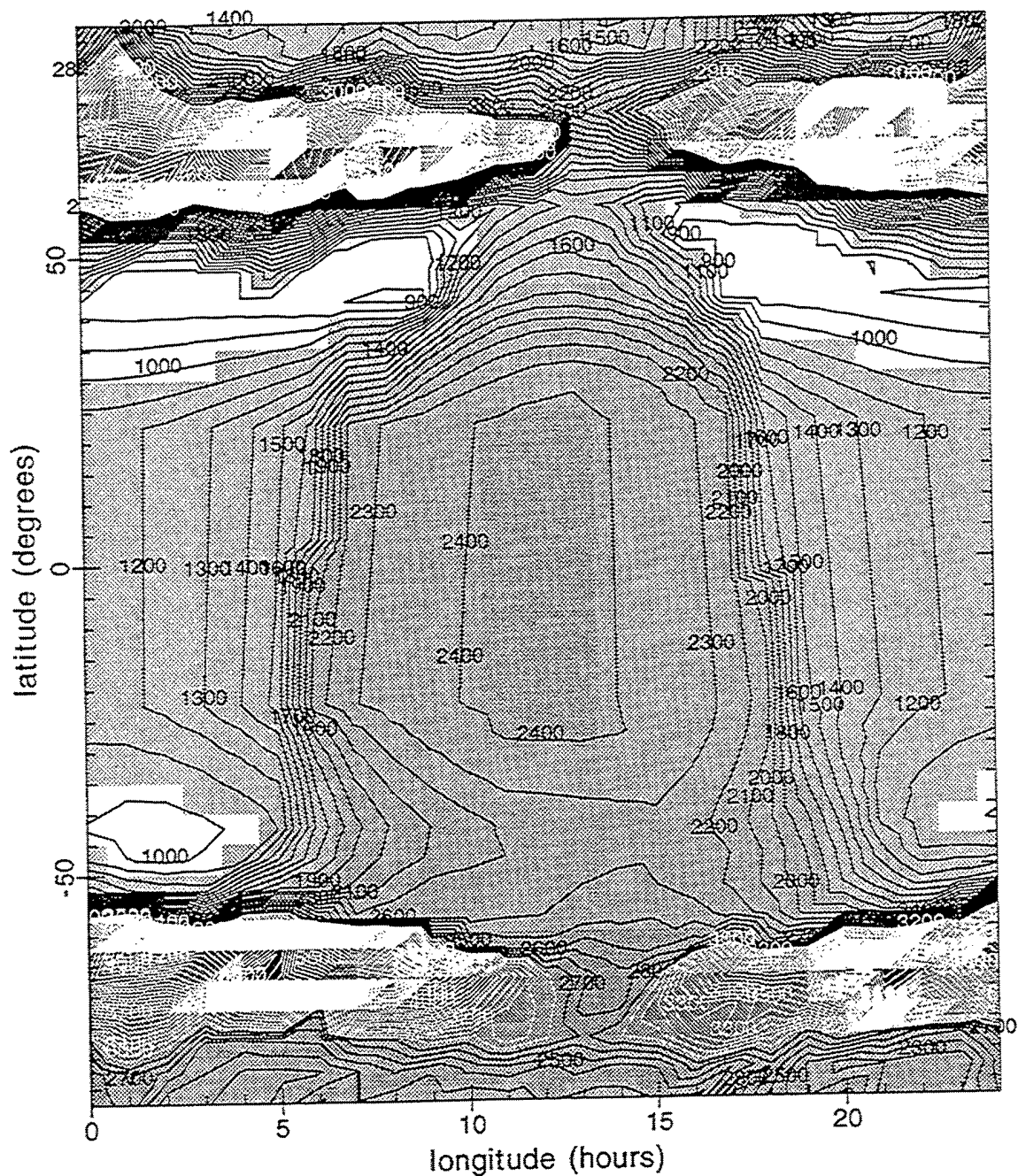
1987 27/06:00

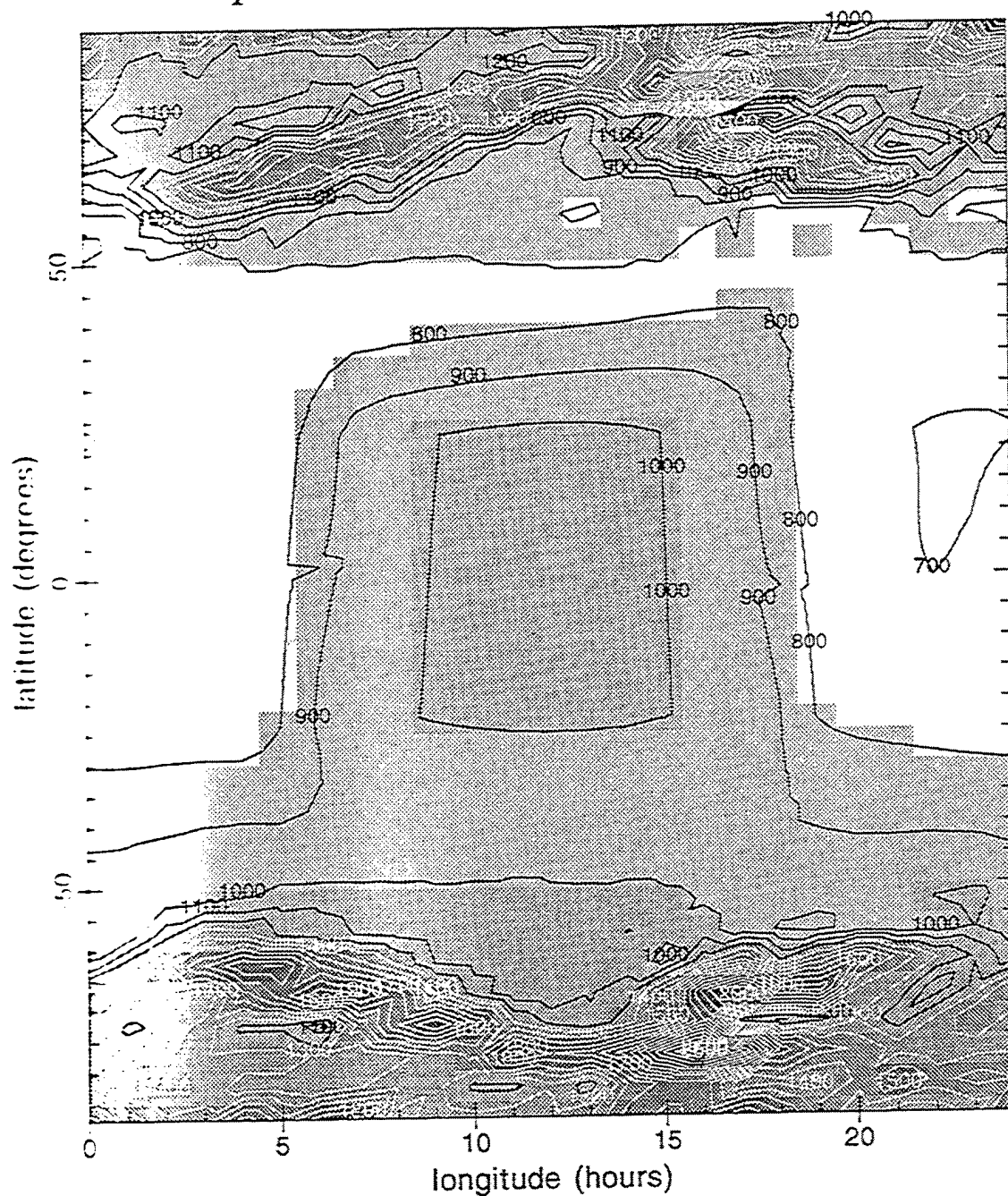$f_{10.7}= 70$ $f_{10.7a}= 70$

$K_p= 6$ $A_p= 86$

altitude = 790

Model = IFM V2.0 (25 December 1995)

Grid = geomagnetic local time

123

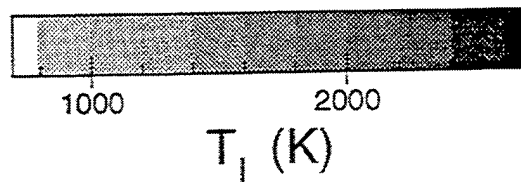Space Environment Corporation

1987 27/06:00
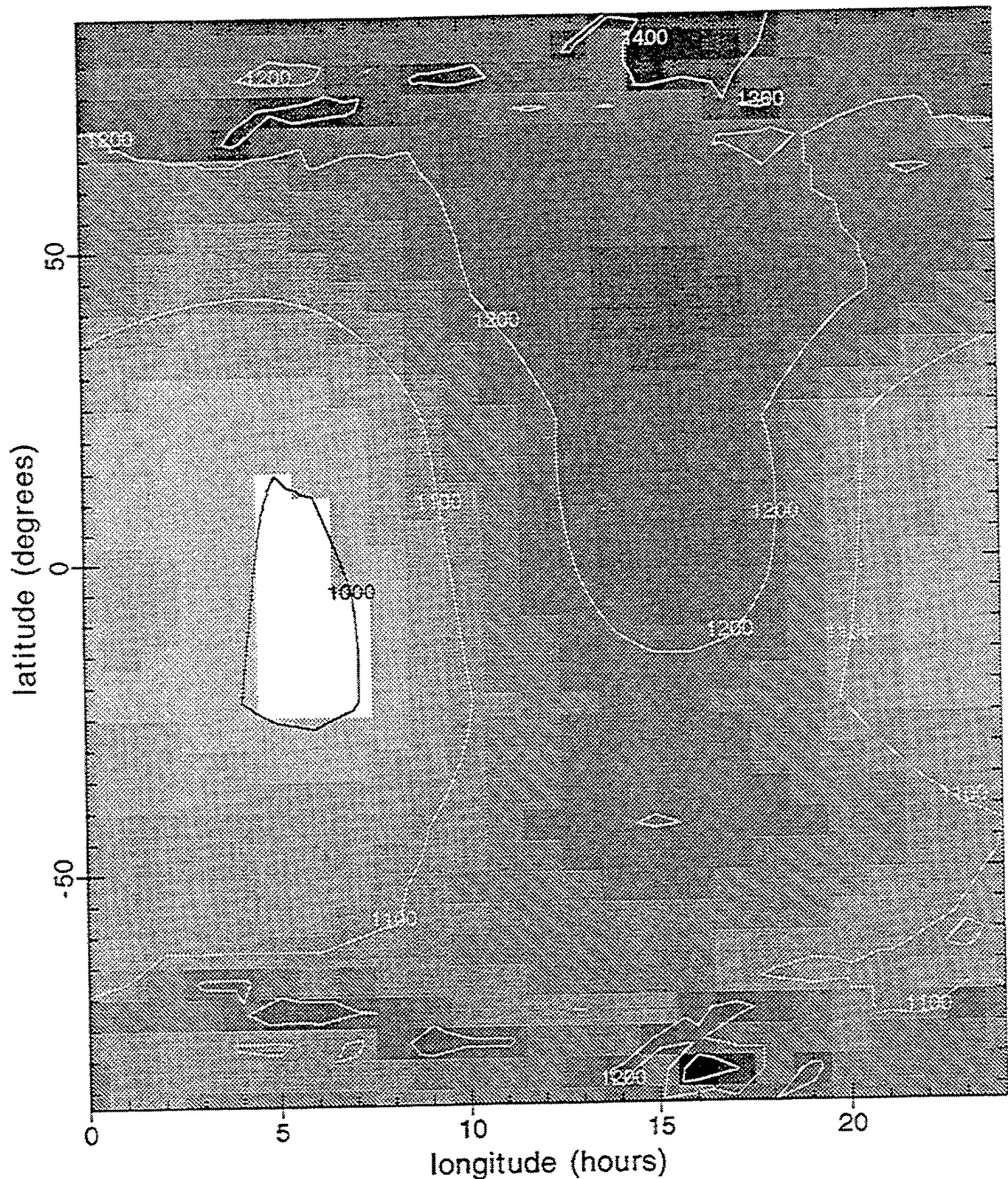
$f_{10.7}$ = 70 $f_{10.7a}$ = 70

K_p = 6 A_p = 86

altitude = 190

Model = IFM V2.0 (25 December 1995)

Grid = geomagnetic local time

T_I (K)

Space Environment Corporation

1991 88/18:00
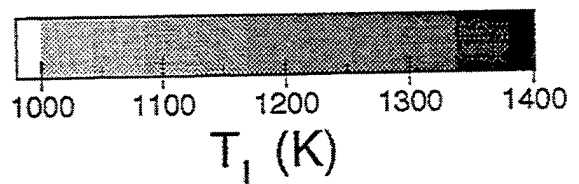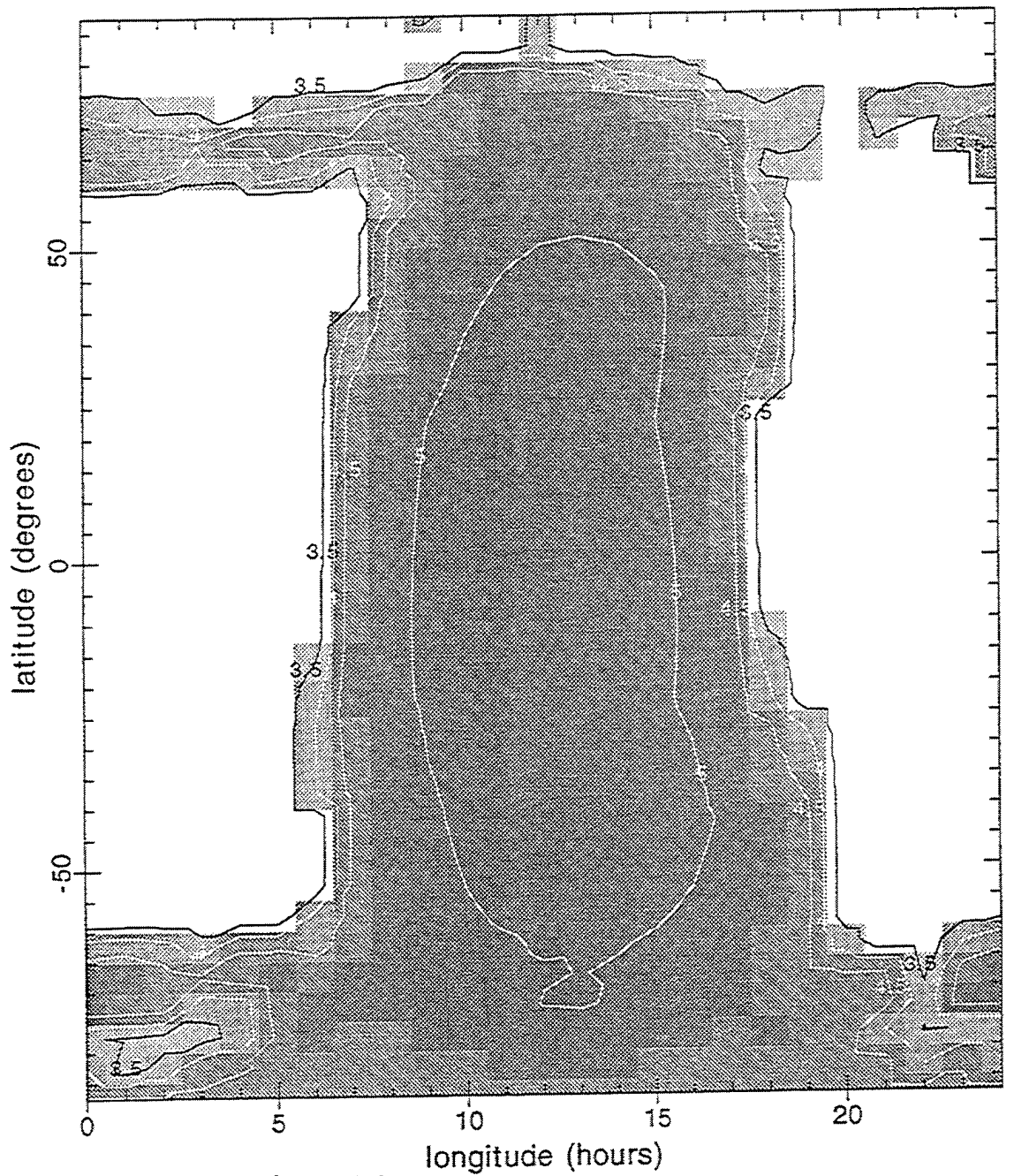
$f_{10.7} = 250$ $f_{10.7a} = 250$

$K_p = 0.7$ $A_p = 4$

altitude = 190

Model = IFM V2.0 (10 July 1995)

Grid = geomagnetic local time

T_l (K)

1987 26/17:00
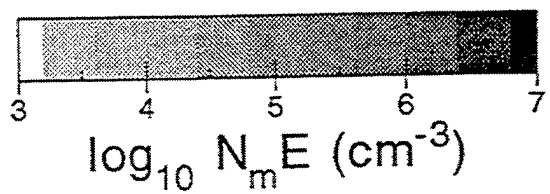
$f_{10.7}= 70$ $f_{10.7a}= 70$

$K_p= 0.3$ $A_p= 4.5$

$\log_{10} N_mE\ (cm^{-3})$

Model = IFM V2.0 (25 December 1995)

Grid = geomagnetic local time

Validation Presented At

January 14, 1997
Models Review Meeting
Boulder, Colorado

Validation of IFM in the Australian Sector

The Australian government through its various branches, IPS and DSTO among other, has extensive ionospheric monitoring and applications capability. This monitoring is not only on the Australian continent but extends both equatorward and poleward in the Australian sector. For this particular validation effort the focus is on the lower mid latitude ionosphere to the equator, 0° to -35° south geomagnetic latitude. The validation is a byproduct of a backscatter ionogram study in which the IFM is being evaluated from the quality of its synthetic backscatter ionograms in the Australian sector. During the month of January 1991 the ionospheric measurements have been extensively studied and an extended data base is available for us to use. This is complemented by the IFM2 validation period 1 data from January 1992.

Data used in this validation

Ionosondes; 4 stations, 1-31 January, 1991

- E-layer F_oE
- F-layer N_mf2
- F-layer M3000 converted to h_mf2
- These data were provided by Phil Wilkinson, IPS, Australia

DMSP, 4 Satellites, 22 January, 1992.

- N_e at 800 km in eight local time sectors.

# Locations of the four ionosondes used in validation

station name	geographic latitude	geographic longitude	magnetic latitude dipole	magnetic latitude invariant
Vanimo	-2.70	141.30	-17.7	-12.3
Darwin	-12.45	130.95	-23.4	-22.9
Townsville	-19.63	146.85	-28.9	-28.4
Norfolk Is.	-29.03	167.97	-34.9	-34.4
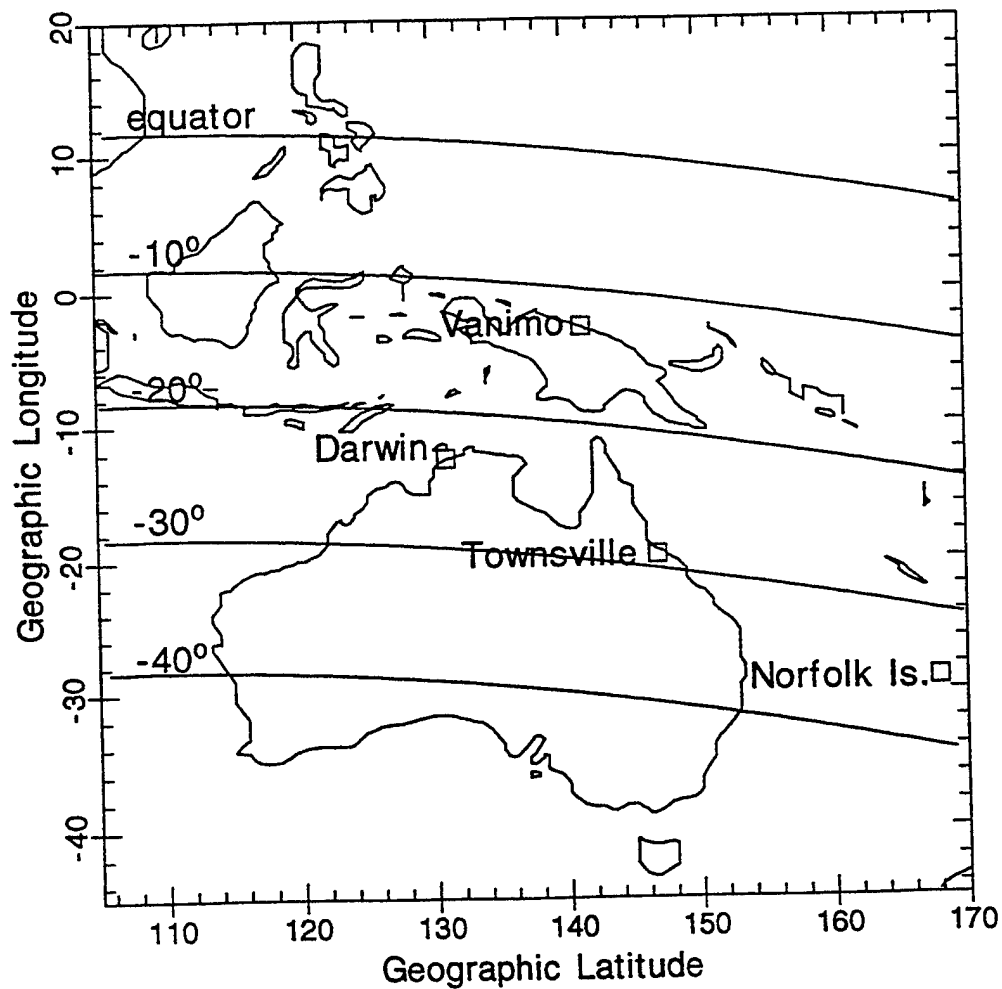
Geomagnetic and Solar Indices, 1 to 31 January 1991

- Kp average is < 2

- Ap daily value average is also very low < 8

- F10.7 is about 200, but from day 20 to 31 it climbs up to 350. The data will be shown for the period prior to day 20.
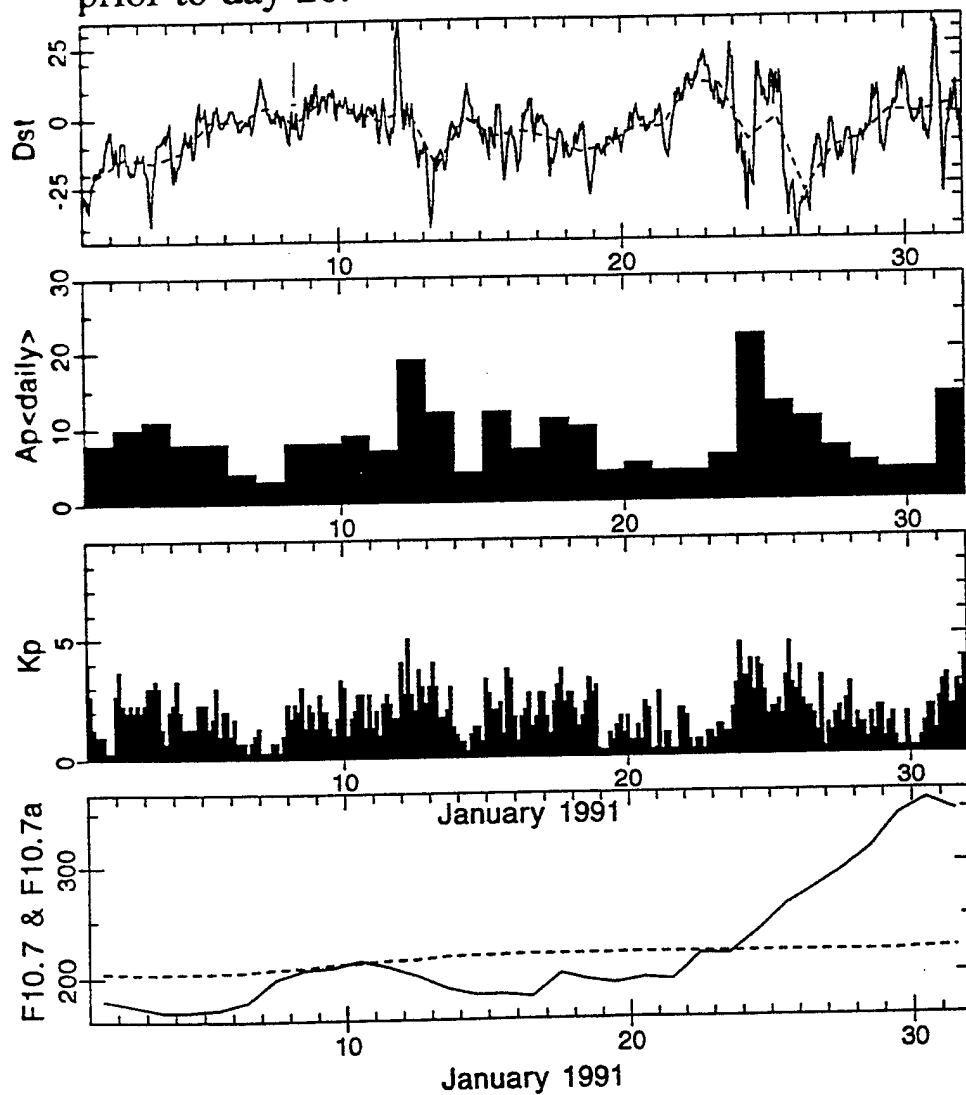
January 1991

F-Layer, N_mf2 and h_mf2, comparison

- During the 1-31, January 1991 period geomagnetic activity was low. This is seen in the ionosonde observations by the repeatability of the diurnal variation in N_mf2.

- The standard deviation of the observed N_mf2 over this 31 day period was;
    - 19.5% at Vanimo,
    - 25.0% at Darwin,
    - 19.4% at Townsville, and
    - 18.5% at Norfolk Is.

- In the N_mf2 plot the error bar on the hour observations uses these standard deviations.

- The N_mf2 IFM model value usually lies within this error bar range.

- Two note worthy exceptions exist.
  At the equatorward stations Vanimo (which is located under the anomaly) and Darwin (under the anomaly shoulder) the pre-noon to about 1400 LT IFM densities are too low.
  The second region is at the most poleward station Norfolk Is at 35^os (magnetic) the post midnight pre-dawn F-layer density in the model is decaying too rapidly and to too low a value. Both of these short comings are discussed further.

- The pre-dawn problem does not showup in the lower latitude stations.

- The h_mf2 variation and comparison is also reasonable, however, other noteworthy differences exist.

- At Vanimo the role played by the equatorial electric field in lifting and lowering the layer to produce the anomaly is evident. In the pre-noon to noon period the model underestimates the layer height. But in the 1800 to midnight sector it overestimates the layer height.

- At all stations the night time layer height is higher in the model than observed, by about 20 to 80 km.

- The two figures are for the 10 January 1991. But are also representative of the other days.

- Overall the N_mf2 from the lower mid latitudes to low latitudes agree with $\leq 20\%$ of the observations, while h_mf2 agrees better than $\pm$ 20km in daylight and tends to be too high at night by 20 to 80 km.
  Note: The simple M3000 conversion used to obtain h_mf2 should be accurate at night when no E-region is present and be more suspect during the day, this trend is contrary to the above discussion.
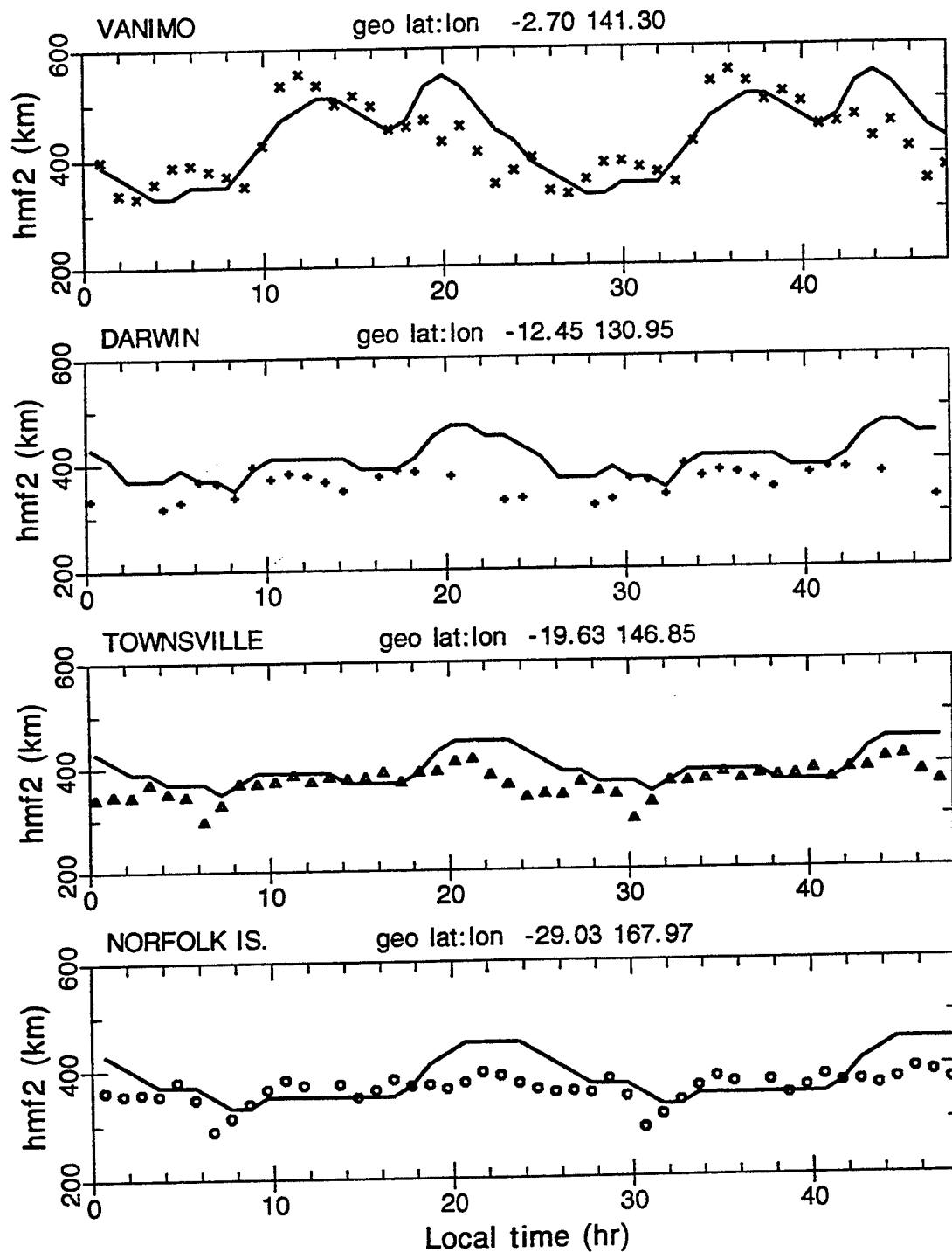
F-layer density comparison on 10 January 1991.

Observations are shown by symbols and IFM by the line
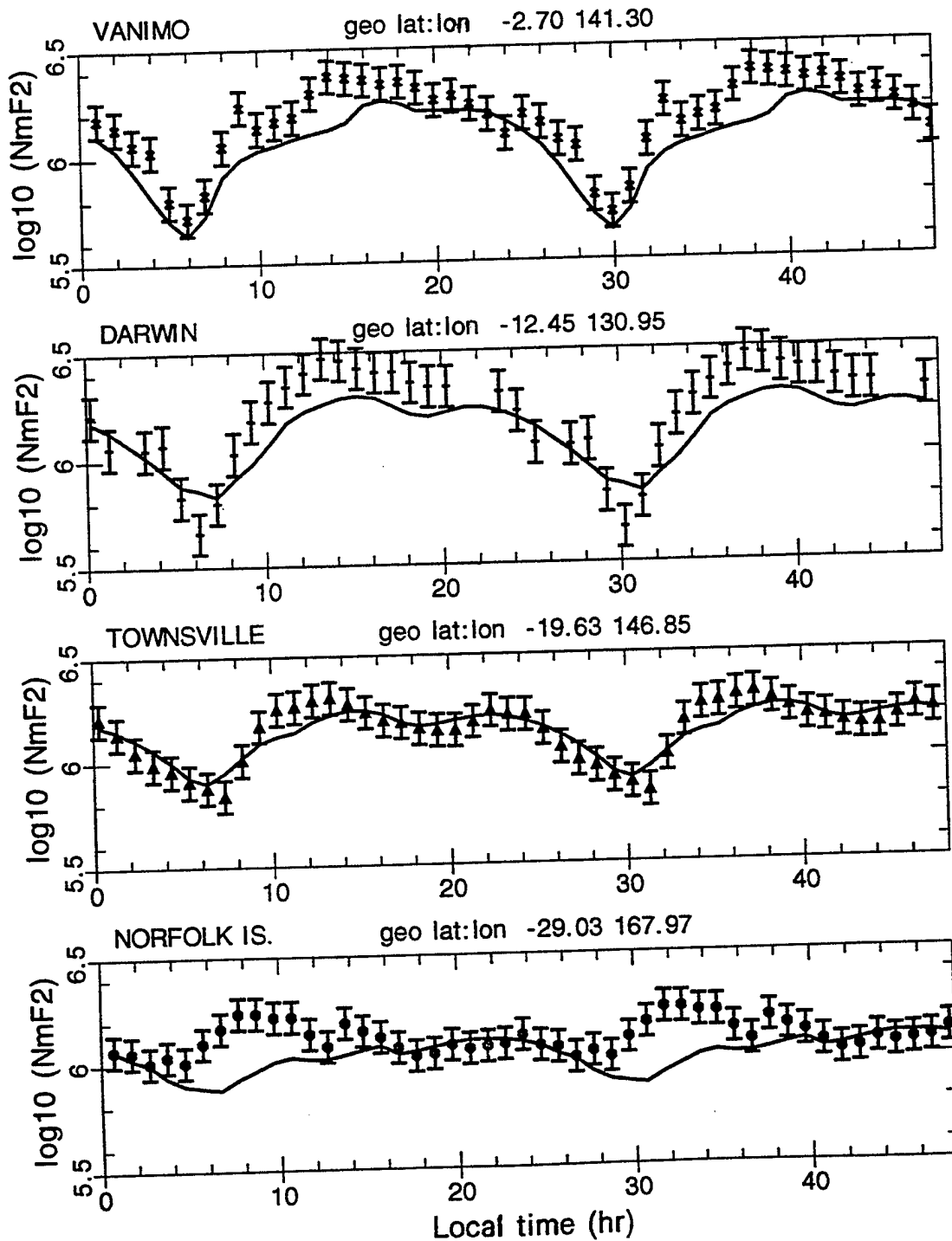
F-layer height comparison on 10 January 1991.
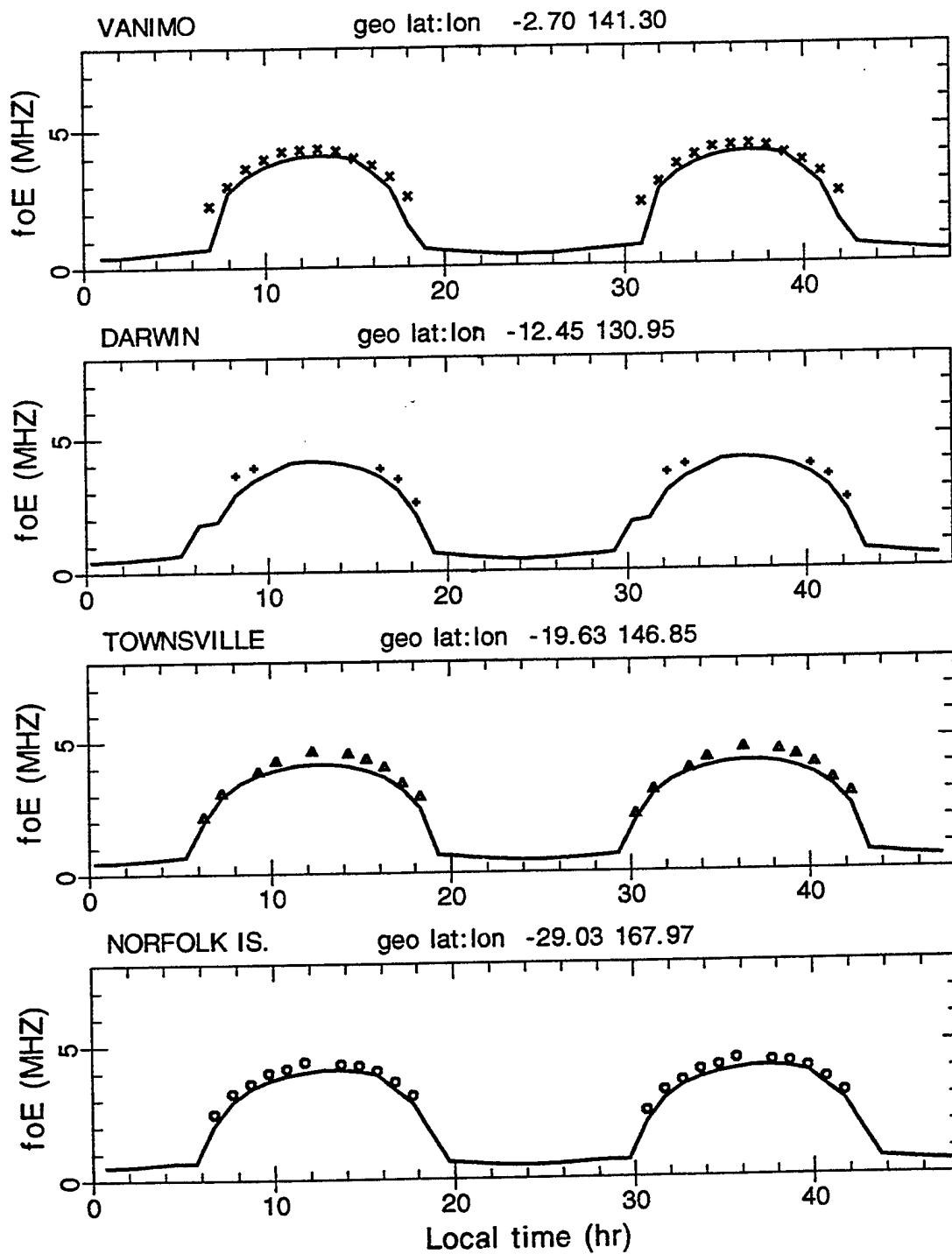
Observations are shown by symbols and IFM by the line

VANIMO   geo lat:lon   -2.70 141.30

DARWIN   geo lat:lon   -12.45 130.95

TOWNSVILLE   geo lat:lon   -19.63 146.85

NORFOLK IS.   geo lat:lon   -29.03 167.97

Local time (hr)

E-Layer density comparison

- Observations are only available during daylight hours when F_oE is greater then a megahertz.

- The E-layer shows almost the same diurnal variation at all 4 stations.

- The electric fields, winds and interhemispheric transport have a small effect.

- The solar flux is the controlling input.

- Over this month the IFM daytime F_oE values are typically smaller than those observed but by less than 0.2 MHz.

- This corresponds to a density difference of less than 10% at 5 MHz.

E-layer comparison on 10 January 1991.
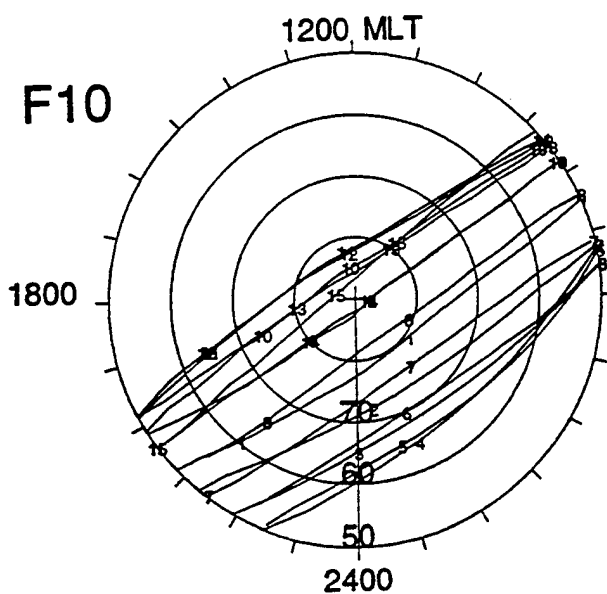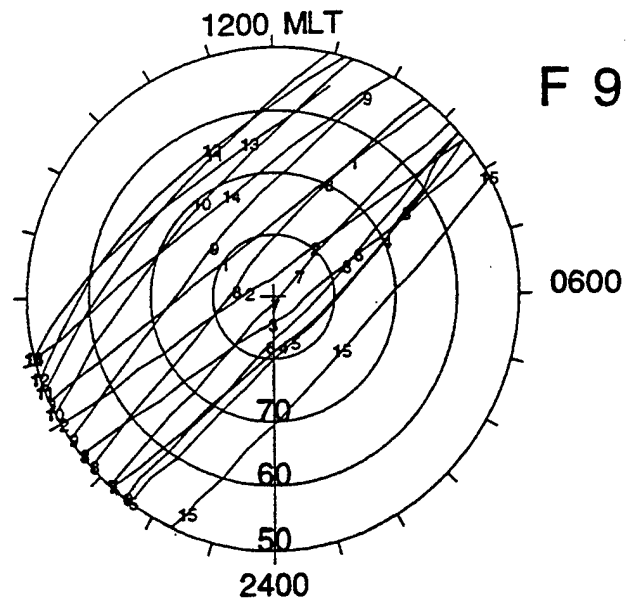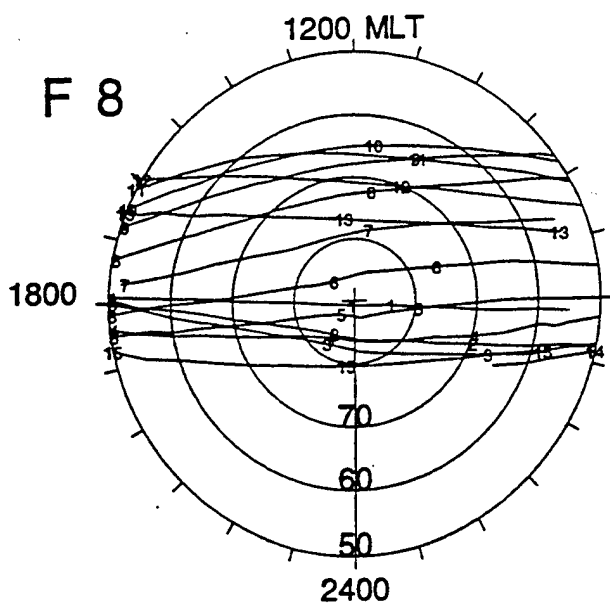
Observations are shown by symbols and IFM by the line

VANIMO   geo lat:lon   -2.70 141.30

DARWIN   geo lat:lon   -12.45 130.95

TOWNSVILLE   geo lat:lon   -19.63 146.85

NORFOLK IS.   geo lat:lon   -29.03 167.97

Local time (hr)

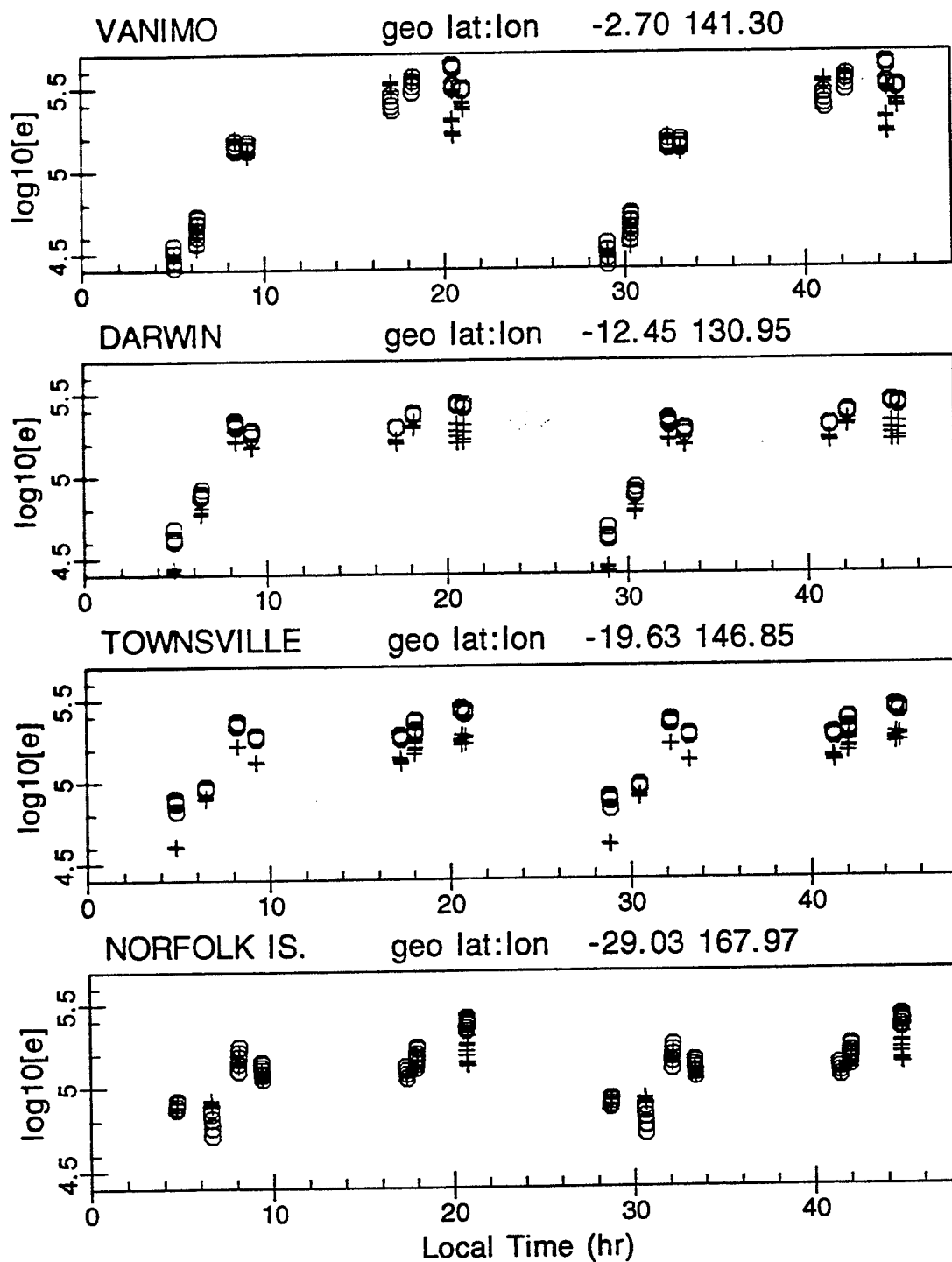# Electron density, at 800 km, comparison of DMSP with IFM

- DMSP Satellites F8. F9, F10, and F11 made N_e measurements at 800 km.

- These were made under very similar low geomagnetic activity and high solar conditions. But these observations were made on 22 January 1992.

- Measurements were extracted when the satellites passed over the Australian sector station latitudes and were within $\pm 15^\circ$ longitude of the station.

- Although 4 DMSP satellites were in different orbits their local time coverage was only 4 different sectors rather than a possible maximum of 8 if their orbit planes had been optimally separated.

- The agreement between the satellite observations (plus symbols) and IFM (circle symbols) is in general sufficiently good that in most sectors the two sets of symbols overlap.

- The most obvious sector in which this is not the case is at 2100 LT. In this case the IFM electron density is significantly larger than the observed. This will be discussed further.

- At Townsville and to a lesser extent all the model densities are higher than observed.
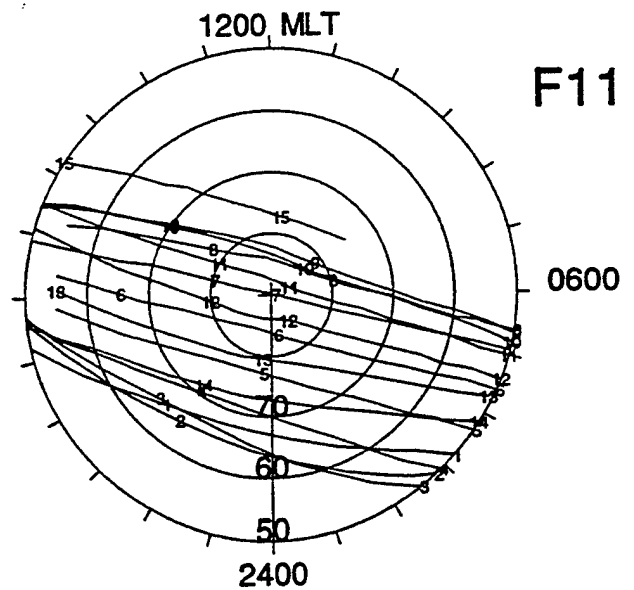
- DMSP southern hemisphere orbits (labeled
  sequentially 1 through 15) for 24 hours during
  validation period 1.

Density at 800km comparison on 22 January 1992.

Observations are shown by crosses and IFM by circles.

VANIMO   geo lat:lon   -2.70 141.30

DARWIN   geo lat:lon   -12.45 130.95

TOWNSVILLE   geo lat:lon   -19.63 146.85

NORFOLK IS.   geo lat:lon   -29.03 167.97

Local Time (hr)

The 2100 LT Discrepancy in N_e at 800 km.

- At 2100 LT IFM N_e at 800 km exceeds observations.

- At 2100 LT IFM h_mf_2 exceeds observed values by almost 100 km.

- At 2100 LT IFM N_mf_2 agrees with the observed values.

- Resolution, the electric field has lifted the IFM F-layer too high.

VANIMO

Local time (hr)
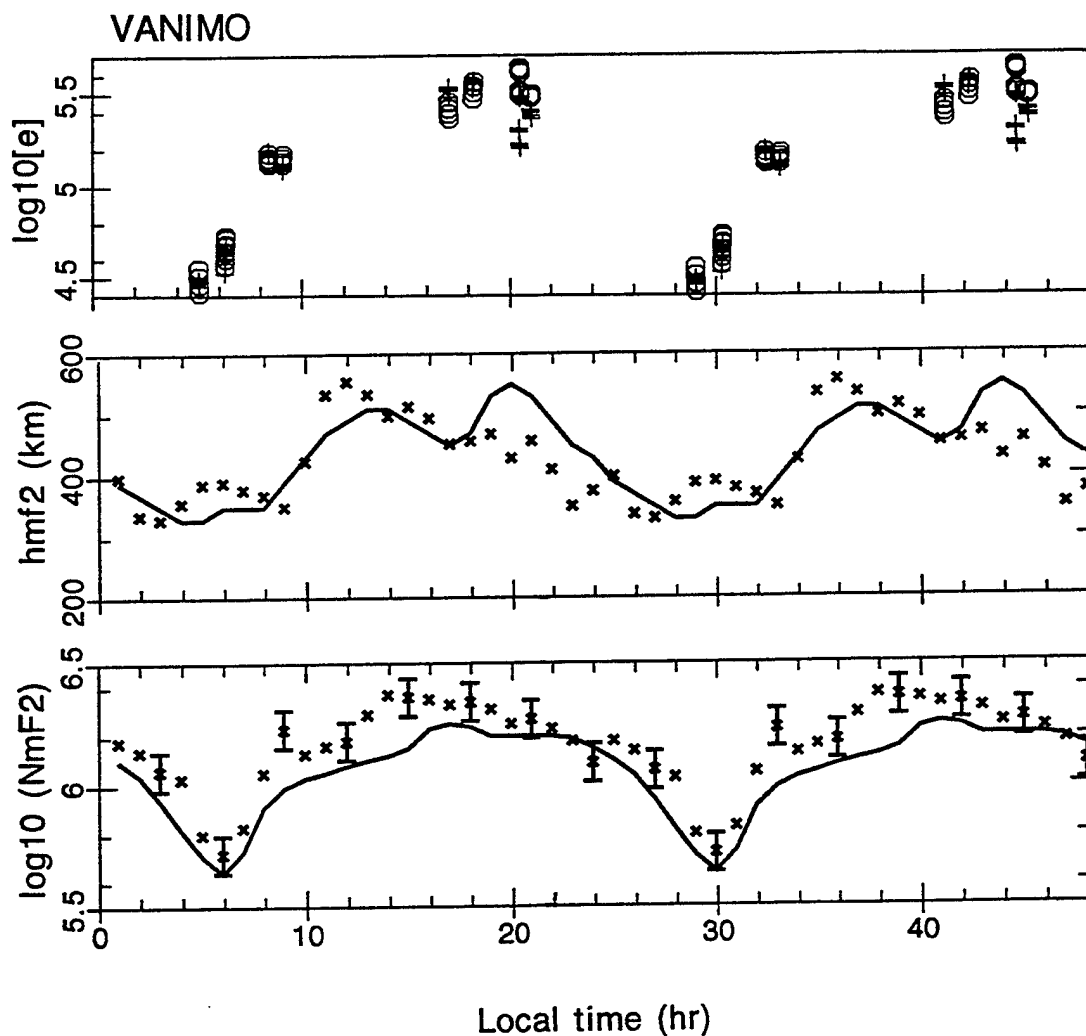
CONCLUSIONS OF THE VALIDATION STUDY

- In general the comparisons are very favourable with the IFM ionosphere being within the observed day to day variability. However, the study has identified several areas where future efforts would lead to improvements.

  o The equatorial electric field is the input that lifts the F-layer, which in turn leads to the equatorial anomaly. This was found to have been lifted too high in the post dusk, 1800 to 2400 LT sector. Fine tuning of the equatorial electric field would lead to improved agreement in this local time sector of the equatorial ionosphere.

  o At the higher midlatitude pre-dawn sector the F-layer had decayed too much in the IFM. This requires an improved topside boundary condition. A topside flux from the plasmasphere is needed to maintain the F-layer. Once again fine tuning of the topside boundary condition would provide improved agreement.

  o In the night sector, at all four ionosonde stations, the IFM F-layer peak height was to high. This could well be indicative of the need to refine the neutral wind which at midlatitudes lifts the night sector F-layer.

  o The IFM daytime E-layer density was found to be systematically low in the IFM. The discrepancy is in general less than 8% in the electron density.

CONCLUSIONS OF THE VALIDATION STUDY (continued)

- In all four cases the IFM inputs need to be improved. In each case the model-obsevation comparison would be the basis for making the changes. <u>A word of caution</u>, in each case such modifications would have to be revalidated at other longitudes and latitudes as well as at other levels of solar and geomagnetic activity.

- The Australian sector validation effort will be continued by extending to higher latitudes in the southern hemisphere. This sector has 'longitudinal' differences from the American sector. Most of the empirical low latitude and midlatitude inputs have been extensively validated against data from the American sector. Hence this extensive Australian data base offers an excellent opertunity to test the global applicability of the IFM. Additional stations being looked at are Canberra, Hobart, Macquarie Is, and then into the auroral region with Mawson.

- The dual ionosonde (F-layer) and DMSP (800km) comparisons enable significantly more insight into the source of model-observation differences than would either technique on its own. This dual approach will be further extended with TEC data when suitable data sets become available.